

NASA Robotic Mining Competition

Engineering Report



*Michael Bush, Collin Chick, Zachary Christy, Cody Cooper,
Kevin Grimsted, Paul Hertfelder, Devon Jones, Austin Kaul,
Sean Kittler, Joree Sandin, Logan Torgerson, Eric Vandervort,
Samuel Vinella*

Sponsors: Moonrockers, NASA SD Space Grant, Self Funding

Advisors: Dr. Jason Ash, Dr. Hadi Fekrmandi, Mr. Lowell Kolb,
Dr. Charles Tolle

Contents

1	Introduction	6
2	Scope of Work	7
3	Conceptual Design	9
4	Collection Subsystem	9
4.1	Design Constraints	10
4.2	Preliminary Design	10
4.3	Data Acquisition/Verification	12
4.3.1	Actuators	12
4.3.2	Updated Collection System	13
4.3.3	Rotating Mounting Structure	14
4.4	Critical Design	15
4.5	Detailed Design	16
4.6	Design Realization	23
4.7	Product Performance	25
5	Deposition Subsystem	25
5.1	Design Constraints	25
5.2	Design Considerations	25
5.3	Preliminary Design	30
5.4	Data Acquisition	30
5.4.1	Larger Side Wall Brackets	30
5.4.2	Deposition Belt Drive Gear	30
5.4.3	Conveyor Wheel Covers	30
5.5	Data Verification	30
5.5.1	Larger Side Wall Brackets	30
5.5.2	Deposition Belt Drive Gear	31
5.5.3	Conveyor Wheel Covers	31
5.6	Design Realization	31
5.7	Product Performance	31
5.8	Final Design Selection	31
5.8.1	Past, Current, and Future plans	31
5.9	Design Schedule	31
5.10	Manufacturing Schedule	32
5.10.1	Manufactured Components	32
5.10.2	Manufacturing plan	32
6	Electrical Subsystem	32
6.1	Design Constraints	32
6.2	Design Considerations	32
6.3	Preliminary Design	33
6.4	Design Schedule	34

6.5	Detailed/Complete Design	34
6.6	Manufacturing Plan	40
6.7	Data Verification	40
6.8	Design Realization	45
6.9	Product Performance	46
7	Autonomy Subsystem	46
7.1	Design Constraints	46
7.2	Design Considerations	46
7.3	Preliminary Design	47
7.4	Critical Design	54
7.5	Environment Mapping	58
7.5.1	Hardware	58
7.5.2	Software	59
7.6	Path Planning	66
7.7	Navigation Execution	70
7.7.1	Introduction and Motivation	70
7.7.2	System Description	70
7.7.3	Controller Specifications	73
7.7.4	Controller Design	73
7.7.5	Test Implementation and Redesign	76
7.7.6	Second Redesign	77
7.7.7	Mapping Changes Impact	77
7.8	Development Plan	78
7.9	Testing Plan	78
7.10	Design Realization	80
7.11	Product Performance	80
8	Project Schedule	81
9	Task Statements	83
9.1	Action Items Tables	85
10	Preliminary Budget	87
11	Project Risks	89
A	Collection System Finite Element Analysis	91
B	Collection Subsystem Drawings	97
C	Custom ROS Message Definitions	103
D	Custom ROS Services	105
E	State Diagrams	106

List of Figures

1	Combined Collector-Conveyor	11
2	Excavator Concept	11
3	Image of icy regolith collection system test.	13
4	Collection system rail	14
5	Implementation of Longer Actuators	15
6	Rotating and Actuating Trench Digger	16
7	Icy regolith collection system.	17
8	Collection system mode of actuation.	18
9	Collection system rotating slide.	19
10	Linear actuator mounted inside of collection slide.	20
11	Collection system mounting structure.	21
12	Mounted linear actuators to rotate collection system.	22
13	Designed collection system implemented to robot chassis.	23
14	Collection system rail brackets	24
15	Updated Deposition System	27
16	Corrugated roof deposition design	28
17	Actuating Roof Deposition System	29
18	View of Both Electrical Boxes and Locations	34
19	Low Voltage Electrical Box	35
20	High Voltage Electrical Box	36
21	High Voltage Enclosure Layout	36
22	HV Box Internal Connector	37
23	HV Box External Connector	37
24	Modularity Connector	38
25	PDB Schematic	39
26	Eagle Library of Components	39
27	Eagle Board Designs	39
28	Thermal Simulation on Old Box	40
29	Thermal Simulation on New Box	41
30	PDB Tested on Breadboard	42
31	ADS - Switch Connected to Power	42
32	ADS - Forward Bias Voltage Input	43
33	ADS - Forward Bias Current Draw	43
34	ADS - Switch Connected to Ground	44
35	ADS - Reverse Bias Voltage Input	44
36	ADS - Reverse Bias Current Draw	45
37	Overview of all sensors and interconnections	47
38	AR tag used in previous years	48
39	10,000 Accelerometer and Gyroscope readings at rest	49
40	IMU Vibration damping mount (steel washers affixed below)	49
41	DWM1000 configuration	50
42	Possible Reflection Paths	51
43	Noise distribution of ranging antennae	52

44	Internal electronics of antennas	52
45	Simple State Diagram	54
46	Inter-Connectivity Diagram	57
47	Example Reference Frame Transformation	60
48	Operation of Points2Grid Library DEM Generation	61
49	Visualization of the Mechanical Fuzzy Map	64
50	Visualization of the Operator Display Fuzzy Map	65
51	Visualization of the Controller Fuzzy Map	66
52	Example of Intersection Computation	67
53	Path Planning Flowchart	71
54	Path Smoothing Algorithm	72
55	Example Output from Smoothing Algorithm	73
56	Controller Step Response	74
57	Path Following Flowchart	75
58	Example Execution of Path Following Algorithm	76
59	Loading cases used to run FEA on collection rail	91
60	Finite Element Analysis post processing on collection rail	92
61	Loading cases used to run FEA on collection slide	93
62	Finite Element Analysis post processing on collection slide	94
63	Loading cases used to run FEA on collection mounting structure	95
64	Finite Element Analysis post processing on collection mounting structure without hole	95
65	Finite Element Analysis post processing on collection mounting structure with hole	96
66	Collection Slide	97
67	Collection Shaft Clamp	98
68	Collection Rail	98
69	Collection Slide	99
70	Collection Slide	99
71	Collection Slide	100
72	Collection Motor Mount	100
73	Collection Mount Support	101
74	Collection Mount Strip	101
75	Collection Mount L Bracket	102
76	Mount Title Actuator	102
77	Rail Support	103
78	Startup State	106
79	Traversal State	107
80	Regolith Mining State	108
81	Dump State	109
82	Icy Regolith Mining State	110
83	Deposition State	111

List of Tables

1	Collection Design Rubric	10
2	Collection Design Design Matrix	12
3	Deposition System Rubric	25
4	Deposition Decision Matrix	26
5	Inter-Connectivity Diagram Legend	58
6	Definition of Cost Function Symbols	68
10	Definition of Symbols for Controller	72
11	Definition of Symbols for Algorithm	74
12	Autonomy Subsystem Verification Matrix	79
13	Action item list to be completed before Critical Design Review.	86
14	Action item list to be completed before February.	87
15	Overall labor budget for six electrical and computer engineers and seven mechanical engineers.	87
16	Mechanical, electrical, and computer engineering component budget.	88
17	Convergence study for FEA of collection rail.	92
18	Convergence study for FEA of collection slide.	94
19	Convergence study for FEA of collection mounting structure without hole. .	96
20	Convergence study for FEA of collection mounting structure with hole. . . .	96
21	Map Row Message Format	103
22	Environment Map Message Format	104
23	Waypoint Message Format	104
24	Environment Map Service Format	105
25	Path Service Format	105

1 Introduction

Space is the next frontier for human beings that many are seeking to explore and colonize. There are limitations in space as an environment whether it be air, food, or water. If those issues can be solved, the next is fuel. How do humans get from one place to another in space? The answer is using the resources on the celestial bodies to the advantage of the traveler.

NASA has the plan of traveling to a location and using the natural resources at said location for survival. The NASA Robotics Mining Competition has the goal of sending a robot to Mars that can mine icy regolith [5]. Icy regolith contains hydrazine which is the necessary ingredient for space shuttle fuel. This is important because the fuel collected would be used for a return trip which would otherwise be improbable due to capacity limitations.

NASA hosts the annual Robotic Mining Competition (RMC) to promote the research and development of robotic in-situ resource utilization. The competition awards points to the team that can construct and operate a robot that, through autonomy or telerobotics, can mine the greatest amount of icy regolith buried beneath a layer of basaltic regolith.

For the past 9 years, excluding one of those years, the South Dakota School of Mines has entered a robot into this competition. Aside from the initial 1000 points awarded for a successful inspection, autonomous operation is the most heavily weighted category for a robot's score. Unfortunately, while the School of Mines robot has displayed exceptional mechanical design concepts and received 2nd place in autonomy, it has lacked reliability and fully effective autonomy.

The solution was to use a design that encompasses more multi-disciplinary skill sets to improve upon the current robot design. The goal was to maximize the amount of points awarded to the robot by implementing full autonomy in the final design, and ensuring the quality and readiness of the robot's mechanical systems.

The team was comprised of a multi-disciplinary group of Senior Computer, Electrical and Mechanical engineering students with varying degrees of industry experience. Professors and a large group of volunteer undergraduates, at the School of Mines, advised and assisted the Moonrockers team .

The team of Electrical and Computer Engineering Senior Design students consisted of: Collin Chick, Zachary Christy, Paul Hertfelder, Logan Torgerson, Eric Vandervort, and Samuel Vinella. The Mechanical Engineering Senior Design students consisted of Team Lead Joree Sandin, Michael Bush, Cody Cooper, Kevin Grimsted, Devon Jones, Austin Kaul, and Sean Kittler.

2 Scope of Work

Icy Regolith Collection Focus

The Moonrockers Team, for this year, has dedicated their efforts to focus on the major change in rules, and facet the robot to achieve in reaching, collecting, and depositing icy regolith, in the arena, at competition. As an overview, in order to fit this focus, the robot's current collection system will need to be redesigned. Also, the current electrical box is obstructing the goal of reaching to the depth of the icy level, therefore, another major change to the bot will be to redesign and re-place the electrical box, behind the deposition system, in order to achieve this goal. The deposition system is currently efficient, however, slight modifications will occur in order to optimize its functionality. The chassis system will be maintained for quality and efficiently, but plans to remain unchanged.

A major scoring category for the 2018 NASA RMC is Autonomy. Up to 50% of qualification mining points can be scored by implementing full autonomy. Full autonomy is defined as the robot being able to navigate within the arena, collect icy regolith, and deposit it with no human interaction.

A more detailed description for the scope of work is listed:

Constraints:

- Maximum Width: 0.75 meters
- Maximum Height (Before competition starts): 0.75 meters
- Maximum Height (After competition starts): 1.5 meters
- Maximum Length: 1.5 meters
- Maximum Weight: 80 kg (Point deduction for mass)

Descriptions used for the functional requirements are as follows:

Electrical Box

Functional requirement: Move the electrical box off the collection system's frame to allow for deeper digging.

Collection System

Functional requirement: Be able to dig deep enough (60cm) to gather icy regolith at an efficient rate.

Deposition System

Functional requirement: Be able to deposit icy regolith at an efficient rate into the collection hopper.

The team will be expected to output exceptional work as a whole. This can only be accomplished by ensuring excellence in each subsystem. Therefore, the team put together a list of decision matrix categories in which the team will use to determine the most optimal system for the final design over the course of the preliminary and critical design phases. A list below shows these categories:

Descriptions of the categories used for the design matrices are as follows:

Electrical Box

- Ease of Access: how easy the design will be to access the box
- Lightweight: how light will the design be
- Space Claim: how much space will the design take up on the robot
- Hindering Bot Functionality: how will the design hinder other functions on the robot
- Cheap: how inexpensive will it be to add to the robot
- Manufacturability: how easy will the design be to make
- Ease of Implementation with Current Bot: how easy will the design be to add to the robot
- Compactness: how much space will the electrical components take up inside the box

Collection System

- Dust Mitigation: how much dust is created
- Mass: how light will the design be
- Space Claim: how much space will the design take up on the robot
- Collection Efficiency: how well will the design collect
- Cost: how inexpensive will it be to add to the robot
- Manufacturability: how easy will the design be to make
- Reliability: how unlikely is a design failure
- Integration with Current System: how easy will the design be to add to the robot

Deposition System

- Dust Mitigation: how much dust is created
- Lightweight: how light will the design be

- Space Claim: how much space will the design take up on the robot
- Deposition Efficiency: how well will the design collect
- Cheap: how inexpensive will it be to add to the robot
- Manufacturability: how easy will the design be to make
- Reliability: how unlikely is a design failure
- Ease of Implementation with Current Bot: how easy will the design be to add to the robot

3 Conceptual Design

The SDSM&T Moonrocker's team completed their Preliminary Design Review on October 23rd, 2017, which was to present the various designs made for each sub-system of the robot. With the help of the advisors, the team was able create a decision matrix that analytically determined which design fit best for our needs and objectives. These are the four main sub-systems that are the focal point for design changes for the upcoming 2018 NASA robotic mining competition.

1. Collection System
2. Deposition System
3. Electrical Box
4. Autonomy

The next sections of the report consists of the concepts chosen for each sub-system. Each design is heavily evaluated on functionality, reliability, and feasibility.

4 Collection Subsystem

The collection system was the primary focus for implementing major changes for the 2018 NASA RMC. When coming up with our preliminary design concepts for the robot, we had to consider the new rules and major changes to NASA's 2018 RMC. The main change being the target material collected during digging. Before points were only awarded for mining or collecting the top layer of BP-1 (like moon sand), but now NASA is only awarding points for mining the Icy Regolith (like gravel) which is underneath the BP-1. This year, there was 12 inches of BP-1 on top of 12 inches of Icy Regolith, which means our robot had to be capable of digging at least two feet deep. The icy regolith is a valuable resource on Mars that can be utilized for rocket fuel on trips back to earth, and is also being further researched and developed for sustaining life on Mars.

4.1 Design Constraints

The Moonrocker's senior design team created a design matrix based on functional requirements, in order to help focus our research. With that said, these were the categories that the team thought were most critical in ensuring a valid design process.

Each of these categories were then ranked from 5 to 1, with 5 being the best option and 1 being the worst option. Each number has quantitative reasoning to justify the rankings from the team. The final rubric for the collection system decision matrix can be seen in Table 1

Table 1: Collection Design Rubric

COLLECTION SYSTEM RUBRIC					
Criteria:	5	4	3	2	1
Collection Efficiency: Predicted icy regolith collection amount	30+ kg	30-20 kg	20-10 kg	10-1kg	1-0 kg
Mass: Estimated mass	0-40 kg	40-55 kg	55-65kg	65-80kg	80+ kg
Reliability: Predicated chance of failure/complexity of system/# of degrees of freedom	1 degree of freedom/1-2 motors/actuators	More complex than 5	1-2 degrees of freedom/2-3 motors/actuators needed	Less complex than 1	High predicted failure/Complex system/ >2 degrees of freedom with > 4 motors
Integration with Current System: # of systems to redesign	0	1	2	3	4+
Space Claim: # of systems modified	0	1	2	3	4+
Manufacturability: # of hours to manufacture	0-20 hrs.	20-40 hrs.	40-60 hrs.	60-80 hrs.	80+ hrs.
Cost: Estimated cost	\$0-100	\$100-1000	\$1000-2000	\$2000-3000	\$3000+
Dust Mitigation: Collection transfer height to deposition system	40-50+ cm	30-40 cm	20-30 cm	10-20 cm	0-10 cm

4.2 Preliminary Design

This section shows the collection design concepts presented at the Preliminary Design Review that was completed on October 23rd, 2017. There were a total of 5 concepts for implementing the best ways to mine icy regolith. 1,2, *insert more designs here*. These models were created using SolidWorks, which is critical in designing the prototypes as well as manufacturing the parts.

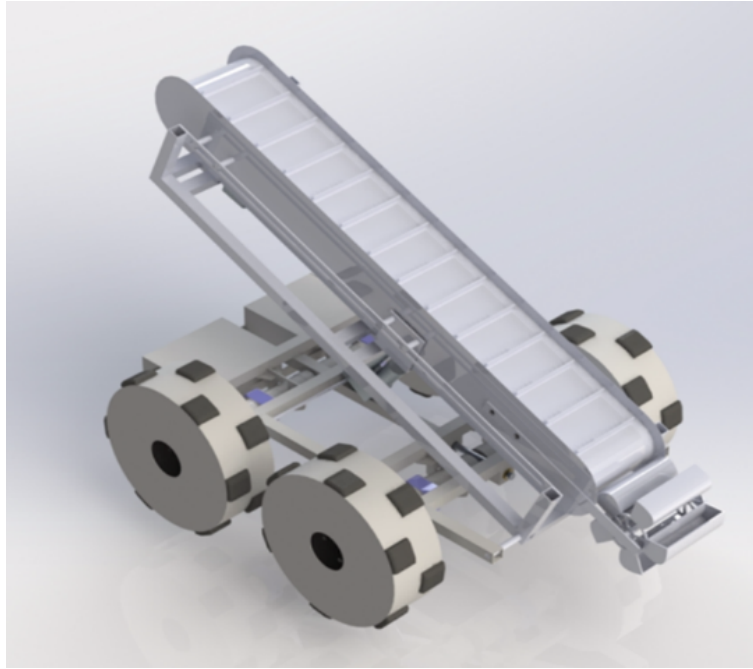


Figure 1: Combined Collector-Conveyor

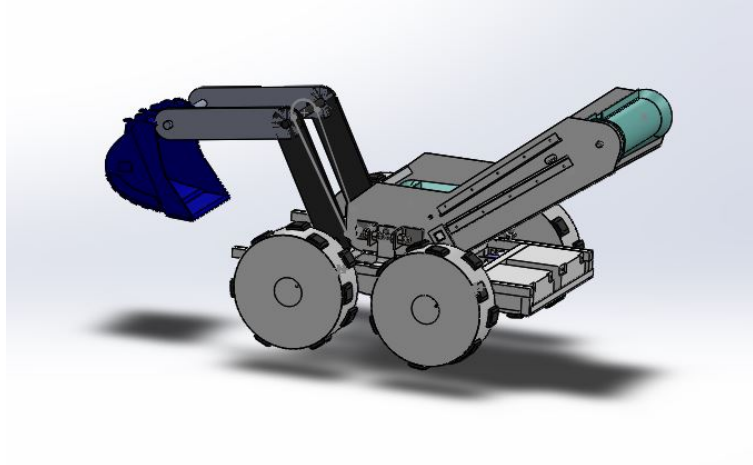


Figure 2: Excavator Concept

Using the collection system rubric made, the team was then able to create a collection system design matrix for a comparative analysis of the preliminary concepts. This design matrix can be seen in Table 3. Each concept was evaluated on each category made from the rubric as shown previously. Although each category was ranked from 1 to 5, the team had to create a new value to represent how important that category was to the functional requirements. Again the scale was 5 being the most important, and 1 being not important. As shown in the design matrix, Collection Efficiency was given a 5 since the objectives are to collect icy

regolith which is twice as deep as the previous years. Manufacturability was given a 1, due to the team assuming that the accelerated schedule will ensure enough time to manufacture any design. Cost was given a 1 since the team's budget is always considered in our design process, and engineering in general is about finding cost effective methods. Dust Mitigation was also given a 1, since it does not play a big factor in the overall grade of our robot during competition. Once each category was given an importance value, that category weight is then the percentage of the total all the categories. The final scores for each design was found by taking the average of each value of the categories.

Table 2: Collection Design Design Matrix

COLLECTION SYSTEM DESIGN MATRIX										
DESIGNS	Collection Efficiency	Mass	Reliability	Integration with Current Setup	Space Claim	Manufacturability	Cost	Dust Mitigation	Total	
<i>Category Importance</i>	5	3	3	3	2	1	1	1	19	
<i>Category Weight</i>	0.263	0.158	0.158	0.158	0.105	0.053	0.053	0.053	1.00	
Auger	4	2	1	3	4	2	2	4	2.84	
Combined Collector Conveyor	3	4	3	2	4	2	1	4	3.00	
Current with Longer Actuators	1	3	5	5	5	5	5	3	3.53	
Rotating & Actuating Trench Digger	5	3	2	4	4	3	3	3	3.63	
Excavator Bucket	3	3	1	3	4	2	2	2	2.63	
Plow & Mine	1	2	5	3	3	4	4	2	2.68	

4.3 Data Acquisition/Verification

4.3.1 Actuators

To dig the required depth, longer linear actuators were implemented. Actuators with optical sensors were purchased and tested. The speed at which the actuators extended was not ideal. Testing was done with pulse width modulation(PWM) to decreased the time of actuation of the 24" actuator. It was found that when the speed of the motor was placed beyond spec, the motor will throw a winding. The limit for the motor when running PWM was noted and used to set a maximum rate of actuation. When implementing two linear actuators that are on the same rigid body, there can be complications with the two actuators not actuating at the same rate. This was evident when testing the two 24" actuators on the collection system. Optical sensors in the actuators were utilized in a control system to ensure the two actuators moved in tandem to prevent unwanted torque on the collection system. Originally, actuators without feedback were going to be implemented to rotate the collection system.

It was decided to purchase actuators with optical sensors to avoid the possibility of the actuators moving at different rates.

4.3.2 Updated Collection System

Digging the icy regolith at a depth of at least 30cm presented a difficult challenge when attempting to modify the previous year's robot. It was realized that the collection system would need to be replaced. A collection system designed for digging to the icy regolith was made by a senior design group from previous years. It was decided to implement this icy regolith collection system onto the current robot chassis. Before designing a mounting structure for the collection system, the icy regolith scoop ladder system was tested to ensure it could handle sand and gravel. A picture of the test can be seen in figure 3 below.



Figure 3: Image of icy regolith collection system test.

The test confirmed the decision to use the scoop ladder collection system designed by a previous years senior design team. A complete SOLIDWORKS model was made of the collection system to assist in the design of the mounting structure. It was found that the motor had to be changed for one with more torque. The same motors used to drive the wheels of the robot was used for the test. The challenge in implementing this collection system was mounting the system and introducing a degree of freedom.

4.3.3 Rotating Mounting Structure

The team looked into modifying the collection system design to include a rotational degree of freedom. This additional feature is intended to allow the maximum digging depth, while also staying within the competition dimensions. The rotating control will allow the digging system and the robot to be within the size constraints when the competition runs start. After the competition starts, the collection system can be rotated to gain maximum digging depth. A system was designed to allow the rotation of the collection system about an axis while also allowing the scoop ladder portion of the collection system to linearly actuate similarly to previous year's designs. This system will be introduced in the Critical Design Section. To validate the design of the mounting structure, Finite Element Methods were used to structurally analyze each part. SIMULIA's ABAQUS was used to conduct the Finite Element Analysis for each part.

The first part analyzed was the rail on the scoop ladder portion of the collection system. It was noticed that there were high force concentrations at the corners of the slot in the rail seen in figure 4 below.



Figure 4: Collection system rail

The part was modeled with 2-D planar elements. Several loading conditions were run. All holes on the rail were fixed rigidly for all loading cases. A worst case loading case where the maximum load that can be applied by the collection motor acted on the thin piece of aluminum below the slot. The loading condition and result of this analysis can be seen in figure 59 and 60 respectively in Appendix A. Table 17 in Appendix A gives the convergence study of this analysis. The analysis revealed that the part would yield. An alternative design was conceived and implemented which can be seen in the detailed design section. The loading conditions, FEA results, and convergence study done for each designed part can be seen in Appendix A. The remaining analysis revealed that the designed parts would not

yield under the proposed worst case loading conditions.

4.4 Critical Design

Following the PDR, the team held meetings to discuss and narrow down the best designs. From recommendations and the completion of our design matrix, the top 2 designs were the *Rotating & Actuating Trench Digger*, as well as the *Implementation of longer actuators*, on the current robot.

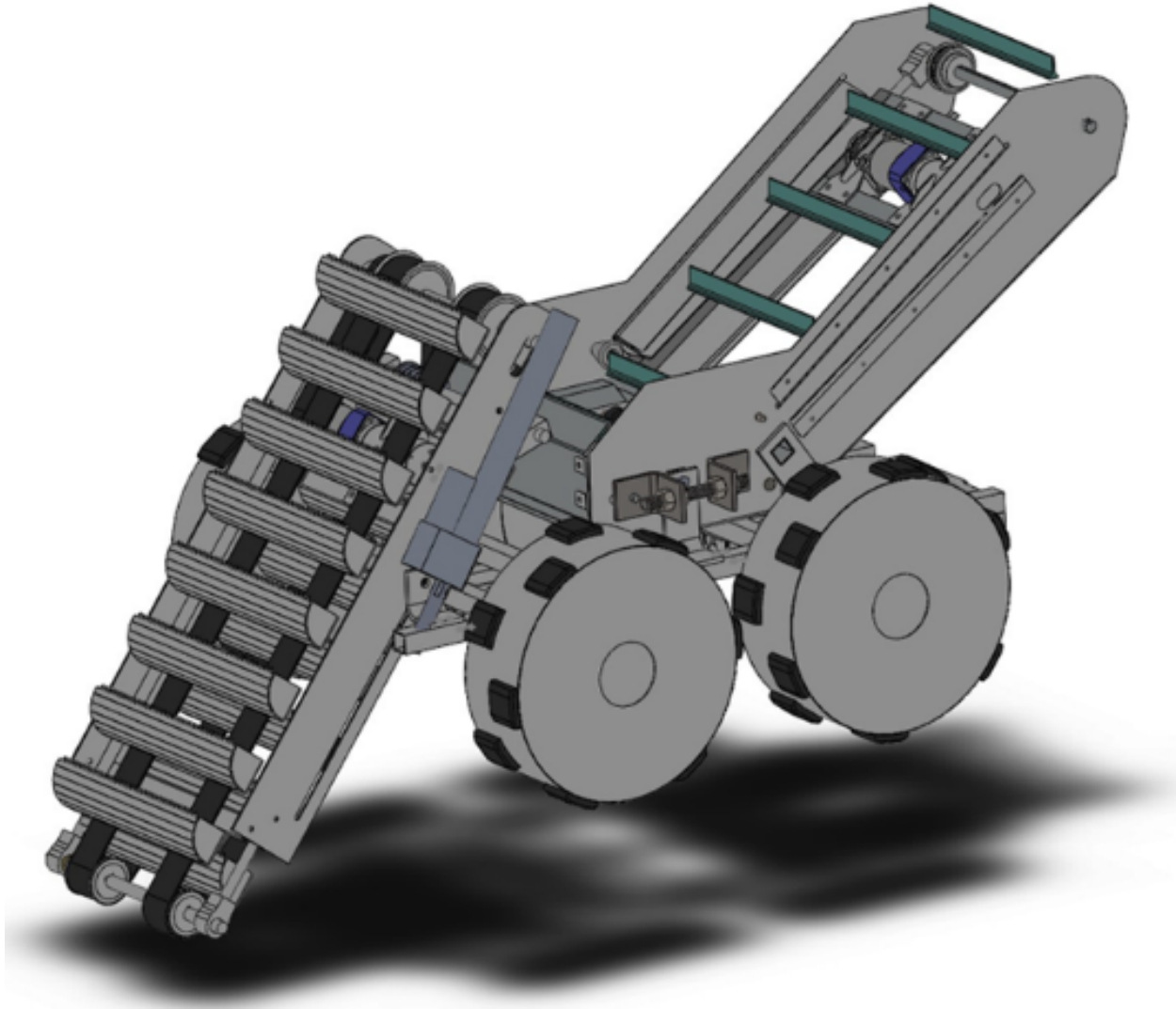


Figure 5: Implementation of Longer Actuators

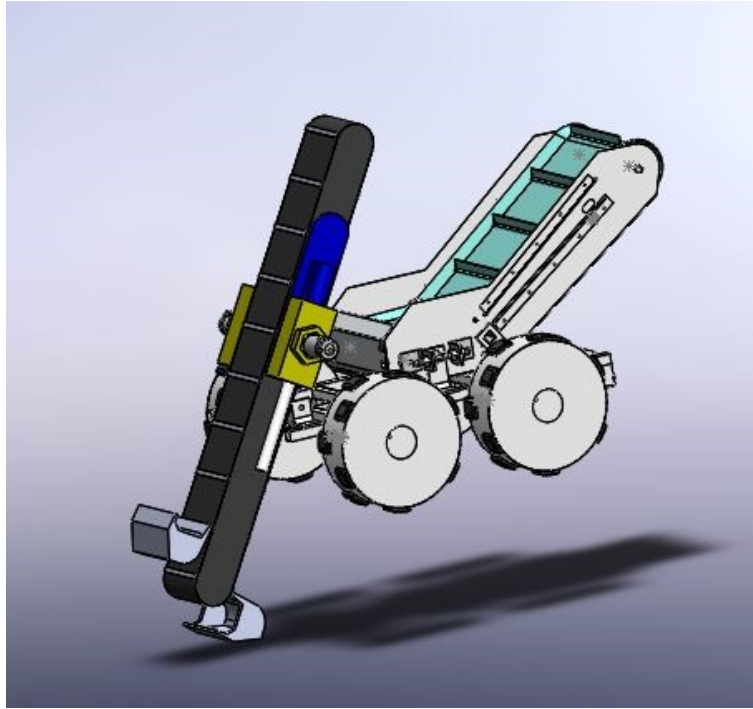


Figure 6: Rotating and Actuating Trench Digger

As shown in the collection system matrix, the Rotating and Actuating Trench Digger Concept received the best score compared to the Combined Collector Conveyor and Current with Longer Actuator concepts. The Rotating and Actuating Trench Digger concept scored a 5 in collection efficiency because of the designs ability to dig down to two feet as needed for competition. Also, this design scored high in Integration with Current Setup and Space Claim due to the fact that the design only requires adding the pivoting control which didn't require drastic changes to the robot chassis.

4.5 Detailed Design

The Preliminary Design Review revealed that the rotating and actuating trench digging concept was the ideal concept based upon the teams given criteria. Before detailed design began, the reuse of a collection system designed during the 2015-2016 academic year for digging icy regolith was considered. This icy regolith system can be seen in figure 7 below.

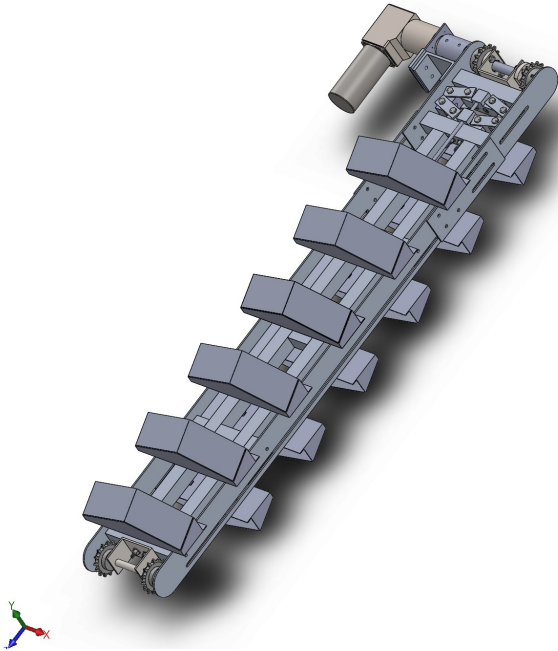


Figure 7: Icy regolith collection system.

It was decided that this icy regolith system would be modified and implemented into the collection system being designed. When implementing the rotating actuating system onto the robot chassis, the icy regolith collection system had to be modeled in a 3-D modeling software. The software chosen to model the already designed icy regolith system was **Solidworks**. After the **Solidworks** model was made for the already designed icy regolith system, a method for attaching the system to the chassis that rotates and actuates was developed. The method to allow the collection system to actuate was adopted from the previous years method. To actuate the collection system, the side rails of the system will have slots that a tab will be inserted to be slide along. Figure 8 below illustrates the side rail of the collection system with the tab to slide along.

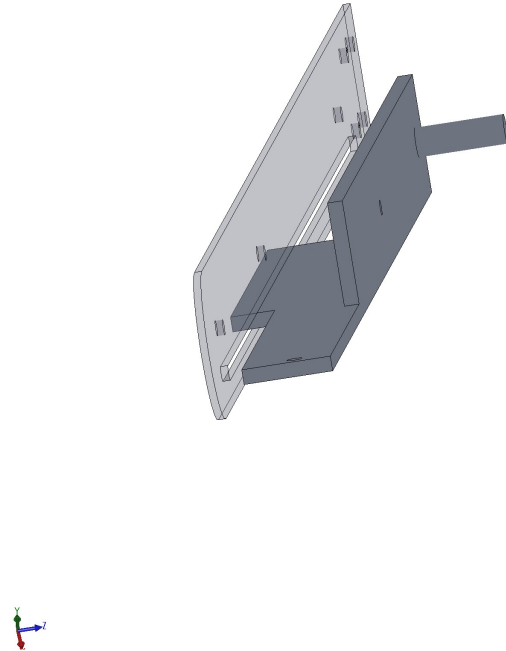


Figure 8: Collection system mode of actuation.

To allow the entire collection system to rotate, a motor must be implemented and an axis to rotate about must be decided. It was decided that the tabs with which the collection system actuates along would be mounted to the axis with which to rotate. The designed slide can be seen below in Figure 9.

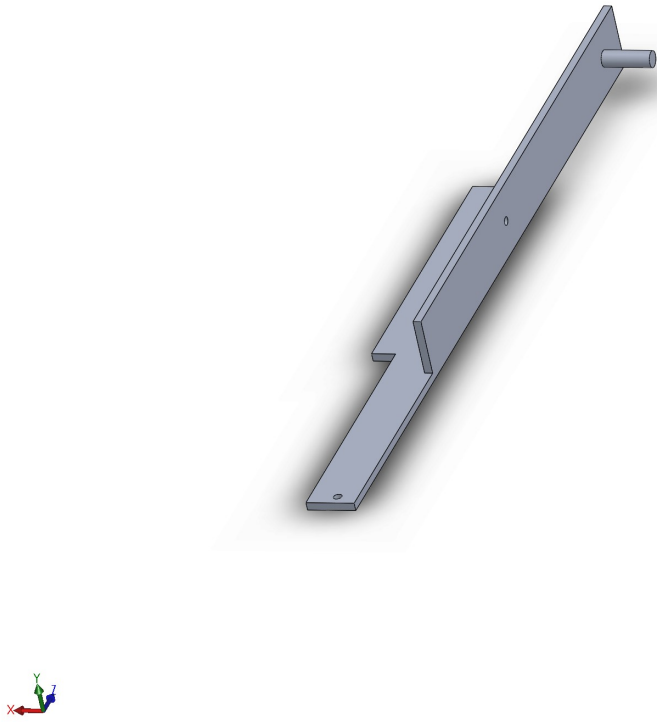


Figure 9: Collection system rotating slide.

As can be seen, the slide has an aluminum shaft to be mounted in a bearing. The bearings were mounted to an aluminum structure that will be directly mounted to the robot. The driving design factor for the placement of the axis with which to rotate was to maximize the digging depth while avoiding the interference with the chassis of the robot. A linear actuator will be used to actuate the collection system linearly and will be mounted to the slide as shown below in Figure 10.

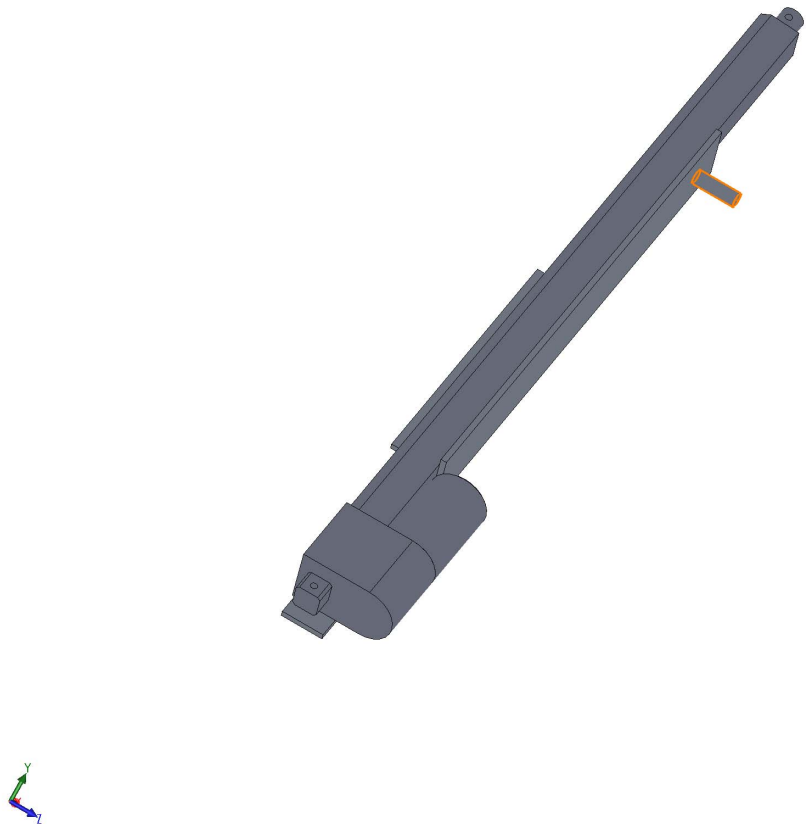


Figure 10: Linear actuator mounted inside of collection slide.

The designed mounting structure to mount the collection system to the chassis was a basic three plate weldment. The fully manufactured structure can be seen in Figure 11 below.

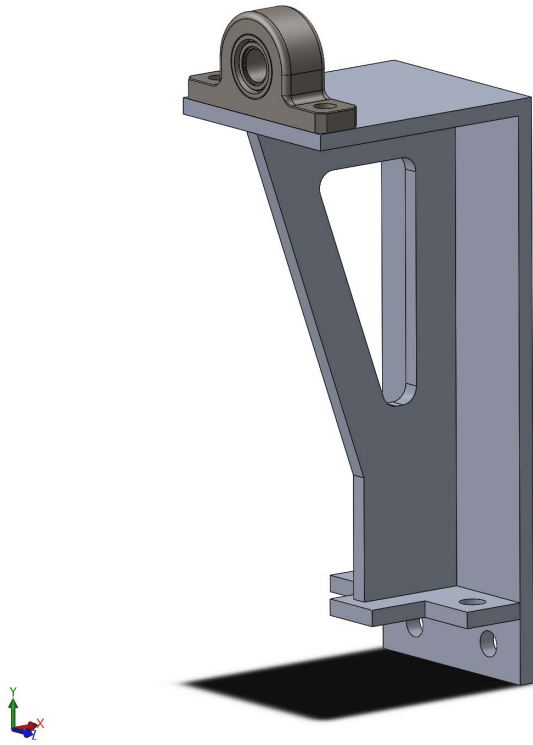


Figure 11: Collection system mounting structure.

To rotate the collection system, a linear actuator was used with pinned mounting joints. Attaching the linear actuator to the chassis and then to the slide allowed the collection system to rotate. The mounted linear actuators to rotate the collection system can be seen in Figure 12 below.

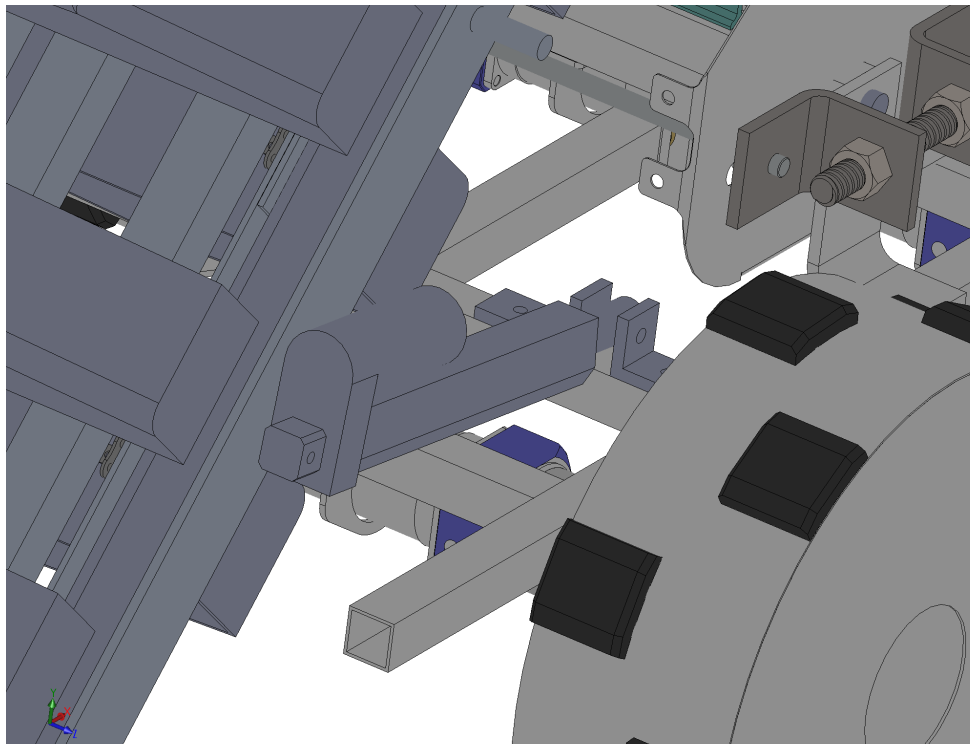


Figure 12: Mounted linear actuators to rotate collection system.

All of the implemented design systems can be seen in the **Solidworks** model in Figure 13 below.

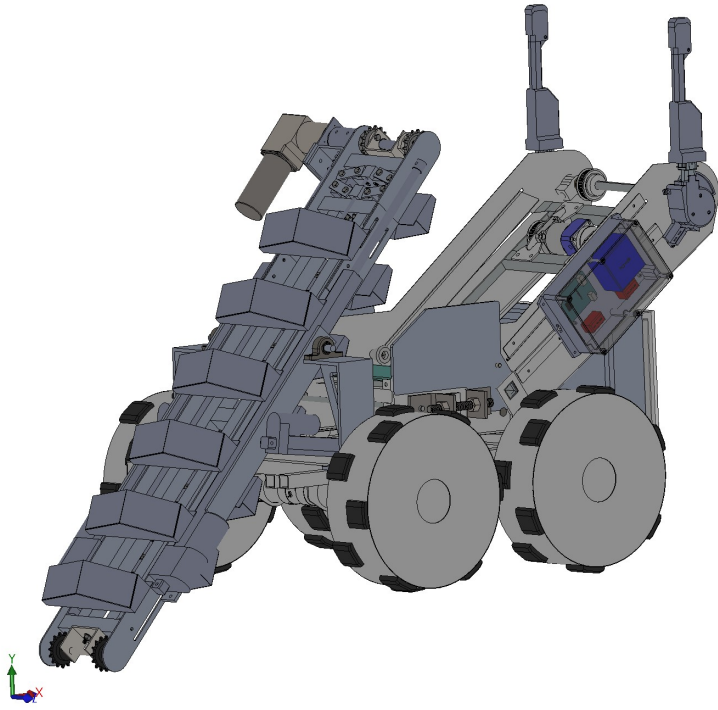


Figure 13: Designed collection system implemented to robot chassis.

4.6 Design Realization

All designed parts for the collection system were to be manufactured from 6061-T6 aluminum. The collection mounting structure parts were water jetted, bent, and then welded together. During the 90 degree bend in the outer plate of the collection mount, the metal cracked. The thickness of the aluminum was too large for a 90 degree bend. Because of the crack, support brackets were placed on the structure to reinforce it. The crack was also welded shut. The angle aluminum that was welded to the collection rails presented many problems. The collection rail is a long piece and tended to warp during the welds. Many manufacturing hours were placed in fixturing to ensure the part did not warp significantly.

During assembly of the robot, small setbacks occurred consistently as parts were added to the robot. In the original SOLIDWORKS model of the collection system, no hardware was implemented. The method in which the collection rails were attached to the collection frame were through expansion blocks that inserted into the tubes of the collection frame. The method designed to mount the collection system interfered with the hardware that mounted the rails to the collection frame. This oversight led to a re-designed method to attach the rails to the collection structure via welded brackets as seen in figure 14 below.

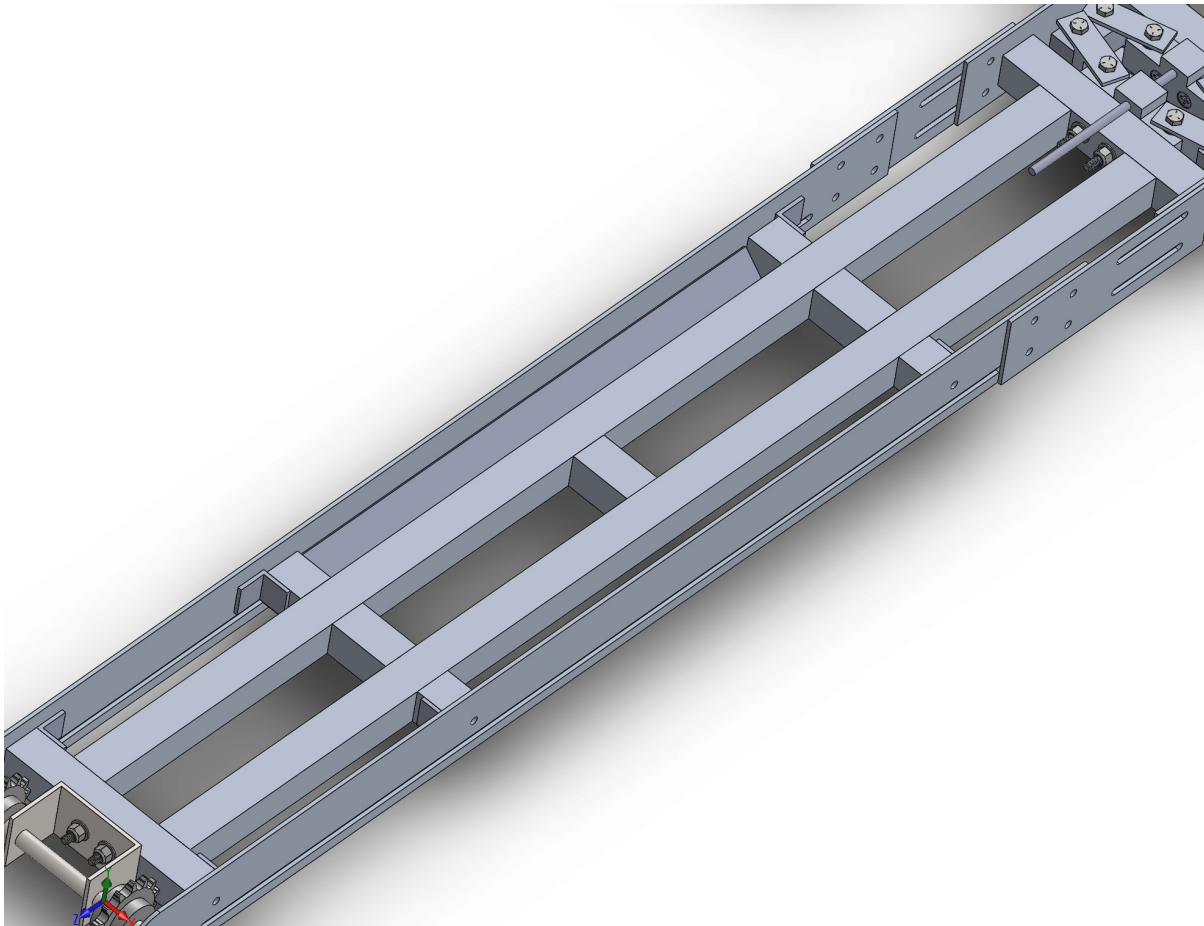


Figure 14: Collection system rail brackets

Another issue that was resolved involved the collection slide. Upon the assembly of the collection system onto the chassis of the robot, it was realized that the collection slide could easily slide out of the collection rail. This was an unforeseen issue and was resolved by drilling two holes in each slide and inserted small bolts on the tabs of the slide. These bolts prevented the slide from completely sliding out of the collection rail.

The dimensions of the angle actuators changed during the assembly process to accommodate for feedback in the actuators. This changed how the actuators were mounted to the chassis. Custom brackets were made that changed the mounting location of the angle actuators on the chassis. This change did not affect any other system.

During the manufacturing process, it was learned that welding can cause high amounts of warping in the parts being welded. It was also learned that during design, there may be oversights that only reveal themselves during assembly and implementation. These issues were resolved quickly by designing alternatives.

4.7 Product Performance

After full implementation of the icy regolith collection system along with its modifications during the assembly process, the system works as expected. All actuators move the system in expected ways and testing was done to ensure the system digs to the required depth. The tests were successful and the robot was able to dig to the required depth. There was concern that the sliding mechanism may bind during actuation. After testing, binding did not seem to be an issue.

5 Deposition Subsystem

5.1 Design Constraints

The deposition system of the Moonrockers robot must be able to function concurrently with the collection system, hold large amounts of icy regolith, and deposit the regolith to the bin without spilling or creating dust plumes. The only constraint based on the competition rules is the height of the final collection bin. The deposition has to deposit above that height in order to receive points for the competition.

The updated design on the current machine constrains volume of material held, torque/weight limit, and the fin size's capability to move larger icy regolith on the conveyor. These and the rule constraints drove the design of the updates and were accounted for in the testing/preliminary design phase.

5.2 Design Considerations

The Moonrockers team has come up with three primary design considerations for the final design of the deposition system. These designs were assessed against each other in a design matrix. The design matrix used categories of complexity, integration with current bot, space claim, weight, manufacturability, dust mitigation, and cost. Refer to Table 4 below for point scoring.

Table 3: Deposition System Rubric

Deposition System Rubric					
Criteria	5	4	3	2	1
Complexity: Number of Motors	1 motor	2 motors	3 motors	4 motors	5 motors
Integration: Number of parts added	1-2 parts	3-4 parts	5-6 parts	7-8 parts	9+ parts
Space Claim: Estimated volume	30,000-60,000 cm^3	60,000-90,000 cm^3	90,000-120,000 cm^3	120,000-150,000 cm^3	150,000+ cm^3
Weight: Weight in metric	1-2 kg	3-4 kg	5-6 kg	7-8 kg	9+ kg

Table 4: Deposition Decision Matrix

DESIGNS	Complexity	Integration	Space Claim	Weight	Manufacturability	Dust Mitigation	Cost	Total
<i>Category Importance</i>	7	6	5	4	3	3	2	30
<i>Category Weight</i>	0.233	0.200	0.167	0.133	0.100	0.100	0.067	1.00
Actuating Roof	3	3	2	4	4	2	5	3.10
Combined Collector Conveyor	3	3	1	5	2	5	1	2.90
Corrugated "Roof"	5	5	3	5	3	2	5	4.17
Sifter Dual Conveyor	2	2	2	3	3	4	3	2.50
Updated System	5	5	4	5	5	5	5	4.83
Yaw Rotation Conveyor	4	3	2	2	3	1	2	2.67

The top design was an updated version of the teams current system. This design won because it was easily implemented into the current system, it was cost effective, and it was a proven method of deposition based off of the past results.



Figure 15: Updated Deposition System

The design that came in second was a corrugated roof design. This design implemented a metal roof on top of the current deposition system which would allow the larger icy regolith to roll down onto the deposition belt, while the fine regolith would fall into the corrugations of the roof and be dispelled off the side of the robot.

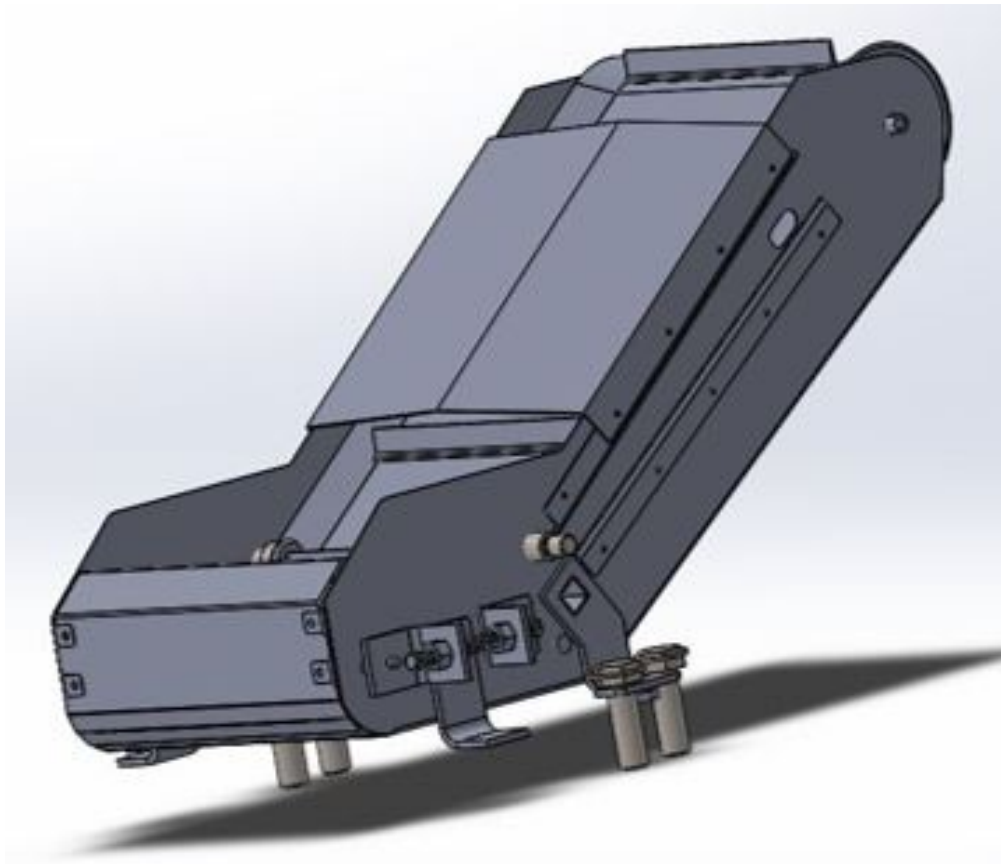


Figure 16: Corrugated roof deposition design

The third place design the team selected was an actuated roof design. This design would be closed to start with, allow the robot to dig fine regolith, and dispel it on top of the roof until the collection system reaches icy regolith. Once the system reaches this point, the roof would then actuate so that the collection of fine regolith is dumped onto the sides of the robot. After dumping, the roof remains open so that the robot may collect only icy regolith for deposition.

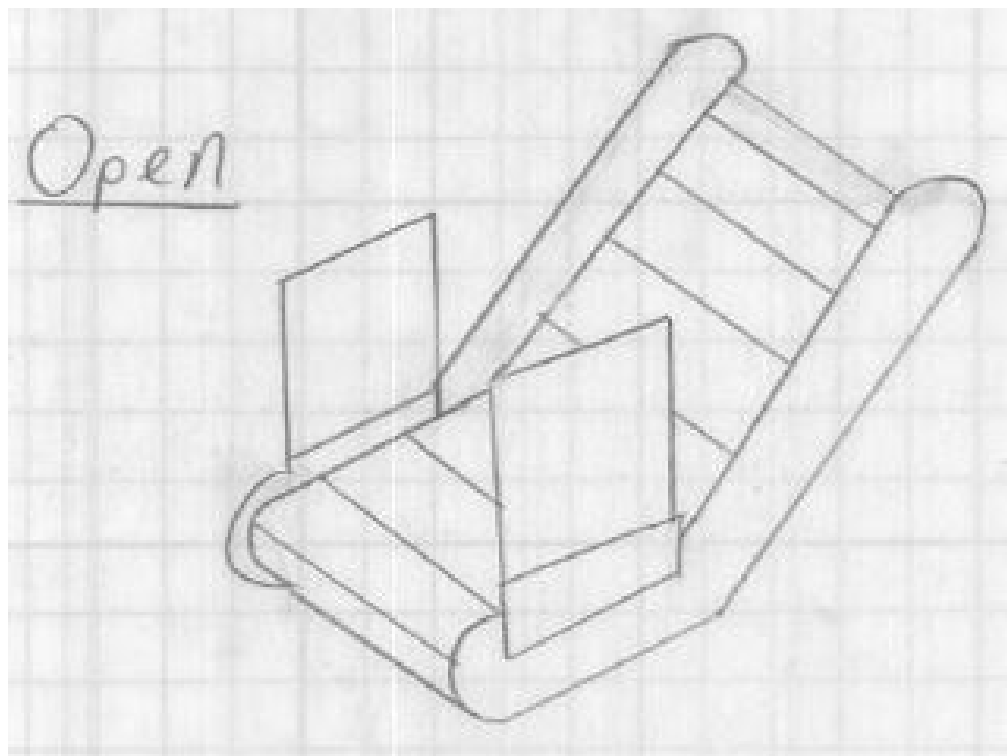


Figure 17: Actuating Roof Deposition System

5.3 Preliminary Design

The current system was chosen as the best option for deposition and updates to the system can improve functionality and ability to operate with the icy regolith challenge. The updates to the current system included higher side walls, chicken wire covers/heavy duty brackets, and improvements on the conveyor drive gear. The higher side walls would hold more regolith before depositing so as to mitigate wasting of time in competition. The chicken wire covers and added brackets will prevent the conveyor guide wheels from jamming and bending the sheet metal it was bolted to. The conveyor's drive gear was a 3D printed gear and lacked purchase on the teeth of the conveyor which, with a heavy load, began to slip. The motor and gear still moved, but the conveyor failed to do so. An improvement in the gear's design would increase surface area and increase the normal stress along the gear's teeth, which is necessary to reduce slipping.

5.4 Data Acquisition

5.4.1 Larger Side Wall Brackets

The team will test and validate the implementation of the larger side wall brackets after manufacturing.

5.4.2 Deposition Belt Drive Gear

The Moonrockers needed to test the maximum weight carrying abilities of the current deposition system in order to determine if the current system would be able to deposit the additional weight provided the team implemented larger side bracketing. The team placed a 40 pound box of rocks in the base of the deposition system and ran the belt. The team noticed there was belt slipping during the deposition process. This test allowed the team to come to the conclusion that the current 3D printed drive gear was slipping off the teeth of the belt. In order to mitigate the error, it was proposed that the team increase the length of the drive gear. In doing this, the surface area from the gear in contact with the belt's teeth was optimized in order to maximize the normal stress acting between the two components.

5.4.3 Conveyor Wheel Covers

The team will implement the conveyor wheel covers after the larger side wall brackets are manufactured since they are attached to the new part.

5.5 Data Verification

5.5.1 Larger Side Wall Brackets

The team implemented larger side wall brackets and tested the functionality of them. The side walls worked in order to stabilize the conveyor wheels and increase the volume the deposition system could hold.

5.5.2 Deposition Belt Drive Gear

The initial testing of the belt with a 40 pound box of rocks was tested again and worked with no slipping. The team also tested the deposition process while a 180 pound student sat on the belt and once again the deposition process was performed with no slipping. These test indicate that a design change of increasing the sidewalls height in order to maximize volume on the deposition belt would be possible.

5.5.3 Conveyor Wheel Covers

The team validated the wheel covers worked when they were attached to the deposition system and tested with larger rocks.

5.6 Design Realization

The deposition team ran into a few issues that needed to be changed. The first was the front panel on the deposition system. This piece of metal needed to be removed so that the collection system could lay flat into the deposition system and fit within the required design constraints. The other problem the team ran into was the placement of the holes in the new larger side walls. The team had assumed the system would be symmetric, however this was not the case. The team was able to easily fix this problem by filing out the holes in order to line up with the holes on the deposition system.

5.7 Product Performance

The deposition system performs well with minimal places of concern. The team will make sure that all the bolts, screws, and key ways are up to par in order to keep the system running optimally.

5.8 Final Design Selection

5.8.1 Past, Current, and Future plans

The Moonrockers decided it would be best to stick with the current deposition system and make minor alterations to the side walls, deposition drive belt gear, and wheel covers. These design implementations were necessary due to the nature of the new NRMC rules requiring the teams to only deposit icy regolith. In the future, The team will need to adjust to the changes in rules as subject to NASA's rule adjustments.

5.9 Design Schedule

The Moonrockers design schedule for the deposition system was minimal. There were not any major alterations to the system, only updates to the current system were made. The design process was conducted for the upgrades to the current system. Refer to Table 4 for more information on scheduling.

5.10 Manufacturing Schedule

5.10.1 Manufactured Components

The team will need to have the larger side walls machined. The 3D printed deposition belt drive gear is already printed and will be implemented onto the final robot. The conveyor wheel covers will not need to be manufactured and can be implemented onto the final robot once the side walls have been machined. The ANSI/ASME Y14.5 Drawings can be found in the appendix.

5.10.2 Manufacturing plan

The Moonrockers will be procuring aluminum from Pacific Steel in Rapid City. The team will get together with Dr. Ryan Koontz and go over the drawings and tollerances required for these components. The parts will then be machined in the South Dakota School of Mines & Technology's machine shop.

6 Electrical Subsystem

6.1 Design Constraints

The electrical box on the Moonrocker's robot must contain all critical electrical components such as computers, motor controllers, and power distribution circuitry. The box must isolate the electrical components from the environment and sufficiently dispel heat. Preventing dust from entering the electrical box is also a critical constraint on this system. A red emergency stop switch must also be incorporated in the electrical design.

6.2 Design Considerations

The 2016-17 Moonrockers robot had an E-box mounted to the collection system. This E-box contained all computers, motor controllers, and the power distribution for the bot. With the new NASA Robotic mining challenge to obtain icy regolith, the E-box needed to be independently mounted to the frame from the collection system to allow the collection system to collect icy regolith.

In addition to the mechanical considerations of the Electrical box, there are several electrical considerations. Due to electrostatic dust and the large transient currents used to drive the brushless motors, the operating environment for the electrical components of the robot presents significant EMI risks including computer and/or communication subsystem failure. We were able to use a simple hoop antenna with an oscilloscope probe to measure voltage spikes of up to 70 mV within the '16-'17 E-box when the motors were running under no load. We also observed that loading the wheels of the robot can cause current consumption to increase by a factor of six. It can be assumed this would also cause the voltage spikes to increase multiplicatively, since the voltage across an inductor is proportional to the inductor's instantaneous change in current and magnetic flux. The input voltage to the motor

coils provided by the SBL1360 motor drivers is trapezoidal with a very short rise time. This is likely the source of the voltage spikes since it represents a high instantaneous change in current.

The wiring of the robot represents an area for considerable improvement as well. The current system utilizes a series of industrial wiring fixtures, hand-crimped wiring terminals, screw terminals, and wax string wire lacing. These methods present reliability and weight efficiency concerns. It is imperative that the standard for wiring neatness and accessibility is maintained, as it has been noted that the competition judges admire these features. In order to have a more easily modifiable electrical system, modularity should be incorporated into our subsystems. This involves adding connectors on our wiring harness that can be disconnected in order to remove an individual subsystem from the robot.

6.3 Preliminary Design

While the electrical box being mounted on the front of the robot allows easy access to electrical components and a highly aesthetic design, its current mounting location causes several unnecessary complications. First, the box is attached to the collection system. This causes clearance issues with the collection material both in front of the robot, and between the back of the E-box and large rocks carried by the scoop ladder. The clearance issues could be alleviated by mounting the electrical box to the forward frame instead of the actuated ladder, but since the collection system modifications will provide it with an additional, rotational degree of freedom, this could cause wear on the electrical connections on the outside of the box, leading to intermittent connection losses (an issue which already plagues the current design).

Due to the articulated chassis, and large closely-mounted wheels, the sides of the robot are also unfavorable mounting locations. This leaves the rear of the robot as the best choice for the electrical boxes. Mounting the high voltage electrical box directly above the batteries, and within proximity to 3 of the 6 brushless motors also provides a reduction in conductor cable length. This will increase electrical efficiency and wiring simplicity. To better insulate sensitive mission-critical computer and communication hardware from Electromagnetic noise, it was decided to split the electrical box into a high voltage and low voltage enclosure. The high voltage enclosure will contain the motor control boards, 12V power regulators and a power distribution board that will incorporate fuses, regeneration diodes, a pre-charge resistor, transient voltage suppression diodes, reverse-polarity protection and solid-state power toggling via high current MOSFETS into a small form factor package that is predicted to reduce the current space requirements of wiring and fuses by 60% while adding circuit protection in the process. The low voltage electrical box will be connected to the high voltage box through only 4 wires. These include the 12V power and ground, and CAN bus communication lines from the main computer to the motor controllers. This box will contain the robot's main computer and sensor hardware. The low voltage box will be mounted to the side of the deposition system for greater accessibility, but thanks to the nature of the CAN communication protocol, we can safely mount this box almost anywhere on the robot in relation to the high voltage box.

6.4 Design Schedule

The CAD models of both electrical boxes should be completed before the critical design review presentation. This includes the first schematics and PCB layout of the Power distribution board, along with a list of electrical component part numbers, and any relevant SPICE simulations.

6.5 Detailed/Complete Design

The high voltage box, low voltage box, and power distribution board were further designed to meet the requirements while allowing for improvements from the current electrical box.

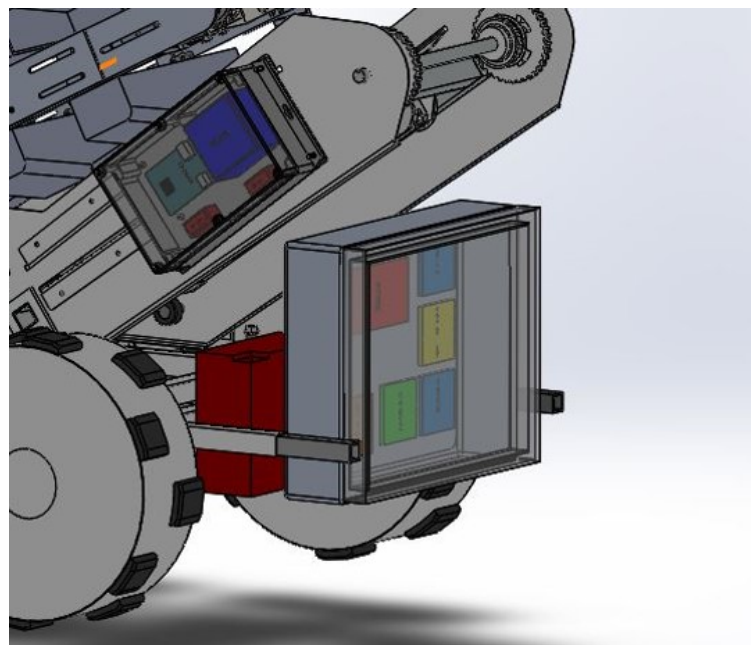


Figure 18: View of Both Electrical Boxes and Locations

The low voltage box that will be housing the computers and sensor hardware will be bought from McMaster-Carr. It will be mounted onto the side of the deposition system. This area could experience a significant amount of dust and further testing will be required to determine if standoffs are necessary to eliminate any chances of dust accumulation. The IP65 rating will need to be maintained as connections to the high voltage box are required. The enclosure is made out of polycarbonate plastic which helps with the weight concern as the alternatives would be to buy or manufacture an aluminum box. This option also saves valuable time that would be spent manufacturing. See Figure 19.

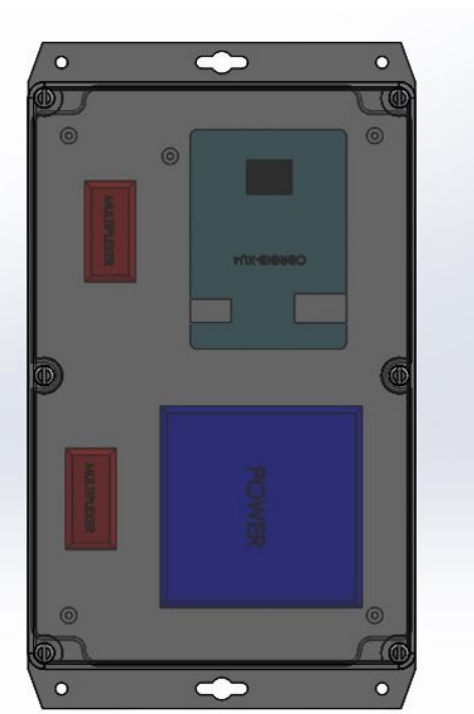


Figure 19: Low Voltage Electrical Box

The high voltage box will house the motor controllers as well as the power distribution board. This high voltage box will be manufactured out of 1/8 inch aluminum sheet and mounted vertically to the chassis behind the deposition system. This will provide ideal accessibility to our electrical components but will in turn sacrifice some accessibility to the batteries. To provide full accessibility to the batteries, the box will be made removable by implementing slide tracks on the chassis. There will be connections from this box to every motor including the wheels, deposition system, and collection system. There will also be connections to and from the low voltage box as well as an emergency stop switch. Connectors will be implemented so that the box can be removed from the robot if necessary. The only time this box is expected to move is when the batteries have to be removed.

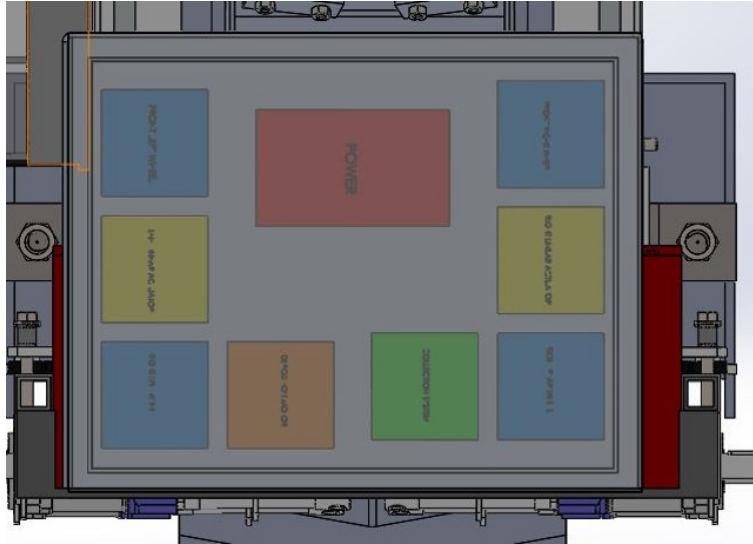


Figure 20: High Voltage Electrical Box

The organization of the high voltage enclosure is as follows:

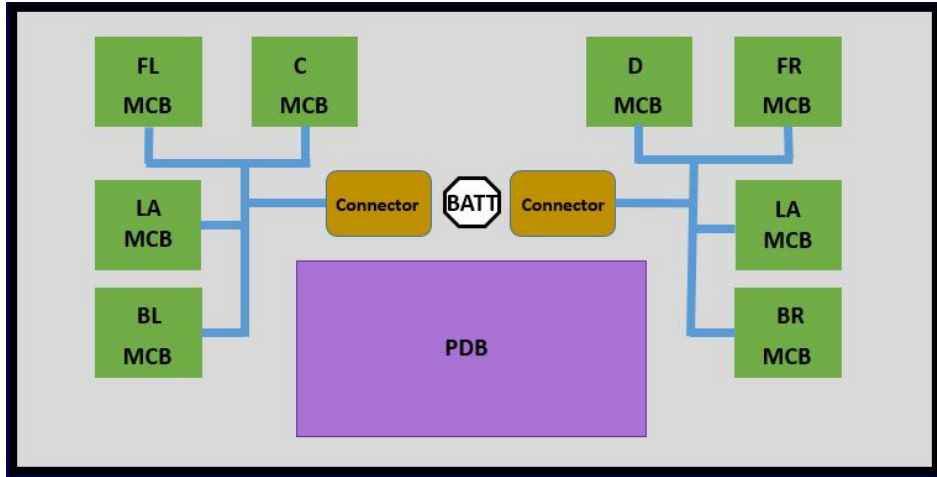


Figure 21: High Voltage Enclosure Layout

The motor controllers were positioned to minimize the heat buildup in any one specific area of the high voltage box. The motor controllers for the four wheel's motors were positioned in the four corners of the box (denoted FL = front left, FR, BL, BR = back right) in order to isolate the controllers most likely to produce heat during competition. Since all wheel motors will be most likely running at the same time, grouping them together will not allow for heat to be dissipated as evenly. The two linear actuator (LA) motor controllers were also placed as far apart as possible, as they would also be running simultaneously to control the collection system. The collection and deposition system motors would likely not be running

together, and are placed as “C” and “D”. Internal wires in the HV box will utilize empty channels between components and run neatly to and from their destinations. Wires run externally from the motor controllers are shown with the blue lines in the diagram. Two IPv65 49 pin mil spec connector will be used on each side of the battery connector on the back of the box. This reduces the amount of connections to the outside which reduces failure points and improves reliability. The ’16-’17 electrical box has an external connector for each motor controller. Figure 22 shows the portion that will be fixed to the HV box using a lock nut. Figure 23 shows the removable connector.

To add to the modularity of our robot, we will add a 19 pin mil spec connector to our collection and deposition system. The connector is shown in Figure 24.

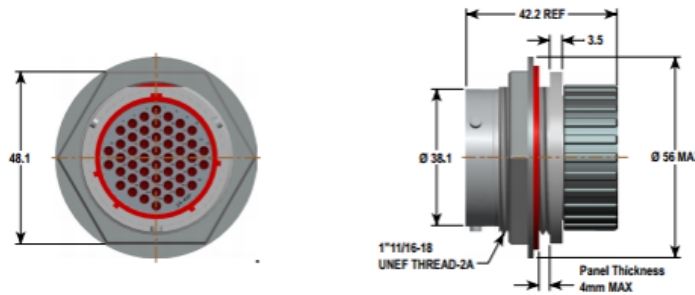


Figure 22: HV Box Internal Connector

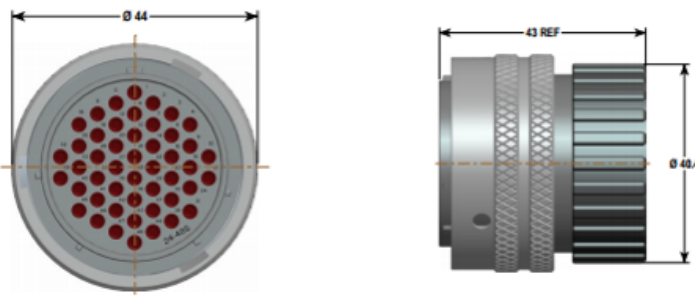


Figure 23: HV Box External Connector

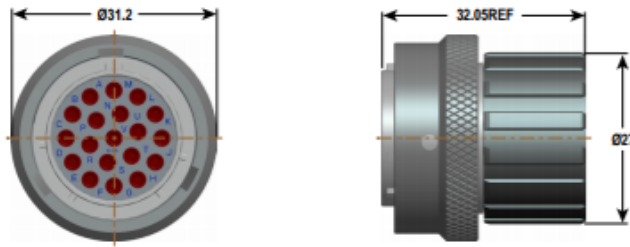


Figure 24: Modularity Connector

To allow for efficient board designs and high current capabilities, two separate boards were designed. A schematic of the power distribution circuit is shown in Figure 25. The required trace widths for a high current were achievable with this design change. The power distribution boards introduce protection circuitry into our system while reducing the amount of space used. The boards incorporate all the features mentioned in the preliminary design section and distributes power to the motor controllers and computers. COTS Meters will be used to individually monitor our 24V and 12V circuits.

Eagle PCB software was used to create a library of parts, schematic, and boards in order to be manufactured. Figures 26 & 27 show the library of parts and boards. The board on the left provides the input power from the batteries, input protection, and ground terminals, while the board on the right provides the power protection for the motor controllers and computers and then outputs the power. Our maximum system current draw is estimated at 30 A, and a reasonable maximum trace width was decided to be 8.5mm to account for the current consumption.

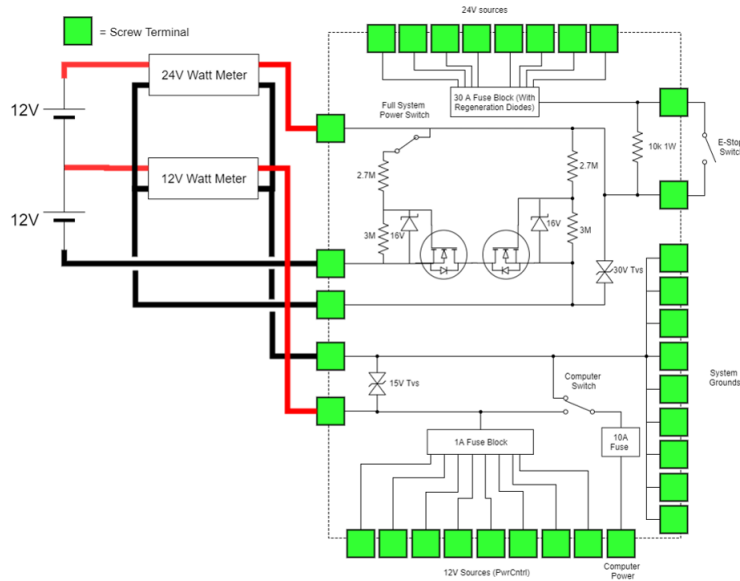


Figure 25: PDB Schematic



Figure 26: Eagle Library of Components

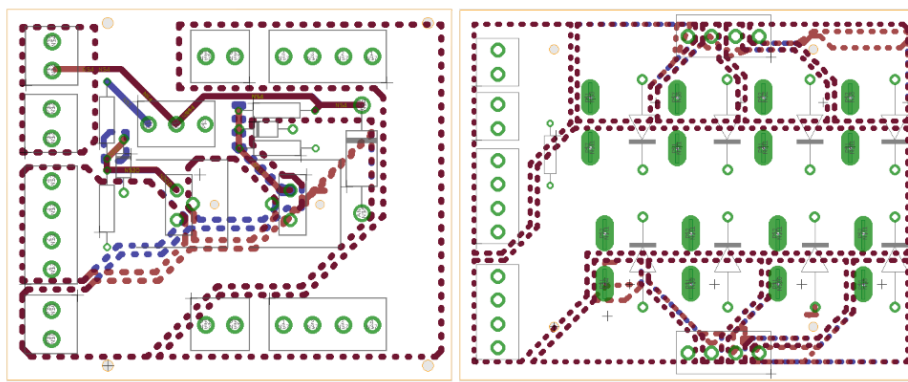


Figure 27: Eagle Board Designs

6.6 Manufacturing Plan

Manufacturing of the boxes will begin after CDR is complete. To minimize the time in which the robot is not operational, we will manufacture both electrical boxes before installing them. After finishing touches are made on the boards, manufacturer files and data will need to be compiled, and finally the board will be milled at SDSM&T for prototyping. A manufacturer such as Advanced Circuits or OSH Park will be used for the final boards. These boards will have a silkscreen to prevent fatal shorting on bare copper. The boards should be in the hands of the team within a few days of the creation of the new boxes so that the new hardware can be installed and testing can begin. The transition from the old boxes and electrical system to the new boxes and new electrical system should take no more than a week.

6.7 Data Verification

A solidworks thermal analysis was done on the '16-'17 and proposed high voltage electrical boxes with the assumptions of max load, 90 degree Fahrenheit ambient temperature, and a convection coefficient of 100. The motor controllers reach a failure point at 85 degrees celsius; the highest temperature recorded for the '16-'17 electrical box was 125 degrees celsius (Figure 28), and 68 degrees celsius for the new proposed box (Figure 29). It should be noted that these analyses were done with open boxes.

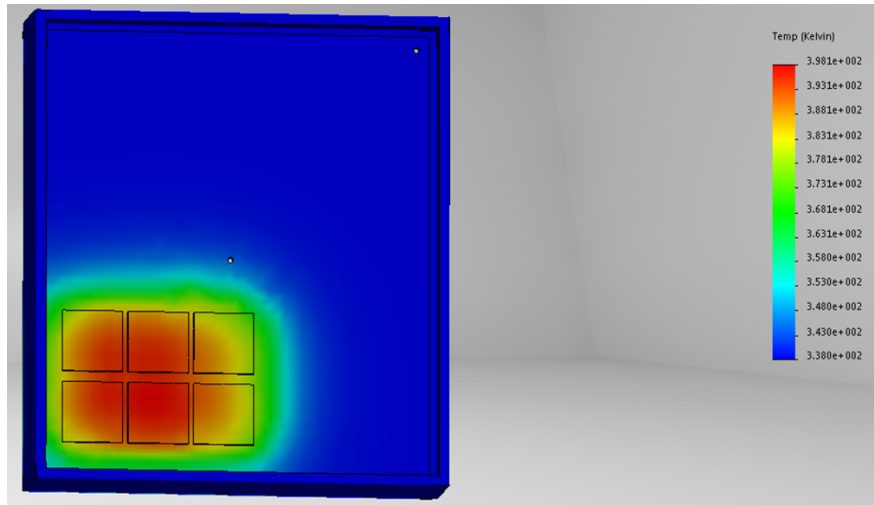


Figure 28: Thermal Simulation on Old Box

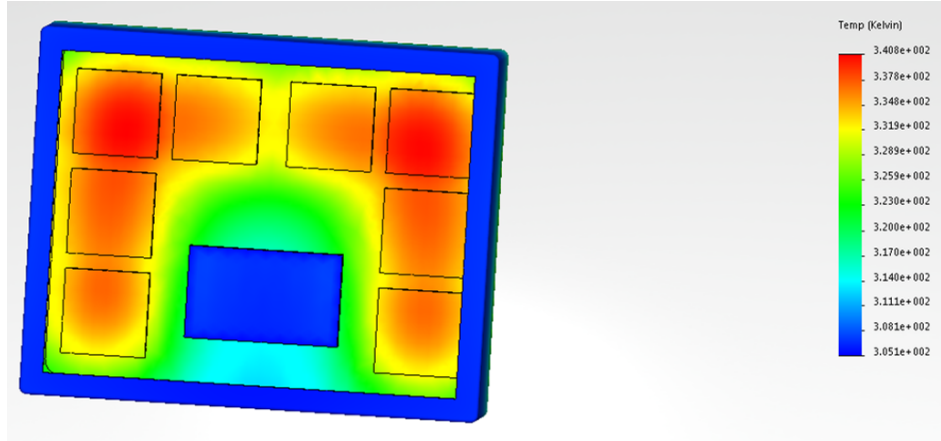


Figure 29: Thermal Simulation on New Box

Using a reputable PCB manufacturer's trace width calculator, we found that a 10mm trace width allows for 28.5 A at 2 oz/ft² copper thickness, 38.2 A at 3 oz/ft² copper thickness, 47.2 A at 4oz/ft² copper thickness, 55.5 A at 5oz/ft² copper thickness, and 63.3 A at 6oz/ft² copper thickness. These options correlate to factors of safety of 0.95 for 2oz, 1.27 for 3oz, 1.57 for 4oz, 1.85 for 5oz, and 2.11 for 6oz. Our choice of copper thickness will vary based on SDSM&T mill capabilities and manufacturer options, benefits, and time frames. The trace widths used for the two boards were 8.5mm and 2mm. The 2mm trace widths allow for approximately 9 A at 2oz/ft² copper thickness, fulfilling requirements; any heavier copper weight will greatly increase the factor of safety for the smaller trace widths.

The reverse polarity protection circuit was implemented on a breadboard to confirm its functionality (Figure 30). This circuit consists of two voltage dividers that, when properly connected, will provide the gate to source voltage necessary to open the gates of both MOSFETS and allow free flowing current throughout the system. When improperly connected, current will be stopped at the drain of the second MOSFET as the gate will remain closed because there will be no gate to source voltage. 16 V zener diodes are implemented to protect the MOSFET against voltage spikes. The power distribution board will also include a 30 V Transient Voltage Suppression diode. This component is implemented for extra protection as this will limit the voltage across the voltage divider to 30 V.

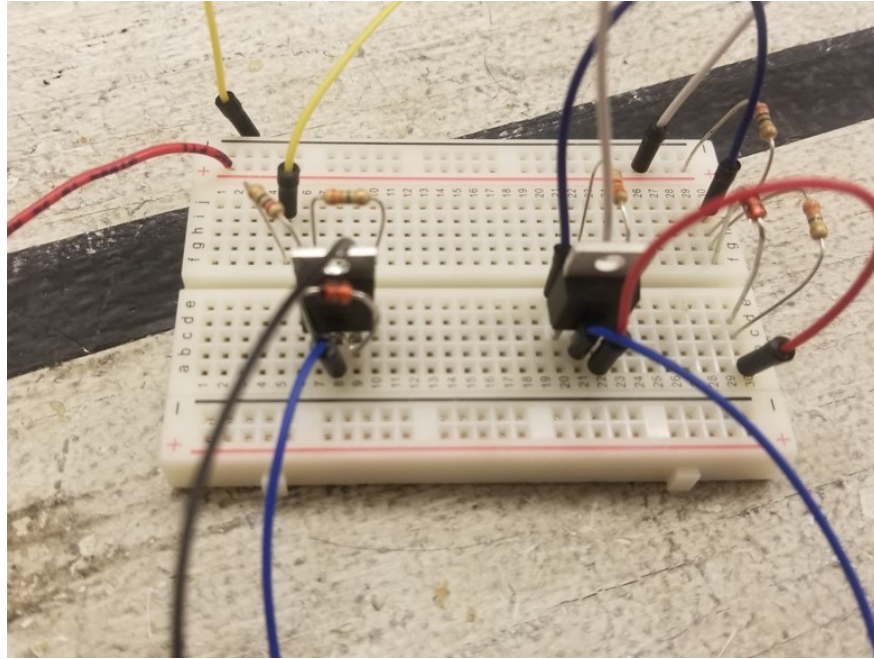


Figure 30: PDB Tested on Breadboard

The reverse polarity protection circuit works as it will draw current when properly connected and will not draw current when improperly connected. The only thing to note with this is that the first MOSFET got significantly warmer than any other component. Heat sinks will be implemented on the board to mitigate this issue.

The power distribution board's main function of reverse polarity protection was simulated in ADS and verified. With the switch connected to power, and an input voltage of about 28 V, the current of a one ohm load was about 20 mA. With the switch connected to ground, and the same input voltage, the current was on the order of uA. See Figures 31, 32, 33, 34, 35, and 36 below.

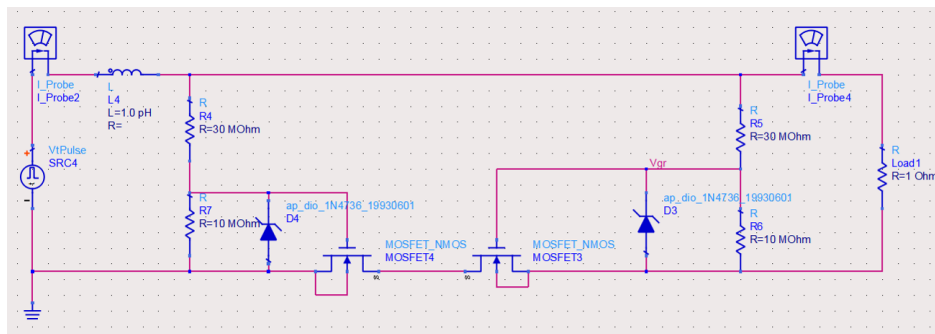


Figure 31: ADS - Switch Connected to Power

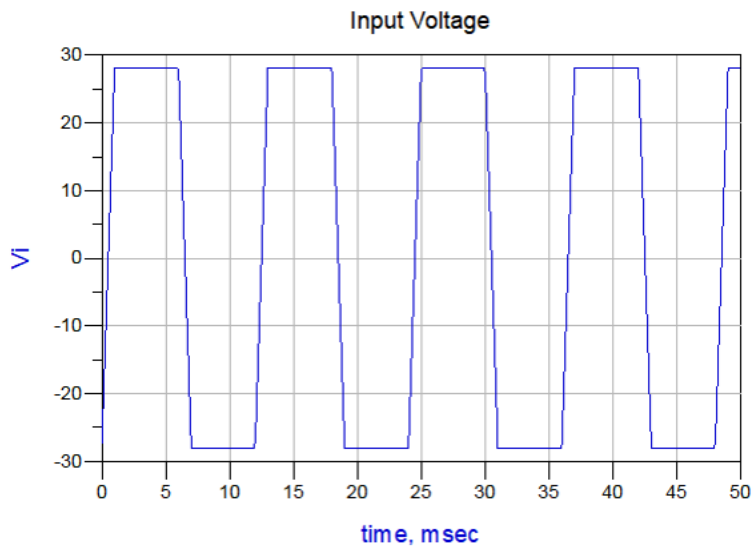


Figure 32: ADS - Forward Bias Voltage Input

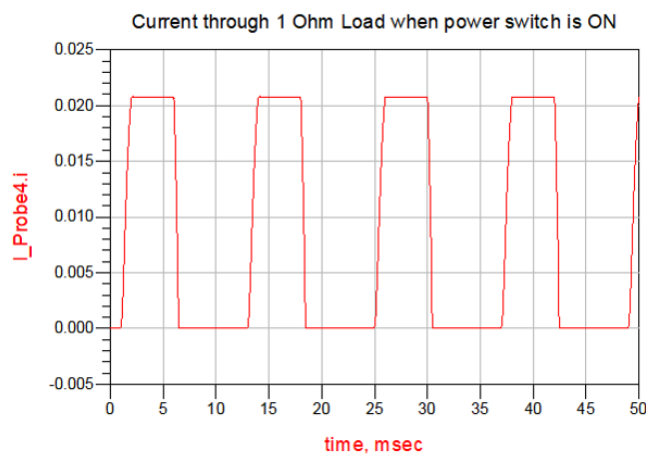


Figure 33: ADS - Forward Bias Current Draw

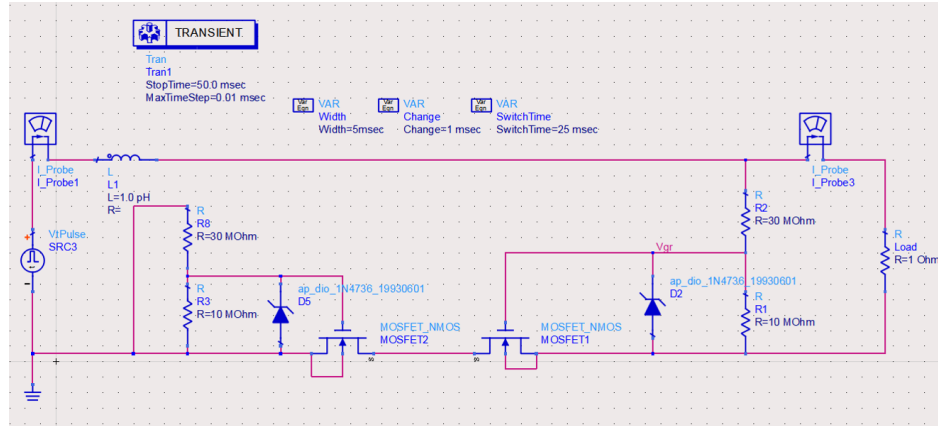


Figure 34: ADS - Switch Connected to Ground

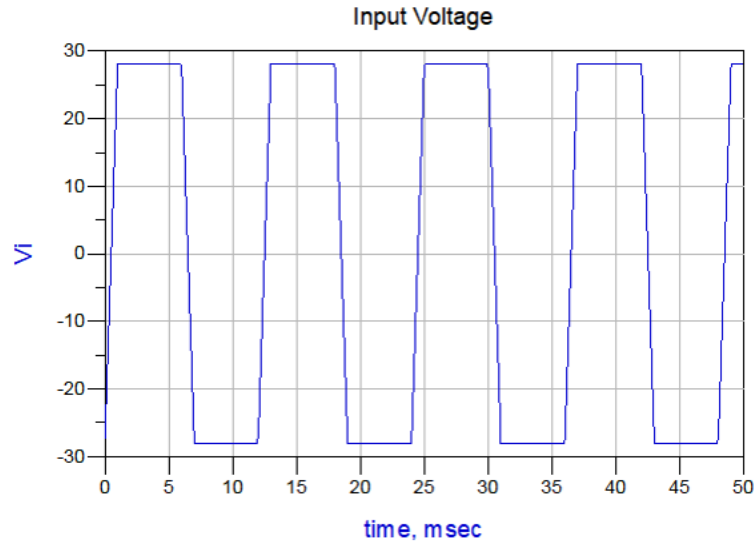


Figure 35: ADS - Reverse Bias Voltage Input

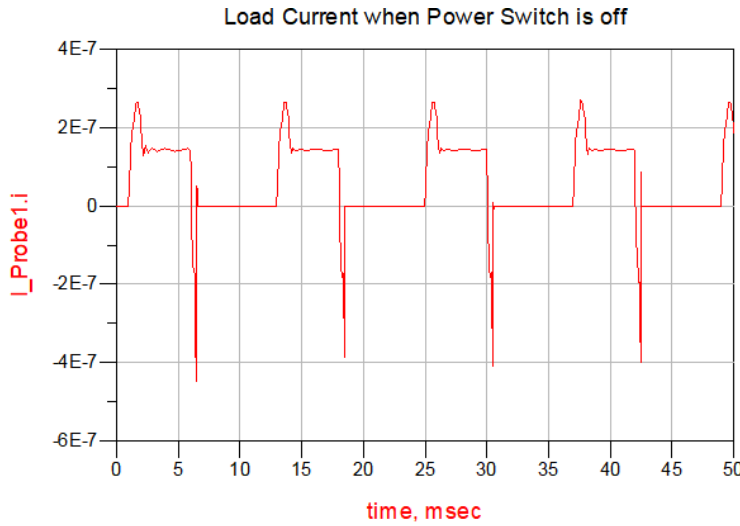


Figure 36: ADS - Reverse Bias Current Draw

6.8 Design Realization

As the new systems began to be built and new designs were implemented, flaws were discovered and improvisations were necessary. In order to create a wiring harness for the entire system and implement it efficiently, a bird's-eye-view plan was necessary. If something was forgotten or the order of crimps, solder, heat shrink, connectors, and routing the wires was not followed, time and material would be lost. As different subsystems were being reconstructed, teams needed to work together because sometimes one job could not be completed without the other. Throughout the entire rebuild process, time was taken to make strong and reliable connections, crimps, and solder joints, and care was taken to maintain appearance of neat wire management.

The power distribution boards were changed several times as impracticalities were found in the design. For example, it was found that copper material with a thickness of >3 oz/ ft^2 was hard to find and is expensive to mill through a fabricator. A free sample of Rogers RT/Duroid 6002 with 20 mils (approx. 8 oz/ ft^2) of copper on one side was given to the team and would have been able to handle the robot's high current requirements, however, the laminate was too thin (0.25 mm) and allowed the material to bend enough to prevent effective milling. Prototypes were milled with Rogers 4003C 1 oz/ ft^2 because it was readily available material. In the end, it was decided to order both boards through OSH Park with their max capability of 2 oz/ ft^2 copper. These boards would be double layer, with the bottom layer duplicating the top layer and creating 4 oz/ ft^2 material. Trace widths were essentially made much wider as empty spaces on the boards were filled with more copper. This added a lot more surface area for the current to flow and dissipate heat. As time became a problem, 1 oz/ ft^2 "super swift service" was selected from OSH Park to guarantee the boards were received before leaving for competition. Since they have two layers, this creates 2 oz/ ft^2 boards, which was justified since copper now filled the empty spaces and increased copper

surface area.

6.9 Product Performance

The current state of the electrical system allows for manual control of all the subsystems and therefore functions as intended.

7 Autonomy Subsystem

Autonomous operation is a major source of points for the mining portion of the competition. Compared to the starting total of 1000 points, a fully autonomous, 10 minute run gives 500 bonus points, making it a very attractive goal for competitors. In the past, we have done relatively well in this category, taking 2nd place in the 2015-16 competition in the autonomy category with a partially autonomous run. We will be expanding our existing system with the goal of having a fully functional autonomous system for competition.

7.1 Design Constraints

Many of the constraints for the autonomy system deal with the types of sensors we are allowed to use. For example, we are not allowed to use any form of GPS sensing on the robot, as GPS positioning would not work on Mars. Magnetometers are also not allowed since Mars does not have a polar magnetic field. Sensors also must not utilize the competition walls for localization. Generally, all sensors must adhere to the spirit of the competition, in that their basic operating principles would be applicable to a Martian environment.

7.2 Design Considerations

Under autonomous operation, there are four main questions that the robot will have at any given time:

- Where am I?
- What is around me?
- What should I do next?
- How should I get there?

These questions will be answered by the Localization, Environment Mapping, Decision Making, and Path Planning subsystems, respectively. To successfully implement these subsystems, more sensing hardware and improved software algorithms are needed.

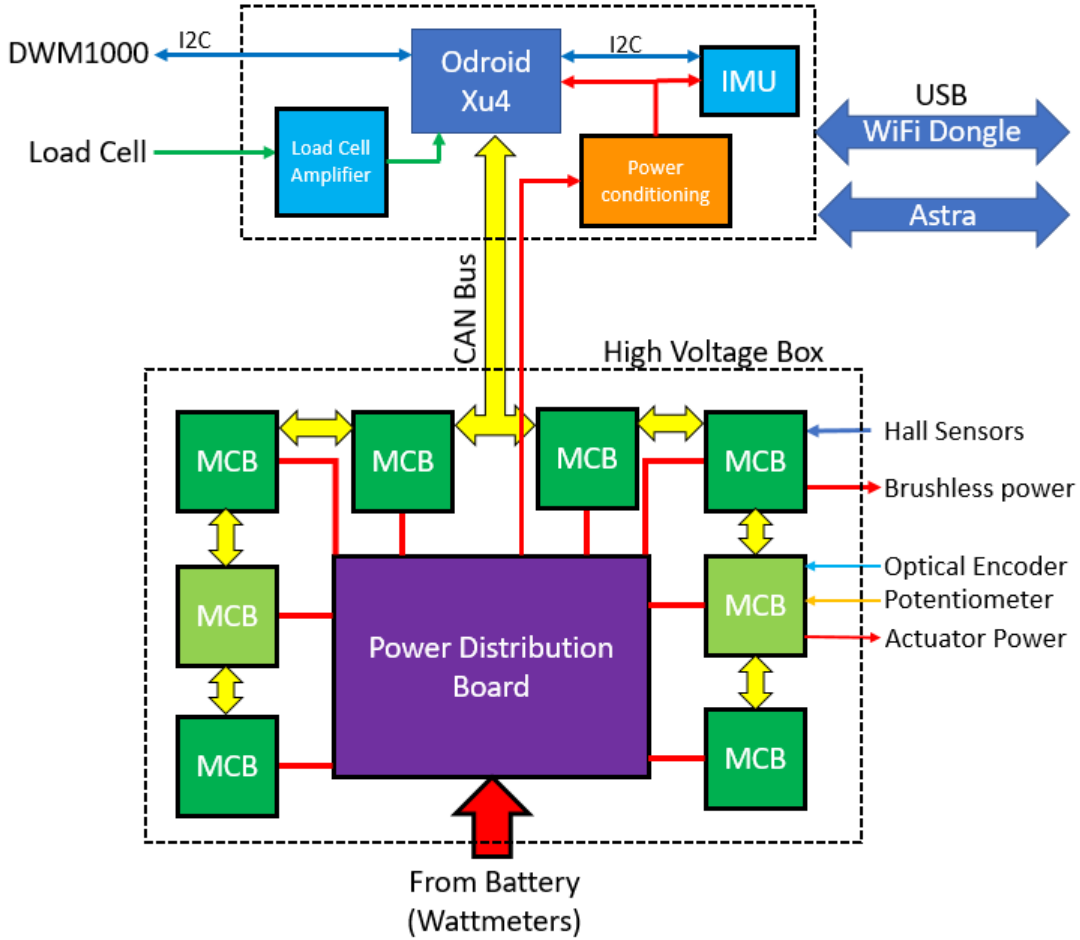


Figure 37: Overview of all sensors and interconnections

7.3 Preliminary Design

Sensor Overview The sensor subsystems can be divided into two categories. Localization, and Robot State Monitoring. Localizations sensors are primarily concerned with positioning the robot within the competition arena, whereas Robot state monitoring sensors are intended to give the main computer feedback on the position of actuators, power monitoring, collected material load sensing, and other various diagnostic information. A diagram of the individual sensors and their interconnectivity can be seen below, and each sensor will be described in detail in the following section.

Localization The Localization subsystem allows the robot to get an estimate of where it is currently located. This is done by using a variety of sensors to gather both absolute and relative position data. The sensors used for localization are listed below:

- Augmented Reality (AR) tag and camera (via Astra camera)
- Inertial Measurement Unit (IMU)
- DWM1000 Ultra-Wideband Antenna

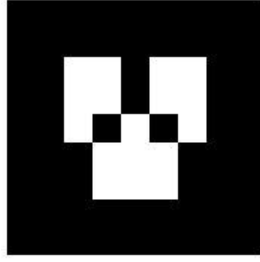


Figure 38: AR tag used in previous years

- Hall Effect sensors

The AR tag and camera are the only sensors that existed in the previous autonomy system. The AR tag is an image on paper placed in front of the hopper. A camera placed on the robot then uses computer vision software to locate the tag. Once the tag is located, the robot's distance from and angle relative to the AR tag can be calculated, giving the robot information about where it is. Some issues with this sensor in the past included "losing" the AR tag, thus leaving the robot with no idea where it is located, and detecting the AR tag where there is none (a "false positive"). These issues have been detrimental to the Localization subsystem in the past, but adding redundant sensors will keep the impact of these problems minimal.

The inertial measurement unit will provide periodic information about the current acceleration in the X, Y and Z directions, as well as the angular velocity about the X, Y and Z axes. This information is enough to extrapolate incremental translation and rotation state of the robot, as well as absolute roll and pitch orientation. Many IMUs incorporate the magnetometer for measurements of yaw orientation, but we ensure that our design does not use these sensors, as they are banned from the NASA RMC since Mars does not have a polar magnetic field. These raw measurements will be fed directly into a ROS Extended Kalman Filter (EKF) node. In order to use an Extended Kalman Filter, it is imperative that the sensors have a Gaussian, or near-Gaussian noise profile. In order to ensure that the IMU had a Gaussian noise profile, the distribution of the gyroscope and accelerometer readings were obtained by creating a histogram of the sensor readings at rest.

The vibrational characteristics of the IMU were measured by using a speaker and a signal generator to apply a waveform to the sensor and monitor its ability to reconstruct a signal. By incrementally increasing the frequency of the input signal, we determined that the accelerometer began to see aliasing in its signal reconstruction after approximately 100 Hz. This lead us to select 75 Hz as our cutoff frequency for our mechanical damping system. Using anti-vibration grommets, and by adjusting the mass to which our IMU will be attached by affixing steel washers to the piece to which the IOMU is attached, we can create a tuned spring-mass damping system.

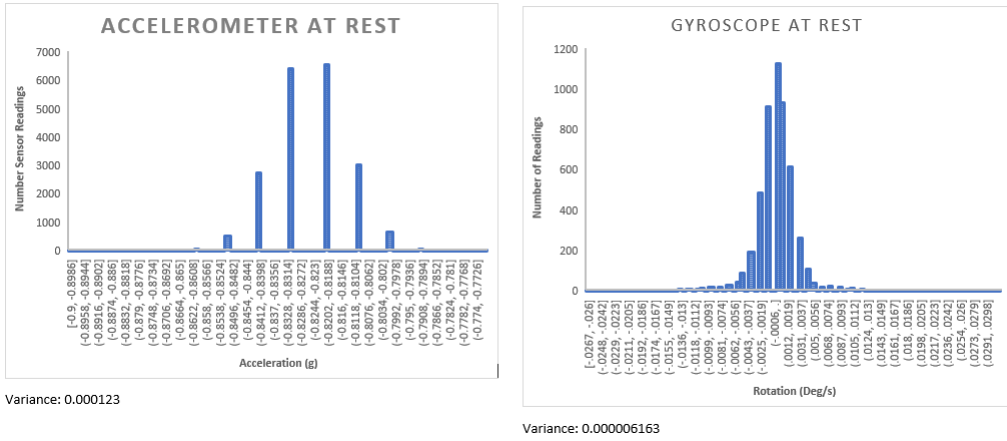


Figure 39: 10,000 Accelerometer and Gyroscope readings at rest

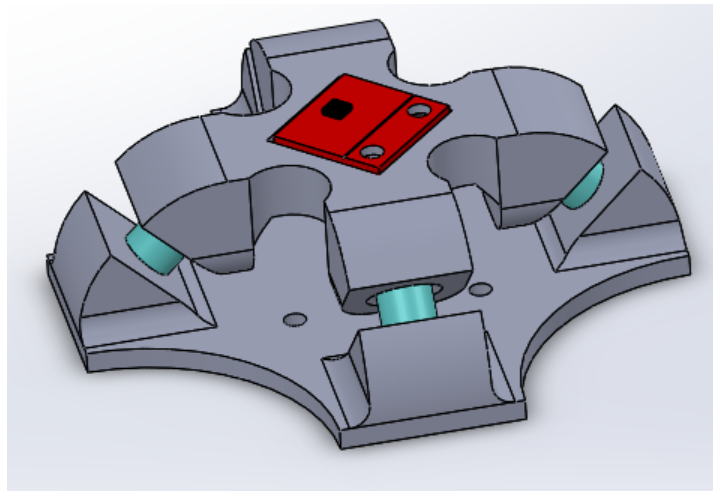


Figure 40: IMU Vibration damping mount (steel washers affixed below)

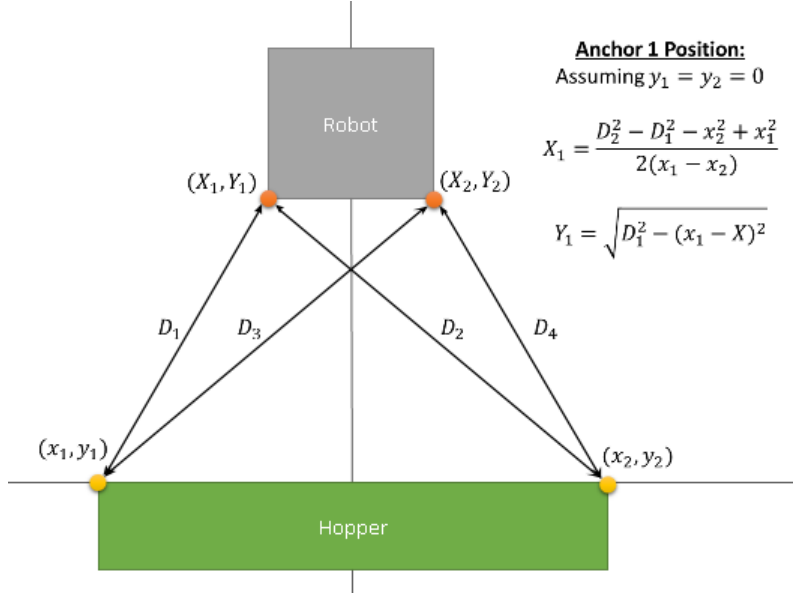


Figure 41: DWM1000 configuration

The DWM100 ultra-wideband antenna will function as an omnidirectional, vibration insensitive absolute location detection system. The antennas operate on a frequency above WiFi, below the maximum dB limit for non-control radio frequencies set by NASA. The Ultra-wideband system operates by sensing the distance between antennas designated as "Tags", and antennas designated as "Anchors". Using multiple anchors, the system can use distance measurements from a single tag to triangulate that Tag's position . These anchors cannot be located co-linearly, since this would not contribute to the accuracy of the system's position estimate. It is for this reason that the anchors should be mounted to the robot to function as the system's fixed reference frame, while the tags should be mounted on the hopper with its own power supply and USB wattmeter. The configuration for absolute position sensing can be seen below.

The antennas mounted on the robot will be mounted on torsion spring-loaded mounts that will begin in a configuration that allows the robot to fit within the required competition volume. After the competition run begins, the antennas will be released via a solenoid and the antennas will be deployed above the robot. the antennas need adequate clearance above the robot to ensure that the measured ranges are representative of the shortest direct path between the anchors and tags, and are not corrupted by the length of any reflection paths. Since the robot's chassis is made primarily of aluminum, this means that it would be the primary source of any such reflection paths. The rule of thumb to mitigate these reflection paths is to ensure that the antennas are at least 10cm away from any reflective medium. This is because any single range measurement can be expected to be accurate to within 10cm, and the DWM1000's internal circuitry is capable of filtering out any reflection path longer than this distance. A diagram depicting this distance can be seen below.

Direct path: ————— L_D = Length of direct path
 Shortest reflection paths: ————— L_R = Length of shortest reflected path

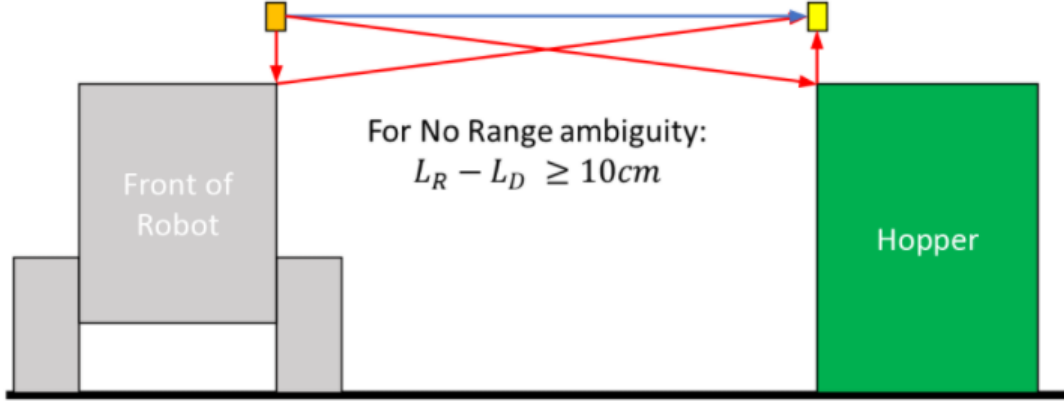


Figure 42: Possible Reflection Paths

Both antenna chassis will contain all the necessary electronics to read and filter the range measurements from the DWM100 modules. This includes an Arduino Pro Micro, a DWM1000 with a breakout board, and a 3.3v to 5v level shifter. The Arduino will receive asynchronous range measurements from the DWM1000 antennae, and use a moving 1-dimensional Kalman filter to estimate the current range state. This range state will be read by the main computer via I2C bus. The main computer will also assign a variable in the Arduino denoting the current velocity estimate using the DWM1000 position estimates and IMU accelerometer data. This velocity estimate will be used in order to factor in the variance of the positional data received by the ranging antennae. A block diagram of the antenna electronics, as well as the noise profile of the DWM range antenna is provided with this document. In the noise profile, a large spike can be seen within the Gaussian distribution. This spike can be attributed to reflection paths interfering with range measurements. These will be mitigated in the final design thanks to the aforementioned deployable antennas.

The SBL1360 brushless motor controller requires a hall effect sensor to operate the brushless motors. This position feedback is stored in a 32-bit register inside the Controller, and can be read via CAN bus commands by the main computer. This Encoder information can be used to improve the robot's state estimation using wheel odometry.

The readings from each of these sensors is then used as input into an EKF, which compiles the information into a single robot state that can then be used by other subsystems. Due to time constraints, we have utilized the EKF implementation provided by the `robot_localization` library in the Robot Operating System (ROS) framework for our system.

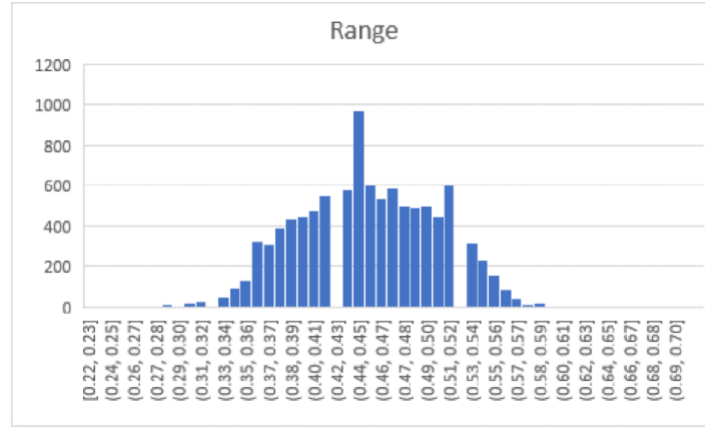


Figure 43: Noise distribution of ranging antennae

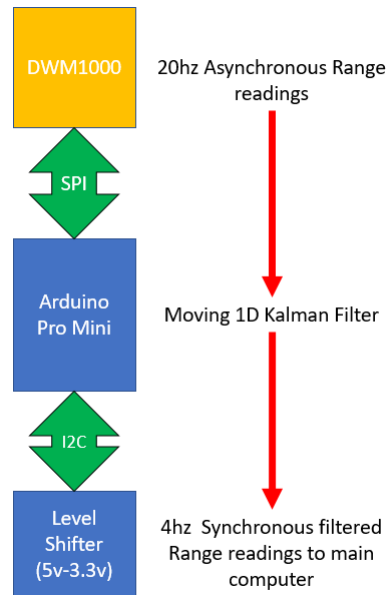


Figure 44: Internal electronics of antennas

Robot State Monitoring Additional sensors will be incorporated into the robot’s design in order to factor various state information into the decision making process of the Autonomy. The primary sensors that constitute this category of sensors include the following:

- Linear Actuator optical encoders
- Rotational Actuator potentiometer
- Load Cell

The main mining actuators used to extend the collection system into the ground contain optical encoders which can be used by the SDC2160 brushed motor controllers to gain incremental information about their position. The encoders can be ”zeroed” by running the actuators in one direction until their stop switch is triggered, and zero current flows through the actuator. The rotational positioning actuators will have their absolute position read via a potentiometer mounted coaxially with the slide axle.

The load cell voltage will be read by the main computer’s ADCs after being amplified by a dedicated load cell amplification integrated circuit. The load cells will provide the main computers with a means to monitor the amount of collected material. By monitoring the rate of change in measured weight, along with the rate of rotation of the collection system, the main computer can also estimate the composition of collected material.

Mapping The Environment Mapping subsystem will require a sensor or sensor suite to detect the landscape around the robot and large obstacles in its vicinity. Due to availability and budget concerns, the Orbbee Astra 3D camera was chosen for the sensing hardware to accomplish this task. The team already had the Astra, so cost and procurement were of no importance. Objects behind the robot will not affect its trajectory or decisions. An elevation heatmap will be generated from the data gathered by the Astra. The Astra data will be mapped as a delta from the modal height of the first dataset from the Astra. Large objects will be saved for use by the Decision Making subsystem.

Decision Making The Decision Making subsystem is the “brain” of our robot. The subsystem consists of a traditional state machine that determines what the next target of the robot should be. At a high level, the state machine consists of five main states: Startup, Traversal Out, Mining, Traversal In, and Deposition (shown in Figure 8). The Startup state is where the robot begins its operation. It attempts to determine where it is located in the arena and determines a target mining location in this state. It then moves to Traversal Out, where it traverses the arena to the mining area, avoiding obstacles along the way. The robot then enters the Mining state, where it mines for icy regolith until the robot is full. It then enters the Traversal In state, where it returns to the hopper to deposit the gathered icy regolith. Lastly, the robot enters the Deposition state, where it aligns itself with the hopper and deposits its payload. After Deposition, the robot loops back to the Traversal Out state and begins the process again.

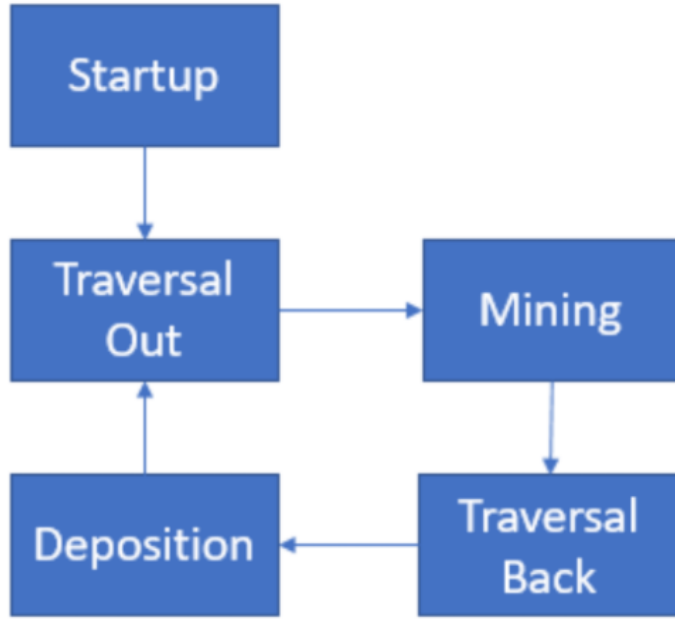


Figure 45: Simple State Diagram

Path Planning The last subsystem, Path Planning, will also be a purely software solution. Several graph traversal algorithms were evaluated as a solution: potential functions, Dijkstra's algorithm, A*¹, D* Lite [3], and a fuzzy logic algorithm proposed by Dr. Tim McJunkin². The D* Lite algorithm was chosen because of its optimized performance and acceptable global path efficiency. The Path Planning subsystem will submit its calculated path to a hardware control library to direct the robot along the selected path. A portion of Dr. McJunkin's algorithm will be used to display the local environment to the operator when the robot has reverted to manual control.

Summary Testing that all these solutions work, individually and as a whole, using conventional methods on the robot hardware would push development verification and validation to an unacceptably late date. A simulation environment will be created to approximate the hardware and environmental conditions so the team can ensure the quality of the solutions. This will facilitate verifying the solution with sufficient time to fix bugs and other issues.

7.4 Critical Design

The critical design phase included developing algorithm and equation specifications for all software subsystems. The final designs are detailed below.

¹These algorithms can be found in **Introduction To Algorithms** 3rd edition by Cormen, Leiserson, Rivest, and Stein

²The paper describing this algorithm can be found at the url <http://idm-lab.org/bib/abstracts/papers/aaai02b.pdf>

State Machine The state machine controls the decisions the robot makes. The final design for the 2017-2018 robot software involve startup, navigation, mining, and deposition as major states. Each major state has a sub-state flow associated with it. These major and sub state flows are detailed in Appendix E.

The startup state first powers up all of the sensors and components to begin finding the current location of the automated mining vehicle. Once localization has given an estimated location of the vehicle, the state is given the first mining location that has been predefined in mapping. After this occurs, the state machine moves from the startup state to the traversal state.

In the traversal state, localization is used to find the current location of the automated mining vehicle. Path-planning is then used to find a path that was given from the previous state before entering the traversal state. Once the path to target is given, calculated motor controls will be given from the path. The calculated motor controls are then issued to the motors to allow movement to the first point on the path. After movement occurs from the old point to the new point on the path, a check occurs to see if the robot has arrived at its destination. If the destination point is the same as the current location, another check occurs to see if the target/current location is a mining location. If it is a mining location, the state machine will move to the mining of BP1. If it is not a mining location, it will enter the deposition state. If the target location is not the current location, movement of the robot will continue until the robot has arrived at target location.

The mining state prioritizes the removal of the Regolith top layer to maximize Icy Regolith collection in future states. While there could be Icy Regolith in the twelve inches of Regolith, the state machine focuses on maximizing the mining of Icy Regolith below the Regolith. This state diagram begins with checking if the current location is a mining location. If this is not true, the state will move into the traversal state using the target mining location as a destination. If the current location is a correct mining location, the collection system will follow the mining routine that will be determined later. Mining will continue until the load cells give information that the deposition belt is filled with material or the collection system has reached the best depth for the removal of Icy Regolith. Once one of these events occurs, the state machine will enter the dumping state.

When the state is changed to dumping, the robot checks with localization to save this location as a variable that will be used later for future checks if needed in the design. From mapping, the robot will find the nearest dumping location for the removal of Regolith from the filled deposition belt. Once this location is found, the estimated distance is found to find the necessary motor controls to reverse back into the dumping location. After motor controls are issued, a check occurs to see if the current location is the dumping location. Reversal continues until the arrival of the robot at the dumping location or the current location is equal to the target location. After the robot reaches the correct location for dumping, the sub-state is changed to follow dumping routine. This allows the removal of Regolith from the deposition belt. After the deposition belt is cleared of material a check occurs to find what mining location was mined previously. This is to allow two mining locations, which are close

to one another, to have all of the Regolith material removed. If this check does not equal the correct location to mine Icy Regolith then the next mining location is given and the robot moves to the traversal state. If this check succeeds the state moves to mining of Icy Regolith.

The mining Icy Regolith state is entered because two close mining locations have been freed of Regolith material. The start of this state is given the previous mining location; this then leads to getting the current location of the robot. From this information a path is given to calculate the necessary motor controls to move to the target destination. A check occurs to see if the target location is equal to the current location. If this is not true, the robot gives the current location to find a new path to the target and to transmit the proper motors controls. This continues until the robots current location is equal to the target location. Once the robot has arrived at the mining location, the mining routine to mine Icy Regolith is followed. This continues until the load cells have stated the deposition belt has reached max weight, or the max depth of the actuators has occurred. Once one of these checks have reached true, the state gets the hopper location for a target to move to. This information is then sent to the traversal state.

The deposition state is entered from the previous state of traversal. A first check occurs to check if the current location is the hopper location. If this is not true, the state moves from deposition to traversal. If this check is true, path planning is followed to find the necessary motor controls to reverse into the hopper. The required motor controls are then sent to the motors to complete the necessary movement. A check then occurs to find if the current location is the correct location to begin deposition. If it is the correct location, the robot begins to follow the necessary steps in the deposition routine. If it is not the correct location, motor controls are issued to continue to reverse until the correct location is reached. After the deposition routine is followed, the next mining location is given to the next state, which will be to the traversal state.

System Architecture The 2017-2018 Moonrocker’s software is broken into several ROS nodes. A node is a single executable running in the ROS ecosystem that handles one function or one set of functions. The assignment of system tasks and each respective system network communication is laid out in Figure 46. This figure will be referred to as the Inter-Connectivity Diagram (ICD) throughout the rest of this document. Table 5 provides a legend for all messages³ and topics⁴ used in the system network.

Each colored rectangle in the ICD represents a single ROS node. Each arrow represents a ROS network connection. The origin (non-triangle) end of each arrow signifies a publisher of the message/topic, and the terminator (triangle) end of the arrow signifies a consumer (subscriber/client in ROS terminology) of the message/topic.

³A message is a data type defined in a .msg file from ROS base types and/or other message types that can be serialized across a ROS network.

⁴A topic is a named stream of messages that ROS nodes can publish messages to or receive messages from.

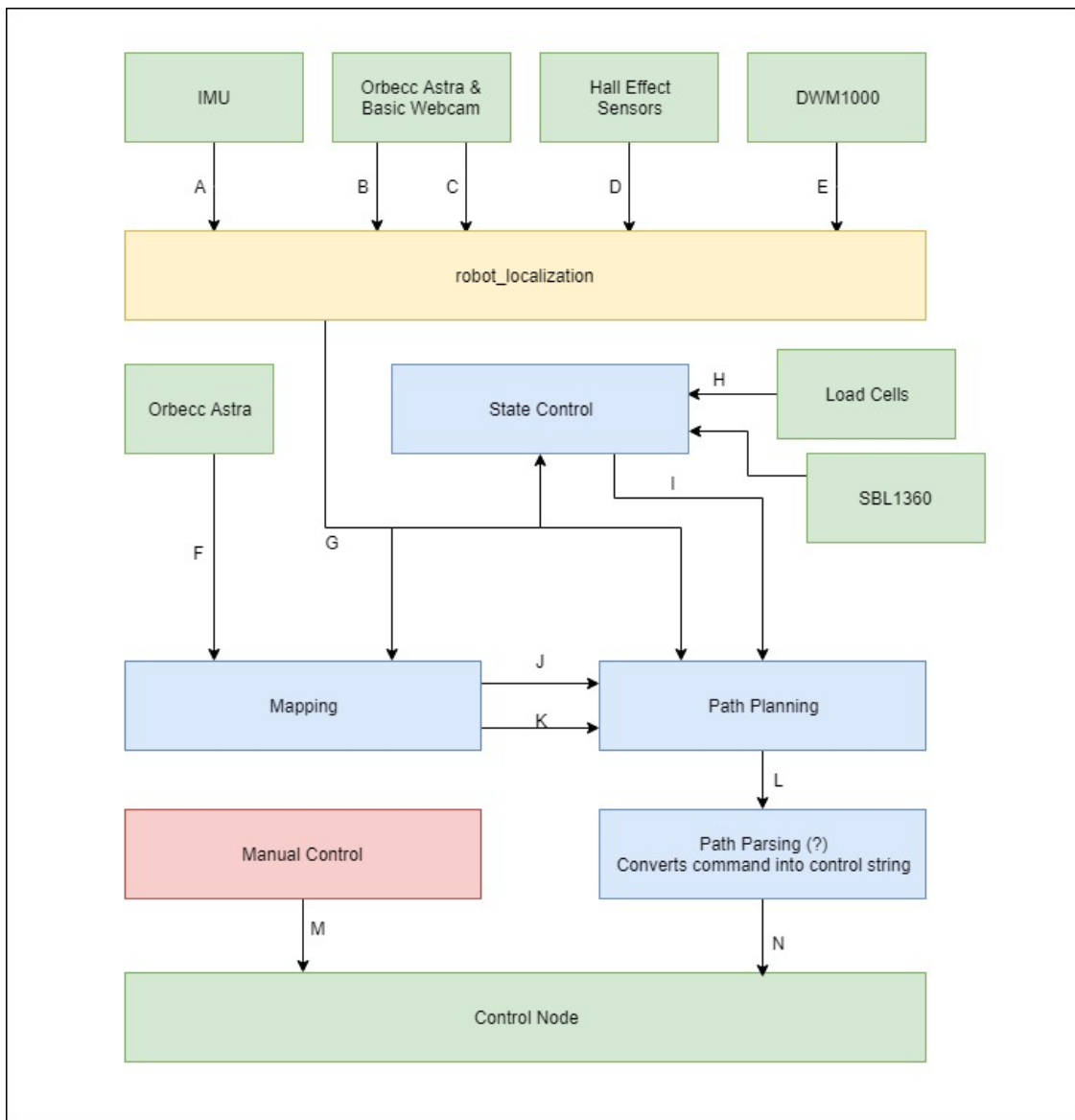


Figure 46: Inter-Connectivity Diagram

Table 5: Inter-Connectivity Diagram Legend

Label	ROS Topic	ROS Message Type
A	/imu	sensor_msgs/Imu
B	/visual_odom	nav_msgs/Odometry
C	/ar_tag	geometry_msgs/PoseWithCovarianceStamped
D	/wheel_odom	nav_msgs/Odometry
E	/uwb	geometry_msgs/PoseWithCovarianceStamped
F	/depth_sensing	sensor_msgs/PointCloud2
G	/odometry/filtered_map	nav_msgs/Odometry
H	/load_cells	/custom_msgs/Mass
I	/current_target	custom_msgs/TargetType
J	/map/local	custom_msgs/FuzzyMapType
K	/map/global	custom_msgs/GlobalMapType
L	/plan/path	custom_msgs/AStarPlan
M	/manual_control	custom_msgs/ControlString
N	/autonomy_control	custom_msgs/ControlString

7.5 Environment Mapping

The mapping component of autonomy answers the question “What is around me?” Like localization, mapping also involves a mix of hardware and software so a section will be provided for each

7.5.1 Hardware

The mapping hardware includes the sensors and controllers that will measure the terrain and obstacles surrounding the robot.

Preliminary Design Two sensors were proposed for mapping hardware: a 3D camera and a LIDAR. Since the robot will only drive in one direction, the team decided multiple terrain sensors would be unnecessary, so one had to be selected.

3D Camera A 3D camera provides a unidirectional picture containing color and depth information. The camera is limited to a given field of view (FOV) horizontally and vertically. A 3D camera typically measured depth with an infrared projector and camera combination. The disadvantages to using a 3D camera are that the picture is limited to a single direction and the camera lens can distort distance measurements.

LIDAR LIDAR provides a panoramic, continuous picture containing only depth information. Its FOV is only limited vertically. The LIDAR accomplishes this by spinning a depth camera in a circle quickly while continuously taking measurements.

The drawbacks to LIDAR are that the data stream is intense, the mounting location can introduce certain time periods where the data must be ignored, and the panoramic nature of the data lends itself to using the competition arena walls for navigation purposes.

Selection Evaluation The team chose the 3D camera for mapping based on its less intensive data stream and its lack of panoramic data. If the system would use the walls for navigation, the team would be disqualified from competition. The embedded hardware that the team had available would better handle the 3D camera data stream more adeptly than the LIDAR.

Detailed Design TBD

7.5.2 Software

The mapping software is the component that translates the measurements taken by the mapping hardware to a data structure that is useful for other software components.

Preliminary Design The mapping software had a simple decision for design of the mapping software. The system could either maintain and update a global absolute map or could create a fuzzy map based on current data.

The deciding factor was that the arena size is small relative to the precision constraints of the system. Global maps provide better tools for other software components than local maps. Their main drawback is the memory and processing required to maintain and update them. The 2017-2018 design will provide a global terrain map.

Detailed Design The detailed design for mapping involved analysis of the use-cases, storage data structure, data delivery, input data translation, and algorithm definition.

Use Cases The use cases for the map data are as follows.

- Calculating a path the robot should take under autonomous operation.
- Detecting objects and threats in the robot's vicinity
- Alerting the manual operator to terrain conditions.

Storage Data Structure The data structure used to locally store the mapping information was dictated by the use cases. The structure must be detailed enough to provide information for the most detailed use case. The object detection requires the most data since 3-dimensional objects must be detected. This lends itself to point cloud data storage.

Mapping is the process of translating the robot's sensor data to a format the rest of the robot can understand and use to navigate the environment. The map should store 3-dimensional data so that future systems could use the full data set for object detection. Preprogrammed libraries are available for interpreting and blending this point cloud data.

Algorithm Initialization When the package launches, the global point cloud is a null set. No data will be retained over a power-off event. This is because there is no way to guarantee that, at power-on, the robot will be in the same environment.

Algorithm Loop At a 1 Hz rate, the mapping component will retrieve a new data frame (point cloud) from the Orbbec Astra. The current global point cloud and the new cloud will be voxel filtered to smooth the data using the Point Cloud Library (PCL) VoxelGrid at 1-centimeter resolution. The new cloud will then be outlier filtered using the PCL StatisticalOutlierRemoval filter.

After filtration, the new cloud will be coarsely transformed into the global reference frame using the estimated robot pose coupled with the reference frame transforms generated by the tf2 library. Next, a fine transformation will be generated using a PCL IterativeClosestPoint-NonLinear registration object. The new cloud will then be transformed and merged with the global cloud using the calculated transformation. An example of this transformation can be seen in Figure 47.

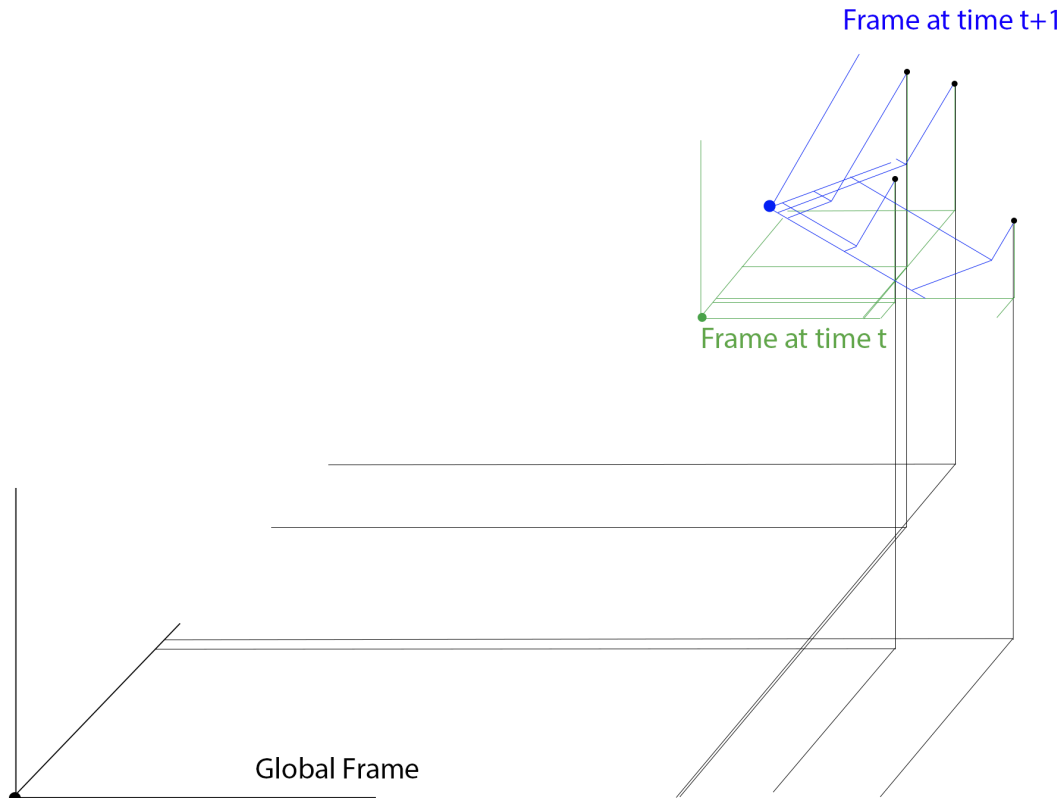


Figure 47: Example Reference Frame Transformation

The final step in the loop is to re-smooth the global point cloud using a PCL VoxelGrid. This will remove any duplicate points and reduce stutter (closely but not perfectly aligned points).

Map Changes When changes are made to the surrounding terrain as will be done when the robot is mining, the mapping component will provide an interface to specify a rectangular

prism that was changed with a flag to specify if an object should be detected in the prism or if open space should be detected in the prism.

Terrain Map The mapping component will provide a service for a global terrain map. When a map is requested, the mapping component will initialize a 5-meter by 10-meter grid with 1 centimeter subdivisions to zero. This grid will represent the terrain height throughout the competition area; this is also known as a digital elevation model (DEM). The grid is oversized to represent a total operational area to avoid concerns of directly using the walls for any significant calculations.

The global point cloud will be projected onto the DEM using the Points2Grid library. This library averages and interpolates data within a radius from each defined point in a grid. See Figure 48 for an example of this.

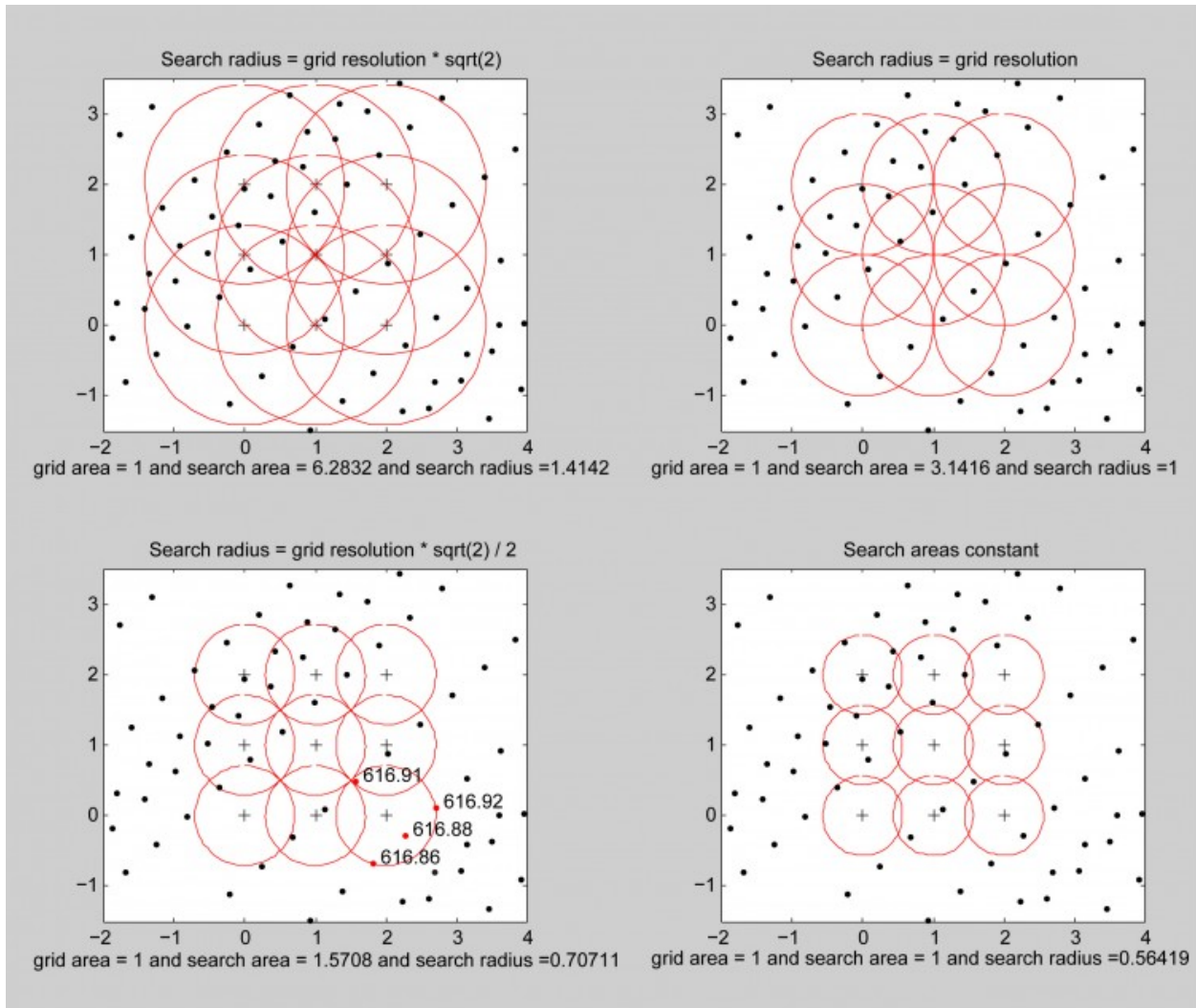


Figure 48: Operation of Points2Grid Library DEM Generation

The global point cloud will be projected onto the DEM using the Points2Grid library. This library averages and interpolates data within a radius from each defined point in a grid. See

Figure 48 for an example of this.

Testing Test cases were written for the algorithm detailed above to ensure that the mapping algorithm would sustainably operate in the background without consuming unreasonable hardware resources. The test cases revealed that, even when running on a laptop, the execution time for a single loop of the software took 0.5 seconds initially and tripled within a minute. This data showed the need for a better design.

Final Design The team analyzed several other available mapping techniques that could save computation resources: Fuzzy Mapping (FzM) [4], Large-Scale Direct SLAM (LSD-SLAM), and Direct Sparse Odometry SLAM (DSOSLAM). The latter two options were eliminated because they are primarily focused on providing robot odometry rather than environment map data [2][1]. That left FzM as the lone contender.

Overview FzM is a mapping strategy designed by Dr. Tim McJunkin [4]. The algorithm is largely based on Fuzzy Logic. The strategy maps the measurements of the current world around the robot to a given number of 'fuzzy' regions. Each of these regions is given a membership from 0 to 1 representing how dangerous the area would be to move into. The memberships for each region are not discarded when new data is available. Rather, they are flowed to the other regions based on the overlap of the regions at the previous time and the current time.

This algorithm is minimally computationally expensive and is robust over infinitely large regions. The complexity is $O(n * m * k_a + k^2)$ where $n * m$ is the resolution of the depth sensor, k_a is the number of active fuzzy regions, and k is the total number of fuzzy regions. The design required for the Moonrockers' application of FzM are the following:

- Zones
 - Size
 - Location
 - Active or not
- Membership flow parameters

Zones Fuzzy logic's central idea is to make the rules and operations described to be identical to human thought process. Therefore, the ideal geometry for the FzM would be one that works flawlessly mechanically and is perfectly representative of human references. With these ideas in mind, design proceeded as follows.

Shape Several shapes of fuzzy zones were evaluated including ovals, circles, and rectangles. Ovals and circles felt like they represented the area that a person would reference while driving, but they presented problems with the mechanics of the algorithm. Notably, they caused membership to move normal to and against the direction of motion when closely

packed enough to cover all space and bled membership to the aether when sparsely packed enough to abate the previous issue. Rectangles resolved the algorithm's mechanical issues but poorly represented areas that humans would reference.

The resolution between the disparity between the solutions and the ideal was to use each geometry in the situation where it excelled. Rectangular regions were used to perform the mechanics of the algorithm (i.e. the membership assignment and tracking), and ovals were used to communicate the map data to both the system and to the operator.

Number and Placement The team wanted to use the full range of the Orbbee Astra depth camera (1.5 meters), have at least 0.5 meters of information for driving backward, and have enough lateral information to turn a full 360 degrees. A 1.5 meter wide by 3.5 meter long mapped area is the minimum to meet these specifications. To meet the 10 hertz performance requirement, the number of active cells cannot exceed 50. In tandem, the cells would have ideally been the same size as the largest object the robot would encounter: 15 cm. An active grid of cells that is 10 wide and 5 long achieved that width and only doubled it in length. To minimize dilution and improper propagation, the cells for the rest of the grid were set to the same size. This resulted in a total of 120 cells that cover a 1.5 meter wide and 3.6 meter long area. A visualization of this map is shown in Figure 49.

To communicate the map data to other parts of the system and to the operator, ovals that more closely represent the areas a driver would consider when moving were placed. The areas that the team decided would fit this description were close forward, forward, far forward, forward left, forward right, left, right, rear, rear right, and rear left. This configuration is shown in Figure 50. The memberships of these zones are calculated by the area-weighted sum of the memberships of the mechanical zones they overlap. These overlaps were calculated using Matlab polyshapes with the intersect() and area() functions.

Due to time constraints and the required time to tune a controller with the complexity of the display map, another, much simpler map was created for obstacle avoidance use. This map contained only 4 areas: far forward, forward, left, and right. This configuration is shown in Figure 51. These zones' memberships and relations to the mechanical map are/were calculated in the same way the display map's are/were.

Flow Parameters With the size, shape, and location of the zones selected, the flow parameters were calculated using Matlab polyshapes. These were calculated as the percentage of the intersection area between a zone in the current and all other zones in the previous step. An example of this is shown in Figure 52. The operator display map was used in Figure 52 to exaggerate the effect. The process was repeated for all mechanical zones for full motion (forward and backward), half motion, and no motion in all combinations of travel and turning. Full motion was determined by the max speed the robot would travel - 0.75 meters per second and 60 degrees per second - times the maximum loop time for the algorithm - 0.1 seconds dictated by the 10 hertz minimum execution frequency.

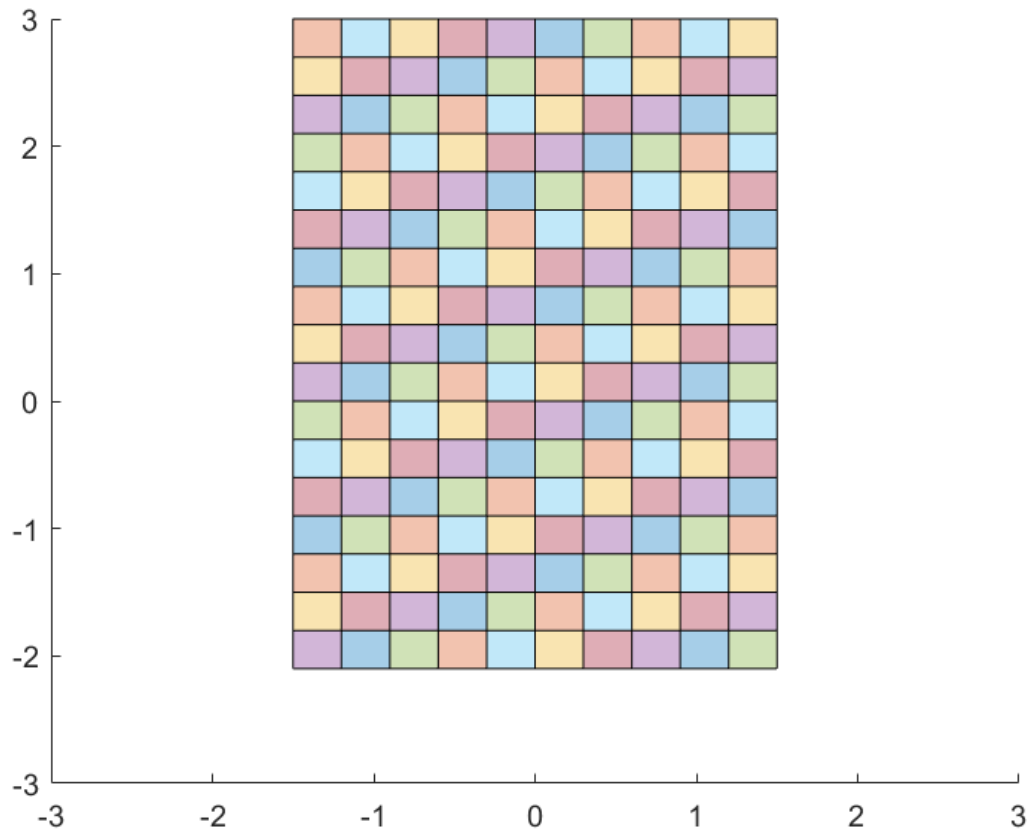


Figure 49: Visualization of the Mechanical Fuzzy Map

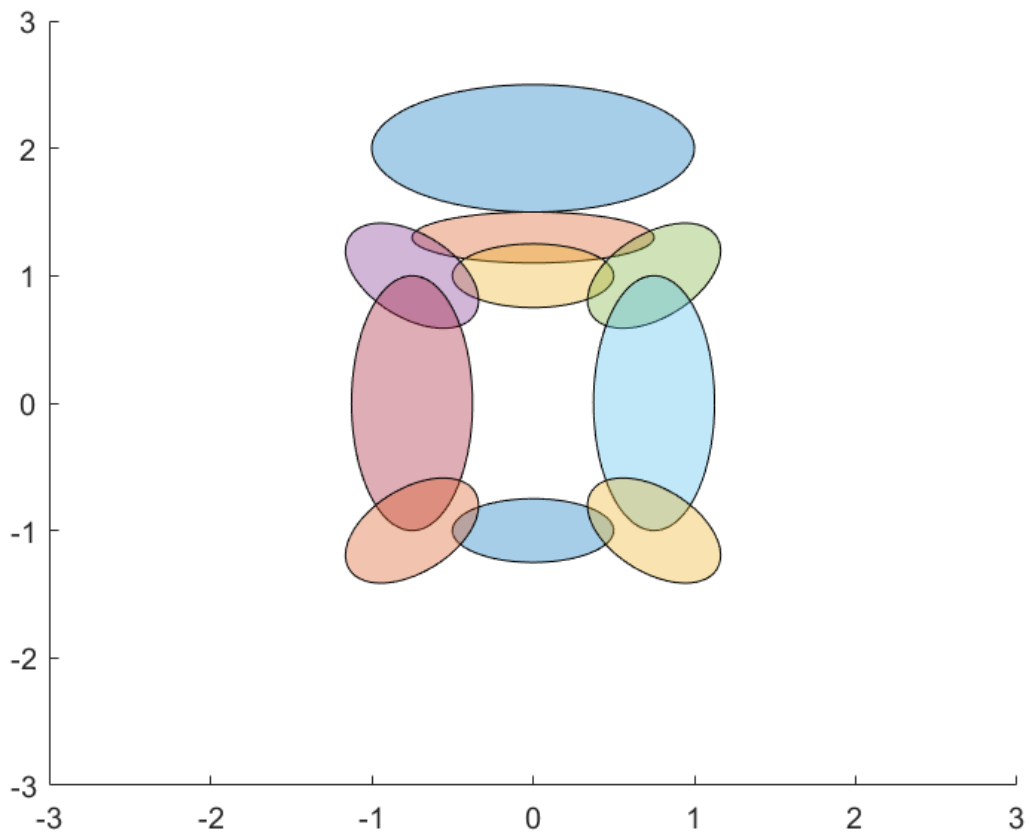


Figure 50: Visualization of the Operator Display Fuzzy Map

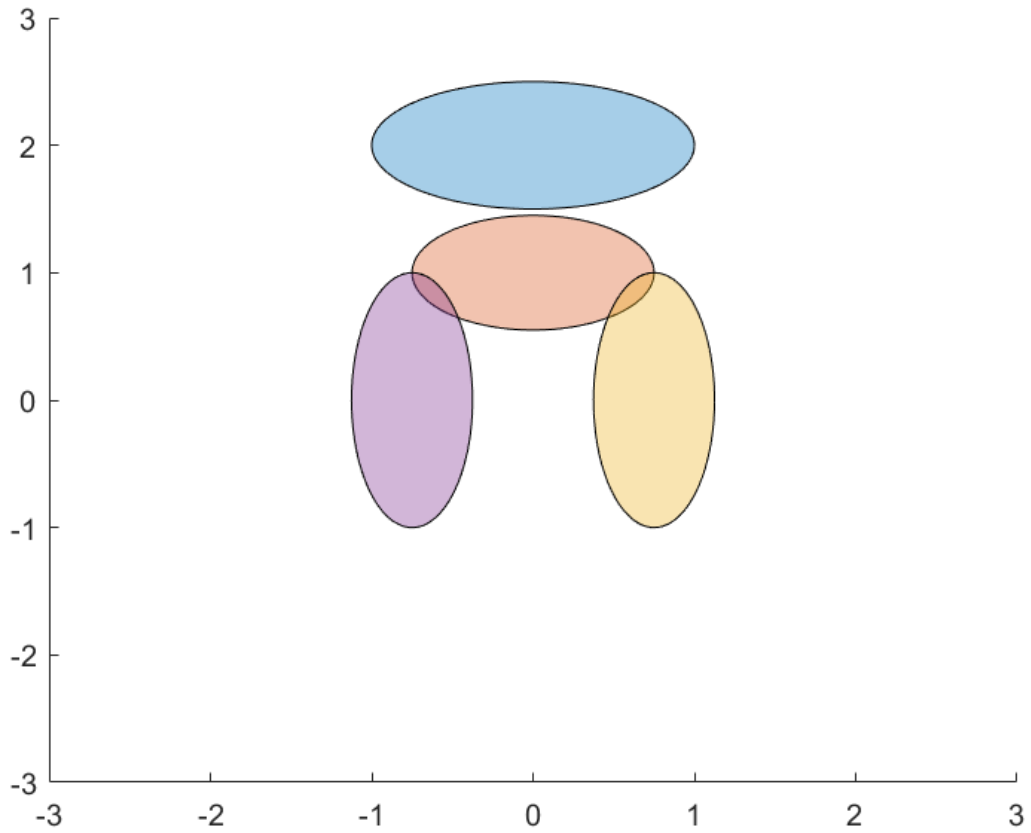


Figure 51: Visualization of the Controller Fuzzy Map

7.6 Path Planning

NOTE: THIS SECTION IS INCLUDED FOR HISTORICAL PURPOSES ONLY. THE 2018 IMPLEMENTATION DOES NOT INCLUDE THE FOLLOWING ALGORITHM DUE TO PERFORMANCE CONCERNS.

See Mapping-Testing section for detailed explanation.

Introduction and Motivation Robotics relies on effective planning to safely and efficiently execute its purpose. Path planning involves determining the fastest, safest, and most efficient line to follow to navigate from a robot's current position to a destination.

Algorithm Description The algorithm chosen for the path planning package is dubbed D* Lite. An overview of the algorithm can be found in the paper available at Dr. Koenig's website[3]. Please see the algorithm description for data storage, initialization, and loop descriptions.

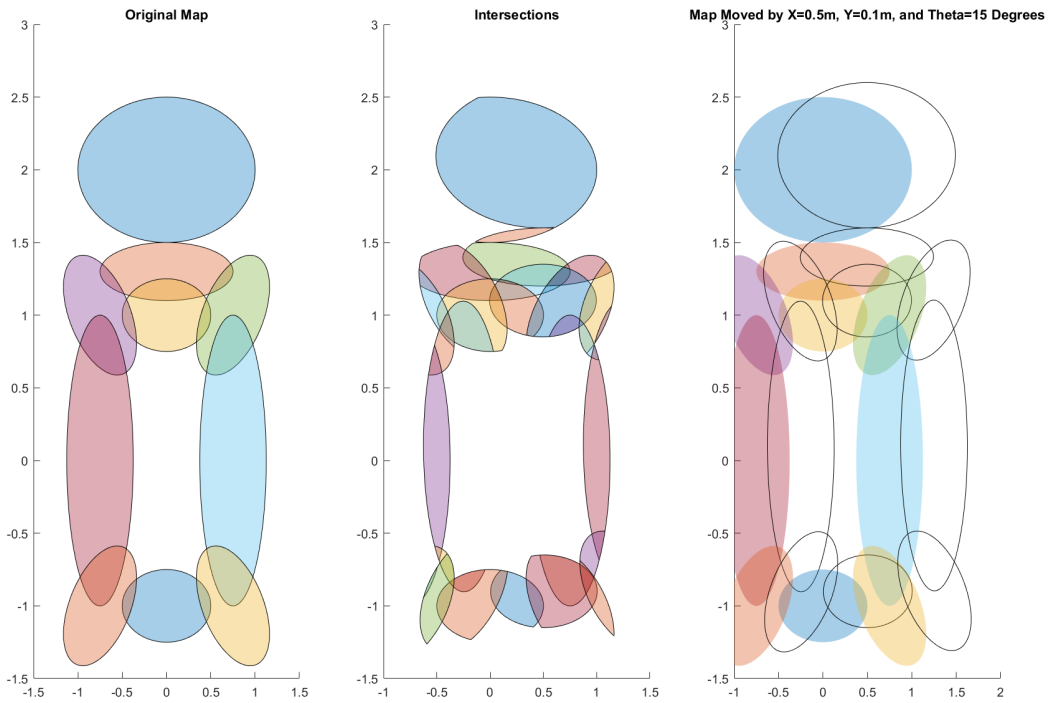


Figure 52: Example of Intersection Computation

Cost Function The purpose of the cost function is to determine how much power and how safe it is to move into the space being evaluated. The Moonrocker's robot has five (5) primary considerations for power requirements and safety: distance to the space, height change from the current space to the space, the terrain grade at the space, the biggest obstacle, and evenness of the terrain.

The cost function and its supporting functions are defined in Table 6.

NOTE: Cross-track refers to a measurement that is referenced orthogonal to the robot's course (θ defined in Table 6).

Table 6: Definition of Cost Function Symbols

Symbol	Definition	Units
C	This size of a cell in the map discretization.	meters
w_{wb}	The width of the robot's wheel base.	meters
h_{cg}	The height of the robot's center of gravity.	meters
L_{wb-r}	The distance from the robot's chassis pivot point to the robot's rear wheels line of contact with the ground.	meters
L_{wb-f}	The distance from the robot's chassis pivot point to the robot's front wheels line of contact with the ground.	meters
θ	The course of the robot measured as the angular difference between the vector normal to the hopper wall extending into the mining arena and the vector from the robot's deposition system to the robot's collection system.	radians
x	The left/right(cross-track) distance from the hopper of a point.	meters
y	The point's distance away from the hopper normal to its wall.	meters
x_i	The x component of the current point being evaluated (the i^{th} point in the planned path).	meters
y_i	The y component of the current point being evaluated (the i^{th} point in the planned path).	meters

Symbol	Definition	Units
x_{i+1}	The x component of the current point being evaluated (the $(i+1)^{th}$ point in the planned path).	meters
y_{i+1}	The y component of the current point being evaluated (the $(i+1)^{th}$ point in the planned path).	meters
M_r	The mass of the robot.	kilograms
M_L	The mass of the regolith load.	kilograms
$D(x_1, y_1, x_2, y_2)$ ¹	The Euclidian distance function.	meters
$H(x, y)$	The height of the terrain at y distance from the hopper with x cross-track.	meters
$\bar{H}(x, y)$	The average height around the point (x, y) .	meters
$\Delta H(x_1, y_1, x_2, y_2)$ ¹	The difference in average height of two locations.	meters
$\sigma_H^2(x, y)$	The variance of the terrain height around point (x, y) .	meters^2
$\sigma_H(x, y)$	The standard deviation of the terrain height around point (x, y) .	meters
H_{max}	The maximum deviation from the average terrain height under the robot (i.e. absolute value).	meters
$P_{x,y}$	The set of all points whose $D()$ from the point (x, y) is less than or equal to $L_{wb}/2$.	points
$F(x_i, y_i, x_{i+1}, y_{i+1}, M_L)$	The cost to move from point i to point $i+1$	meters

1 The subscripts 1 and 2 denote unique but not specific points.

Definition of Equations

$$D(x_1, y_1, x_2, y_2) = \sqrt{(x_2 - x_1)^2 + (y_2 - y_1)^2} \quad (1)$$

$$\bar{H}(x, y) = \sum_{p=(x,y)}^P H(p) \quad (2)$$

$$\Delta \bar{H}(x_1, y_1, x_2, y_2) = \bar{H}(x_2, y_2) - \bar{H}(x_1, y_1) \quad (3)$$

$$\sigma^2 = \sum_{p=(x,y)}^P H(p) - \bar{H}(x, y) \quad (4)$$

$$\sigma = \sqrt{\sigma^2} \quad (5)$$

$$\begin{aligned} F(x_i, y_i, x_{i+1}, y_{i+1}, M_L) &= D(x_i, y_i, x_{i+1}, y_{i+1}) + \left(\frac{M_r + M_L}{M_r} \right) \Delta H(x_i, y_i, x_{i+1}, y_{i+1}) \\ &\quad + \sigma(x_{i+1}, y_{i+1}) \end{aligned} \quad (6)$$

Heuristic Function The heuristic function determines how well the solution is trending toward the destination. It helps to reduce the computational complexity of the path planning calculation.

The heuristic function is defined as follows using symbols defined in Table 6.

$$G(x_g, y_g, x_t, y_t, M_L) = D(x_i, y_i, x_{i+1}, y_{i+1}) + \frac{M_r + M_L}{M_r} \Delta H(x_i, y_i, x_{i+1}, y_{i+1}) \quad (7)$$

Path Smoothing Since the global grid will be generated on a small scale, the resulting path could be noisy and have many discontinuities. To combat this and provide a just complex enough path, the system will find keypoints along the full path provided by the D* Lite algorithm. Keypoints are defined as a point in a path where the path deviates significantly from a straight line. These keypoints will be defined as either the first or last point in the path or the furthest point from the previous keypoint such that, for all points between itself and the previous keypoint, the average normal distance to the line connecting the two keypoints and the standard deviation of the normal distance is less than or equal to 5 centimeters. A depiction of this is shown in Figure 14. The system will use a bisection search to find all keypoints in each path. The system will first test the whole path to see if the entire path fits the criteria stated above that identifies a keypoint exists in the path. If one does, the system will bisect the path until the point being evaluated collides with a boundary past which the non-existence of a keypoint has been guaranteed. In that situation, the point being evaluated is considered a keypoint. The algorithm for the smoothing is shown in Figure 54.

An example of the output of this algorithm is shown in Figure 55.

Output Data The output from the path planning package will be an sequence of positions wrapped in the plan.msg defined in Appendix C.

7.7 Navigation Execution

7.7.1 Introduction and Motivation

A robot is useless if it cannot reliably travel the path that it planned. This raises the need for a path following control scheme. Its purpose is to monitor the current position of the robot and issue new drive commands to continue navigation along the planned path and to correct navigation errors as it does so. A PID control system suits this problem well.

7.7.2 System Description

To maintain the separation of responsibility, the path following control system will be designed around a system to directly manipulate forward drive speed and rotation speed. To simplify the system, forward speed will be constant. To ensure enough additional maneuverability, the constant speed will be $0.75 \frac{m}{s}$ (top speed is $2 \frac{m}{s}$).

With this simplification, the state space equations for controller design are as follows. Table 10 defines all symbols used in the state space definition.

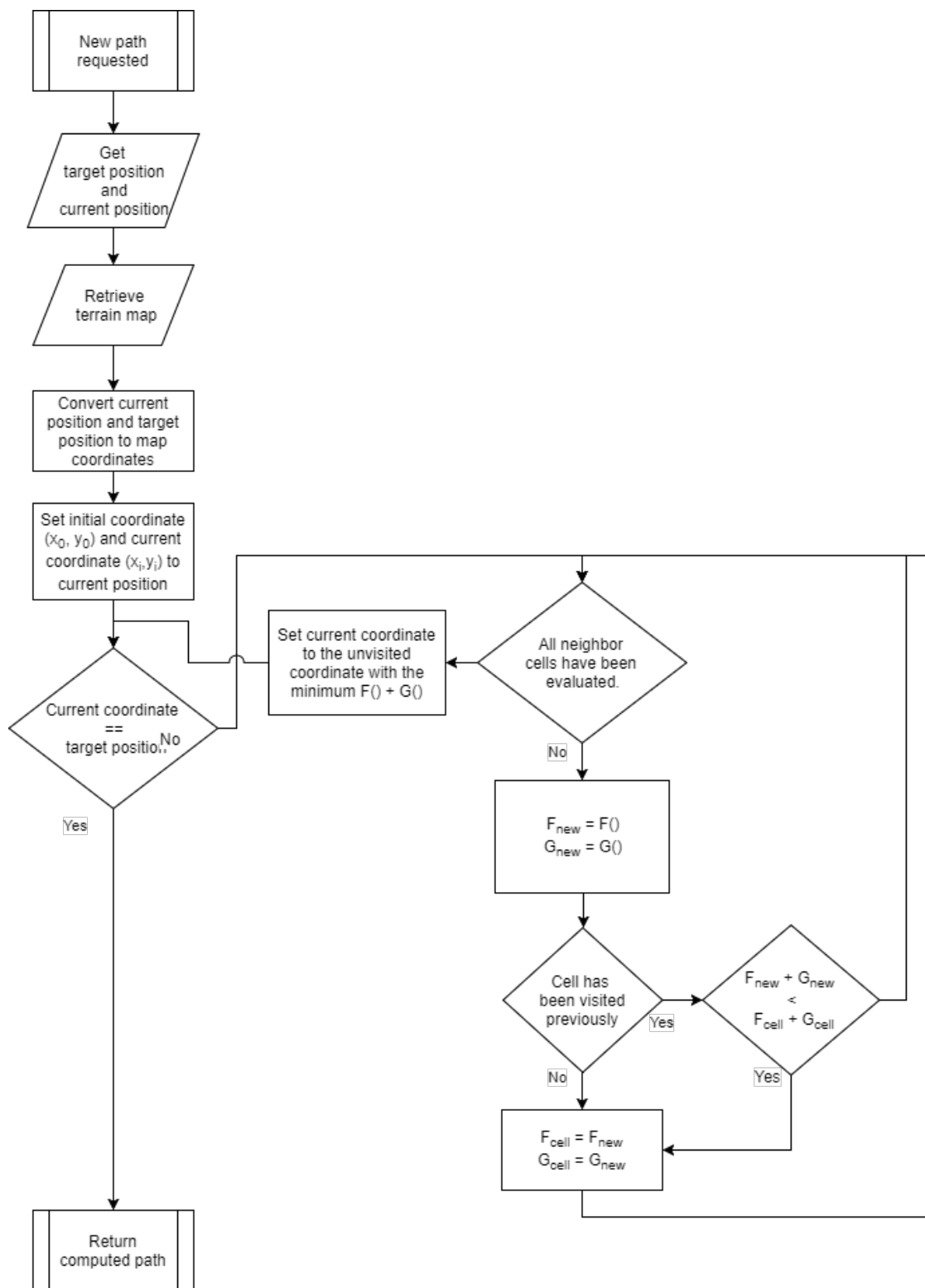


Figure 53: Path Planning Flowchart

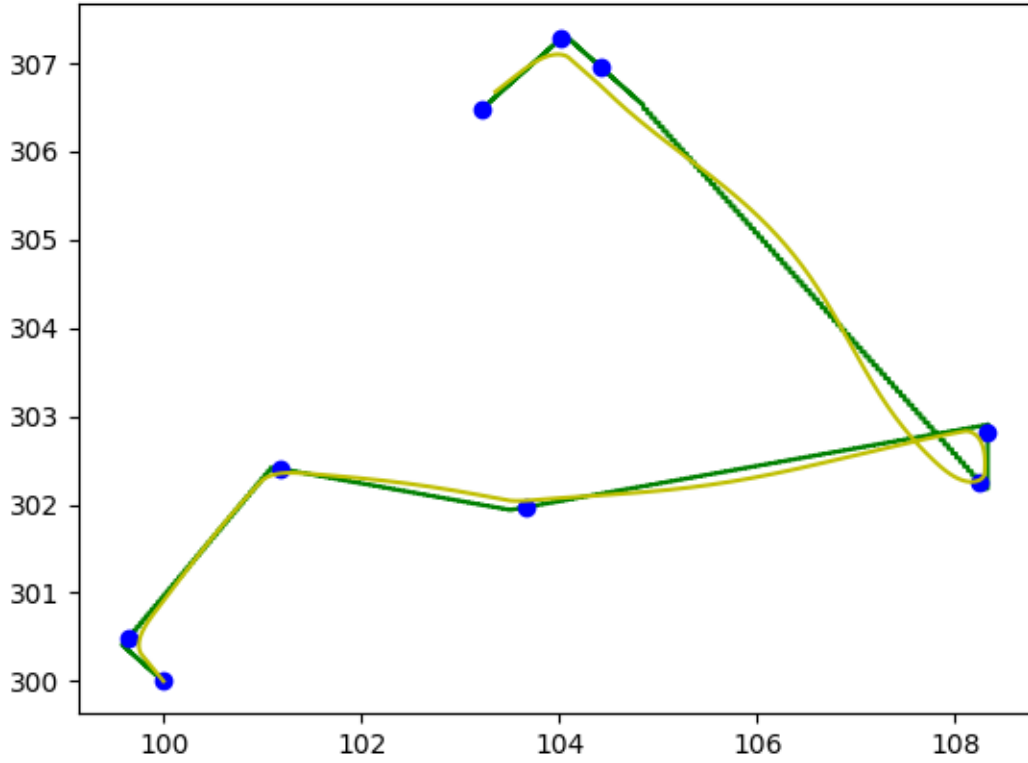


Figure 54: Path Smoothing Algorithm

Table 10: Definition of Symbols for Controller

Symbol	Definition	Units
XTE	Cross track navigation error. This is calculated as the orthogonal distance from the vector between the previous and current waypoints. ¹	meters
v	The along-course speed of the robot. This is constant at $0.75 \frac{m}{s}$.	$\frac{m}{s}$
θ	The course of the robot measured as the angular difference between the vector normal to the hopper wall extending into the mining arena and the vector from the robot's deposition system to the robot's collection system.	radians
Dot Notation	Dot notation signifies the time derivative of the symbol it is applied to (e.g. \dot{x} is the time derivative of x). The number of dots specifies the order of the derivative (\ddot{x} is the second time derivative of x).	N/A

¹ See Path Planning section for definition of waypoint.

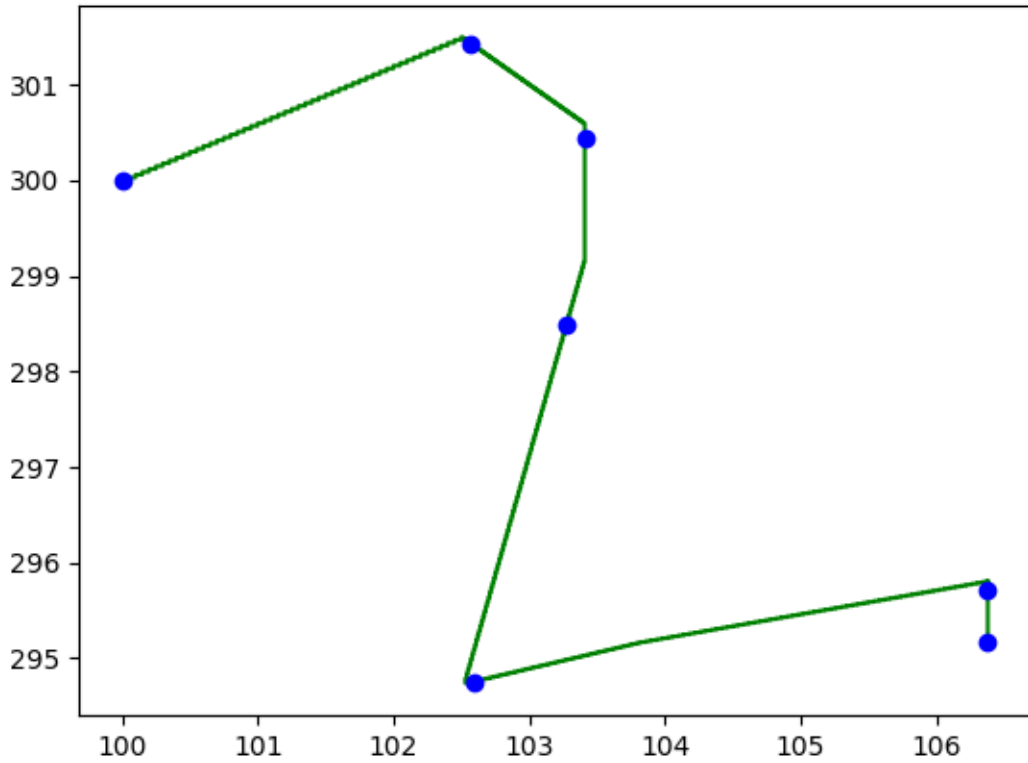


Figure 55: Example Output from Smoothing Algorithm

State Space Equations

$$\begin{bmatrix} X\dot{T}E \\ X\ddot{T}E \\ \dot{\theta} \end{bmatrix} = \begin{bmatrix} X\ddot{T}E \\ v \cos(\theta)\dot{\theta} \\ \dot{\theta} \end{bmatrix} \quad (8)$$

7.7.3 Controller Specifications

The competition arena is approximately 7.5 meters long. This means that a full transition across the arena would take 10 seconds. An appropriate time to fully course correct would be 3 seconds. This specification would allow 3 full course corrections across the arena.

7.7.4 Controller Design

True control design for the system is beyond the scope of undergraduate education at South Dakota School of Mines and Technology (coupled state space equations and saturations and slew rate limit nonlinearities). Therefore, an iterative design approach was taken with a traditional PID controller.

Figure 56: Controller Step Response

After several iterations, a proportional gain of 15, a derivative gain of 15, and an integral gain of 0.15 result in a settling time of just over 3 seconds. This step response can be seen in Figure 56.

Table 11: Definition of Symbols for Algorithm

Symbol	Definition	Units
waypoint (wpt)	(x,y) point used for navigation. The path will be a sequence of these.	meters
$D(wpt1, wpt2)$ ¹	The Euclidian distance between waypoint 1 and 2.	meters
Σ Notation	Sigma notation signifies a sum.	N/A
Δ Notation	Δ notation signifies a change in the variable following it (e.g. Δx means a change in x).	N/A
XTE^2	The cross-track error of the robot measured as the distance from the robot's current position to the vector connecting the previous and current waypoints along a vector normal to that vector.	meters
XTE_{new}	The XTE measured in the current controller loop.	meters
XTE_{old}	The XTE measured in the previous controller loop.	meters
$ND(wpt1, wpt2, wpt)$	The Euclidian distance from a waypoint to the nearest point along the line connecting waypoint 1 and 2.	meters
T_{new}	The time for the start of the new controller loop.	clock ticks since power up
T_{old}	The time for the start of the last controller loop.	clock ticks since power up

¹ See Path Planning section for distance equation.

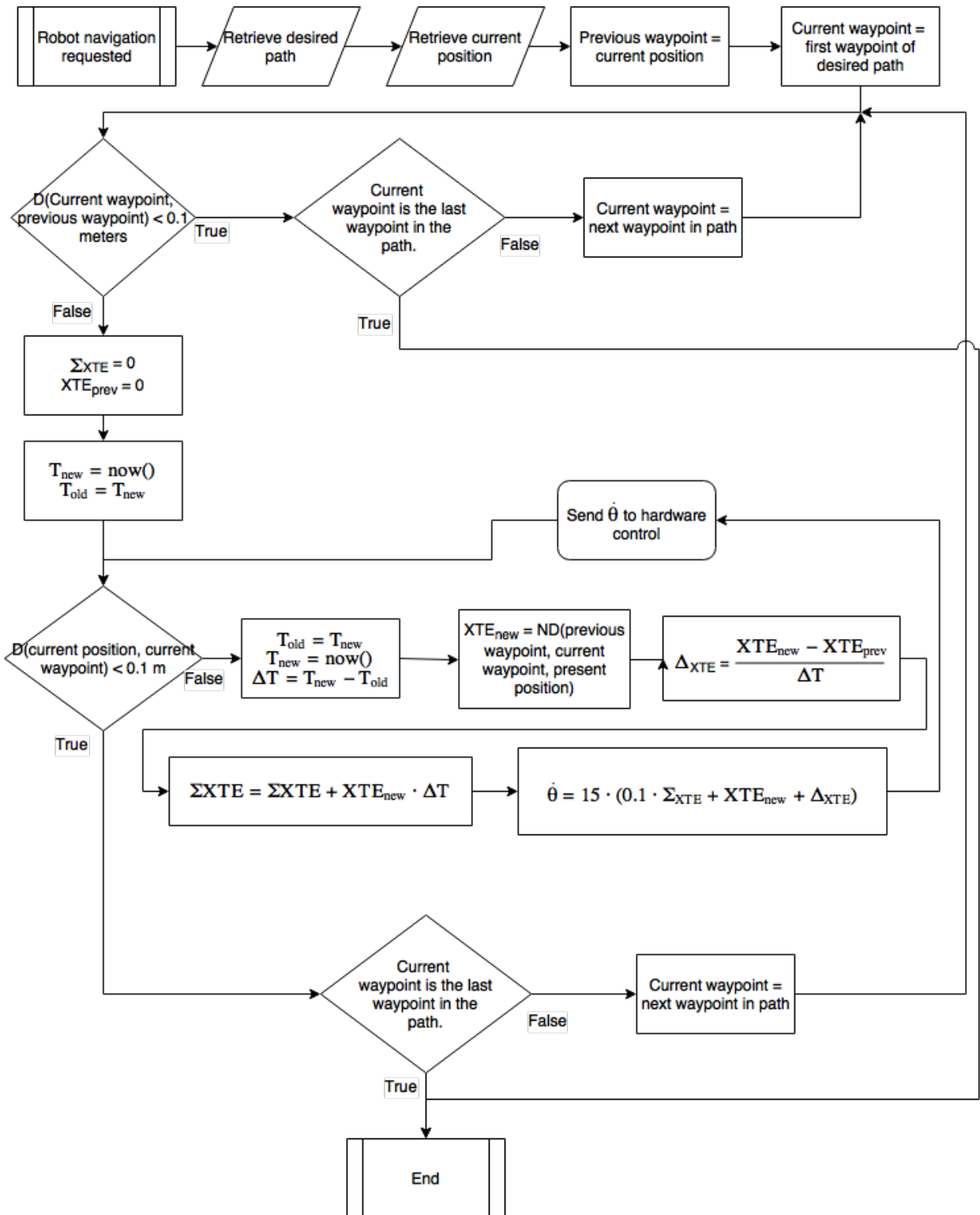
² XTE will be calculated using the ND function.

Note: For the following equation, the subscripts 1 and 2 denote waypoints 1 and 2 respectively, and the subscript p denotes the arbitrary waypoint.

$$ND(wpt1, wpt2, wpt)^5 = \frac{|(y_2 - y_1)x_p - (x_2 - x_1)y_p + x_2y_1 - X_1 * y_1|}{D(waypoint1, waypoint2)} \quad (9)$$

⁵Equation adapted from Wolfram MathWorld [6]

Figure 57: Path Following Flowchart



7.7.5 Test Implementation and Redesign

During algorithm testing, the simulated PID in a discrete simulation environment proved unstable and did not perform to the specifications that the continuous MATLAB simulation indicated it would. Additional designs were iterated in a discrete Python simulation. Initial tests showed the PID struggled to turn corners as the system transitioned from one waypoint to the next. This led to trying two discrete PID systems: one for straight line driving and another for turning corners. The straight-line driving PID met the given system criteria with a proportional gain of -1.0, a derivative gain of -0.15, and an integral gain of 0.0. These gains resulted in a max path deviation of 30 centimeters and an average of approximately 15 centimeters. The cornering PID changed to the course deviation of the robot as a control variable. The gains that met system specifications were a proportional gain of 4, a derivative gain of 0, and an integral gain of 0. The system will transition from the straight-line PID to the cornering PID when the system is less than 0.25 meters from the current waypoint. The system will transition from the cornering PID to the straight-line PID when the system is less than 5 degrees off course and has less than a 1 meter cross track error. Figure 58 shows this control scheme in action on a randomly generated path. Note, this path was preprocessed using the path smoothing algorithm described in the path planning section.

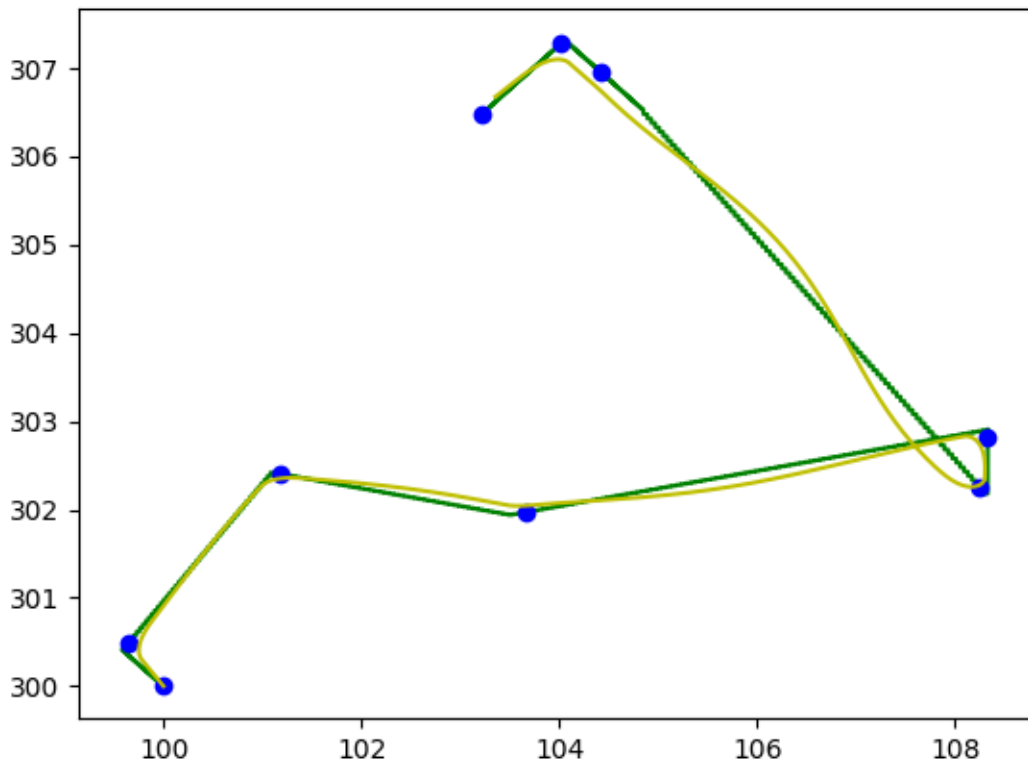


Figure 58: Example Execution of Path Following Algorithm

7.7.6 Second Redesign

Once the PID system described in the previous section was written in C++ and a robust dynamic simulator was implemented to test its functionality, the system was unstable and required redesign. To combat this, the system was reevaluated using state space analysis and the dynamic equations described above. The only addition to the dynamics was that both the course error and the XTE were used as inputs to the controller. Using pole placement, the gains required for 0.1 second settling time were calculated to be 1,333.3 proportional for XTE and 110 for course error. Testing showed this controller to be stable with a settling time closer to 0.01 seconds. This allowed the same controller to be used for the entirety of any given path rather than having a separate controller to turn corners.

7.7.7 Mapping Changes Impact

Due to the changes detailed in the Mapping-Testing section of this report, the execution engine needed to absorb the loss of path planning. Since the design of the mapping moved to fuzzy logic zones, the simplified fuzzy map was used to augment the execution engine. The fuzzy regimes for robot speed were selected as follows.

- Fast - Trapezoid with apex at 0.5 meters per second
- Still - Triangle with apex at 0.0 meters per second

The fuzzy regimes for robot turning rate were selected as follows.

- CCW - Trapezoid with apex at 45 degrees per second
- Still - Triangle with apex at 0 degrees per second
- CW - Trapezoid with apex at 45 degrees per second

The fuzzy logic rules implemented for the controller were as follows:

- If there is something in front, go slow.
- If forward is clear, go fast.
- If there is something left, turn CW.
- If there is something right, turn CCW.
- If there is something large in all zone, stop turning and advancing and call for help.

This fuzzy control was implemented bicamerally with the controller described in the previous section. The combination of the fuzzy control input with the standard controller provided a robust control system that is capable of avoiding obstacles and reach its destination safely.

7.8 Development Plan

Because the autonomy subsystem encompasses such a large scope of work, a plan of attack has been put together to guide the development of the robot's autonomous functionality. This plan serves the added purpose of naturally creating "break points" for the work being done, allowing a partial implementation of the robot's autonomy should the scope of work for this year prove to be too large.

Traversal The first goal for the development of the autonomy subsystem is to implement basic traversal. The first points threshold in the NASA RMC Rules for 2018 states that 50 autonomy points are awarded if the robot is able to traverse from the starting point to the mining area under complete autonomy. To implement this functionality, the localization sensors will need to be fully functional in order for the mapping and path planning software to route the robot across the arena. The environment and mapping software for the robot will need to be in a working state, able to route a path from the current location of the robot to a given target location. The robot will also need some rudimentary target determination to give the path planning algorithm two endpoints to plan a path between.

Regolith Collection After traversal is functional, the next goal is implementation of regolith collection. The NASA RMC Rules state that 100 autonomy points are awarded to a robot that can traverse out to the mining area, collect regolith, and return to the hopper under full autonomy. For this goal, improved target determination and additional state logic will be required to control both traversal from the starting location to the mining area and traversal from the mining area to the starting area, as well as movement around the mining area while the robot is mining. The mining algorithm will also need to be fully implemented for this goal, requiring more additional state logic as well as more fine-tuned localization to facilitate digging in the same hole multiple times.

Regolith Deposition Once the robot can collect regolith autonomously, the final step is to implement regolith deposition. The NASA RMC Rules state that 250 autonomy points are awarded to a robot that can perform a single full mining trip, and 500 autonomy points are awarded to a robot that can complete its full 10 minute run fully autonomously. To complete this, all parts of the autonomy subsystem will need to be in a finalized state, including finalizing the full state logic for the robot and implementing the robot's deposition control. The robot's localization will need to be fully calibrated and fine-tuned at this point to ensure that the robot is in the correct position against the hopper when it is depositing regolith.

7.9 Testing Plan

To aid in verifying the validity of the robot's autonomous functionality, a testing plan was developed for the autonomy subsystem. Table 12 is the overall verification matrix for the autonomy subsystem, which lays out at a high level what needs to be tested for each part of the autonomy subsystem.

Table 12: Autonomy Subsystem Verification Matrix

Subsystem	Parameter	Test
Localization Sensors	Data Accuracy Sensor Variance Localization Accuracy	Failure Testing Sensor Test Cart Integration Testing
Mapping	Map Accuracy Obstacle Detection Accuracy	Unit Testing Navigation Simulation Integration Testing
Path Planning	Path Validity Path Optimality	Unit Testing Navigation Simulation Integration Testing
Path Following	Follow Accuracy	Navigation Simulation Integration Testing
State Logic	Logic Validity	Navigation Simulation Integration Testing

Failure Testing For the localization sensors used by the robot, the first major testing step is to verify that the sensors function properly by themselves. Failure testing encompasses a variety of tests, ranging from testing how sensor data varies in a control state to examining the effect of vibration on sensor readings.

Sensor Test Cart To begin testing the localization sensors' interactions with each other, a simple cart was assembled. Multiple sensors can be mounted to this cart and wheeled around as though they were on a robot in motion to give a basic idea of how they interact with one another.

Unit Testing Testing software has different requirements from testing hardware and thus requires different methods of testing. Unit testing includes writing small tests to verify that individual portions of software are functioning properly given some simple dummy data. This is done for each portion of the overall autonomy subsystem on an individual basis.

Navigation Simulation For more in-depth testing of the navigation software before the robot is fully manufactured, a navigation simulation is being developed using the Gazebo simulation library. This library allows for the modelling of the physical components of the robot, allowing the software to be tested using that model as a substitute for the physical hardware. It goes so far as to allow modelling of sensors as well, giving essentially a complete replacement for the physical robot itself. This simulation is planned to be in development alongside the rest of the autonomy software and may or may not be able to be used for testing this year, but it should be in a state where it is useful to the Moonrockers team in years to come.

Integration Testing The last step in testing any system is making sure that it works correctly as a whole. Integration testing will be the final step in testing the autonomous

functionality of the robot, ensuring that the physical robot and the autonomy software work together to form a fully functional system.

7.10 Design Realization

As this project has progressed from design through manufacturing, much has been learned about how issues in the development process could be mitigated in the future. The most prominent issue that was encountered was the scope of the project. Ideally, this year would have resulted in a robot with the option to run under full autonomy; however, due to the large amount of work required by this task combined with the large amount of work required on the rest of the robot, it was unable to be completed. In the future, breaking down these larger tasks into more clear subtasks would be helpful in allowing for more work to be completed.

Another set of issues encountered involves the computer that the team decided to use. During the design phase of the project, it seemed like the best balance between cost and performance given our budget and requirements. As development progressed, however, it was quickly revealed that there were some issues not foreseen. Firstly, once much of the original mapping algorithm began to undergo testing, it was seen that the performance requirements of the algorithm were much greater than originally predicted. These increased performance requirements were so much greater that they required the original algorithm to be scrapped and a new one to be developed.

Another major issue encountered with the main computer arose in the implementation of CAN bus, one of the robot's major communication protocols. Once development of an interface for this protocol began, it was realized that the implementation of this interface would be much more difficult than initially anticipated. To fix this, the team decided to use a second, less powerful computer with an easier interface for CAN bus to handle the sensor communications, allowing the more powerful computer to handle the more intensive tasks of mapping and path following.

Beyond these issues, the team has also been able to improve skills in working with the technologies used on this project, including using C++ and Python with the ROS framework and using CAN bus and I2C as communication protocols. These skills will be useful to team members in the future in their careers, and the information learned by this year's team will prove useful to future teams.

7.11 Product Performance

At this stage, the development of the functionality of the robot is progressing well. The assembly of the robot is complete aside from a couple of minor pieces. Code to allow telerobotic operation of the robot is completed, meaning that the robot will be able to be manually controlled at competition.

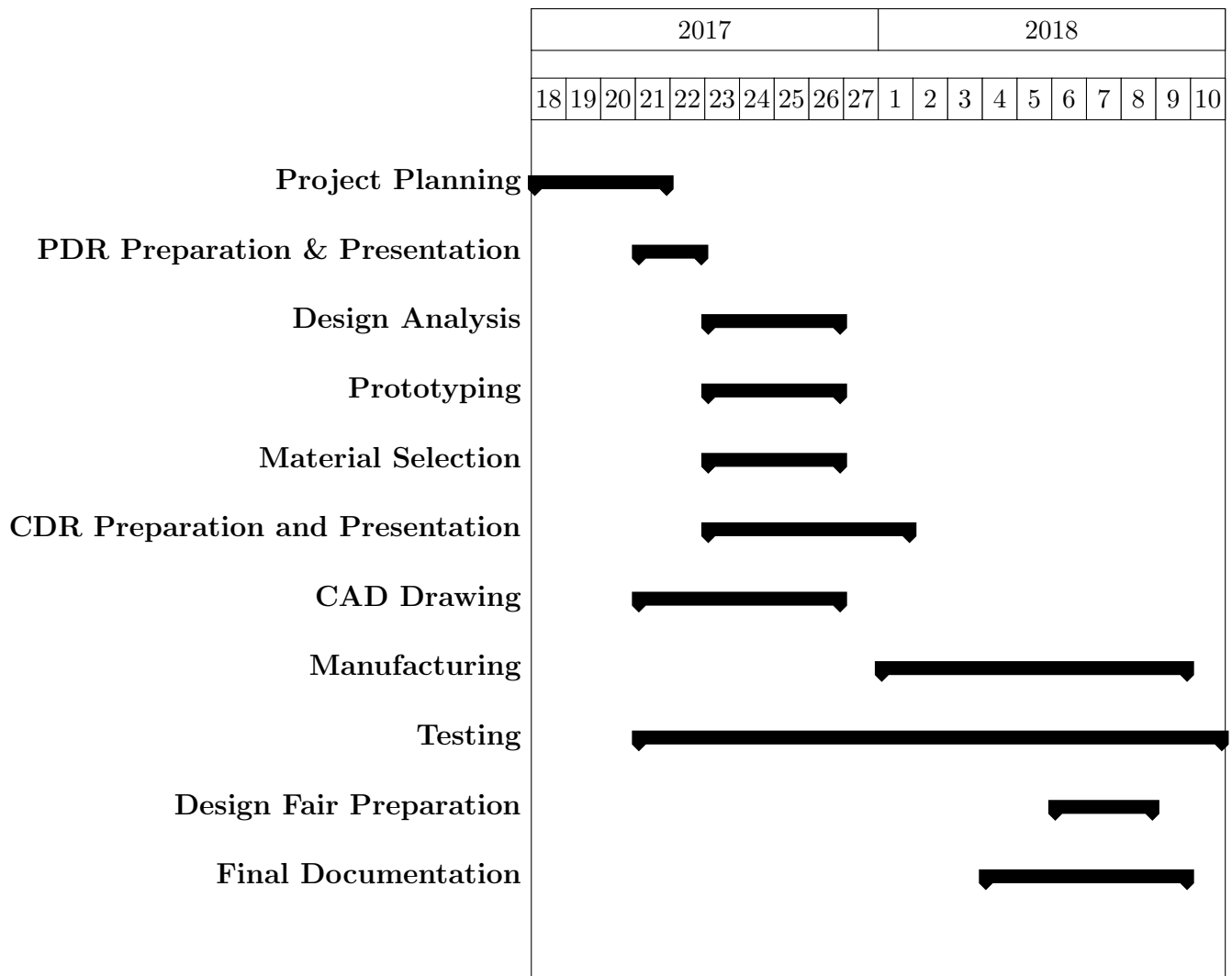
The goal for the autonomy subsystem is still to implement as much functionality as possible without compromising the quality of the product being developed. In completing the manual control code, a substantial portion of the hardware interface code has been written, with code for two major sensors remaining: the IMUs and the DWM antennae. Over the next two weeks leading up to the competition, the development of this software will be completed, and the Kalman filtering for the localization is anticipated to be completed. Given that mapping and path following are nearly completed, the robot should be able to drive autonomously in time for the NASA RMC. Any remaining work will be left as future work for this project.

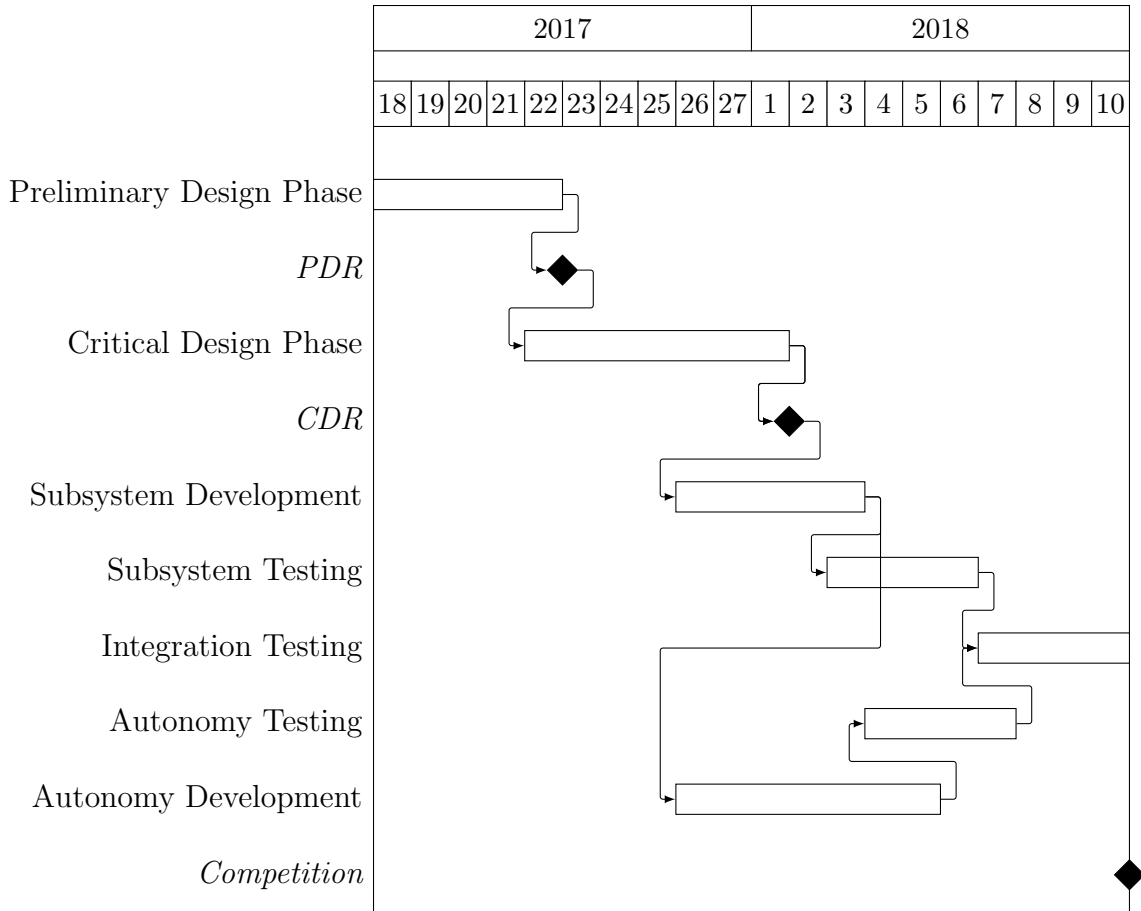
8 Project Schedule

A Gantt chart was made to outline the time line of the senior design team for the 2017-18 academic year. This chart marks the important milestone dates throughout the design process including presentations, design fair, and the NASA Robotic Mining Competition.

Gantt Chart

This Gantt Chart marks every two weeks starting August 17th 2017 and ending May 19th 2018.





9 Task Statements

The Moonrockers team currently appointed officers whose main responsibilities included logistics and management for the non-senior students assisting the team. These officers included team chair Joree Sandin, vice chair Dakotah Rusley, secretary Nick Reynolds, and treasurer Carter Barkley. The senior design team appointed each of its members to system teams with there being a system lead for each team.

Joree Sandin was the Moonrocker's NASA Robotic Mining Competition Senior Design Lead. Joree effectively managed the team and its actions throughout the senior design process by keeping the team on task and schedule. Joree also assisted in the redesign of the collection system and participated as a collection system team member. Joree ensured that all documentation required for senior design and for the NASA competition was done on time and with completeness. Joree was heavily involved in all documentation and reporting of the Moonrockers senior design project.

The ECE members had two system leads and these roles were the Electrical and Computer Engineering Team Lead, Zachary Christy, who led team meetings and managed general hard-

ware development, and the Software Lead, Collin Chick, who led the software development efforts.

The Mechanical systems lead was Austin Kaul who managed and tracked the efforts of the mechanical engineers as the robot systems were updated and redesigned to meet the requirements and challenges of the competition. This lead position involved having in depth knowledge of all mechanical systems and their functions as well as the work completed by each member of the system teams. Austin was also involved in developing the concepts and design of the collection system as well as running the finite element analysis of critical components on the robot. Austin was also heavily involved in the documentation and reporting for the Moonrockers senior design project as well as testing and manufacturing for all mechanical systems.

Michael Bush was the Environmental Mapping and Path Planning development lead and directed many of the Systems Engineering and planning management efforts. He also assisted the collection team to brainstorm and critically evaluate potential concepts.

Kevin Grimsted was the collection system Lead. Kevin primarily focused on developing 3-D models of the proposed collection system, deposition system, and E-box. He was also heavily involved in the design concepts and requirements for the collection system. Kevin assisted in the manufacture and testing of the collection system and provided regular system updates to the mechanical systems lead.

Devon Jones was the Deposition team lead and led the efforts to redesign and update the deposition system. Devon regularly reported to the mechanical systems lead on the progress of the deposition team. Devon was also involved with the manufacture and testing of the deposition system.

Cody Cooper was a member of the deposition system team and was heavily involved with the redesign and analysis of the deposition system. Cody was also the presentation lead which involved gathering information from every system team and developing presentations for the Preliminary and Critical design reviews. Cody was also involved with the manufacture and testing of the deposition system.

Sean Kittler was a member of the deposition team and focused his efforts on the redesign and update of the deposition system.

The team of student engineers was advised by faculty Dr. Charles Tolle (ECE), Dr. Jason Ash (ME), Mr. Lowell Kolb (ECE), and Dr. Hadi Fekrmandi (ME). These advisors remained continuously available to the students, but refrained from active design or construction roles on the robot.

9.1 Action Items Tables

An action items list was made for the time period between the PDR (October 23rd) and the CDR (December 6th) and can be seen in tables 13 and with due dates for each action item and an individual or team assigned to them.

Table 13: Action item list to be completed before Critical Design Review.

Action Item	Subsystem	Assignee	Due Date	Estimated Time (h)
Create Action Items List	Documentation	A. Kaul/M. Bush	11/3/2017	3
Self evaluation form 1 due	Documentation	All	11/9/2017	1
Progress Report 3	Documentation	All	11/9/2017	4
Draft Preliminary Report	Documentation	All	11/9/2017	5
Static Analysis of Robot	Collection	All	11/10/2017	2
Final E-Box placement Selection	E-box	E-Box Team	11/10/2017	5
Solidworks of Collection	Collection	Collection Team	11/10/2017	10
Product Breakdown Sheet	Documentation	Z. Christy	11/15/2017	1
Test Apparatus Built Collection	Collection	Collection Team	11/29/2017	3
Test Apparatus Built for autonomy	Autonomy	All	11/29/2017	3
Unit Test cases	Collection	Collection Team	11/29/2017	3
Unit Test cases	Deposition	Deposition Team	11/29/2017	3
Unit Test cases	E-box	E-box Team	11/29/2017	3
Determine Reliability Checklist	Reliability	All	11/29/2017	3
Solidworks of E-box	E-Box	K. Grimsted	11/29/2017	5
CDR Slides	Collection	A. Kaul	11/29/2017	5
CDR Slides	Deposition	D. Jones	11/29/2017	5
CDR Slides	E-box	L. Torgerson	11/29/2017	5
Integration test cases	Reliability	All	11/29/2017	5
Solidworks of Depostion	Deposition	Deposition Team	11/29/2017	7
FEA of Collection Scoop	Collection	A. Kaul	11/29/2017	9
Decision Matrix of Scoop Design	Collection	Collection Team	11/29/2017	8
Alter Deposition/Matrix	Deposition	Deposition Team	11/29/2017	10
FEA of Collection Structure	Collection	A. Kaul	11/29/2017	10
CDR Presentation	Documentation	C. Cooper	11/29/2017	15
Self evaluation form 2 due	Documentation	All	12/1/2017	1
COTS parts selection List	Collection	Collection Team	12/1/2017	5
COTS parts selection List	Deposition	Deposition Team	12/1/2017	5
COTS parts selection List	E-box	E-Box Team	12/1/2017	5
4th progress report due	Documentation	All	12/1/2017	5
Preliminary report due	Documentation	All	12/1/2017	10
Manufacturing/Component Design Review	System	All	12/6/2017	1
CAD Model of Deposition Changes Finished	Deposition	C. Cooper	12/8/2017	5
Order Parts	System	J. Sandin	12/10/2017	2
Test Apparatus Built Collection	Collection	Collection Team	12/22/2017	5
CAD Model of Collection Concept Finished	Collection	A. Kaul	12/22/2017	10
Machine Design on Collection System	Collection	Collection Team	1/6/2018	1
FEA on Scoop	Collection	A. Kaul	1/6/2018	5
FEA on Slide	Collection	A. Kaul	1/6/2018	8
FEA on Support Structure	Collection	A. Kaul	1/6/2018	8
FEA on Rail	Collection	A. Kaul	1/6/2018	8
Test Apparatus Built for autonomy	System	All	1/6/2018	3
Unit Test cases	Collection	Collection Team	1/21/2018	3
Unit Test cases	Deposition	Deposition Team	1/21/2018	3
Determine Reliability Checklist	Reliability	All	1/21/2018	3
CDR Preparation	System	All	1/22/2018	3
CDR Slides	Collection	A. Kaul	1/22/2018	5
CDR Slides	Deposition	D. Jones	1/22/2018	5
CDR Slides	E-box	L. Torgerson	1/22/2018	5
5th Progress Report	System	All	2/23/2018	5
Draft Report Due	System	All	2/23/2018	7
Self Evaluation Form 3 Due	System	All	2/23/2018	9

Table 14, below, lists the action items to be done by each member or groups of members from February to May after the Critical Design Review.

Table 14: Action item list to be completed before February.

Action Item	Subsystem	Assignee	Due Date	Estimated Time (h)
5th Progress Report	System	All	3/2/2018	4
Draft Report Due	System	All	3/2/2018	40
Self Evaluation Form 3 Due	System	All	3/2/2018	1
Submit Water Jet Parts	Austin	Collection	3/2/2018	2
Machine/Manufacture Parts	Mechanical Systems	All	3/16/2018	20
6th Progress Report Due	System	All	3/23/2018	4
Design Fair Presentation Needs	System	All	3/23/2018	10
Assemble Robotic Systems	Mechanical Systems	All	3/30/2018	30
Test Systems	Mechanical Systems	All	4/14/2018	30
Implement Autonomy	System	All	4/14/2018	40
Design Fair Preparation	System	All	4/17/2018	20
7th Progress Report Due	System	All	4/27/2018	4
Final Report Due	System	All	4/27/2018	20
Self Evaluation Form IV Due	System	All	4/27/2018	1

10 Preliminary Budget

Table 15: Overall labor budget for six electrical and computer engineers and seven mechanical engineers.

Major Items	Count	Hours	Rate	Total
ECE Labor Budget	6	200	\$75.00/hr	\$90,000.00
ME Labor Budget	7	200	\$75.00/hr	\$105,000.00
Total Project General Budget				\$195,000.00

Table 16: Mechanical, electrical, and computer engineering component budget.

Major Items	Count	Category	Cost	Total
Adhesive materials	1	ME/EE	\$50.00	\$50.00
Aluminum sheeting (1/8×36×48 in.)	1	ME/EE	\$150.00	\$150.00
Aluminum sheeting (1/4×24×48 in.)	1	ME	\$180.00	\$180.00
Aluminum square tubing(1in × 8 ft)	2	ME	\$20.00	\$40.00
Bearing structures	2	ME	\$60.00	\$120.00
DWM1000	6	EE	\$26.00	\$156.00
IMU	2	EE	\$30.00	\$60.00
Linear actuators (24 in.)	2	ME	\$150.00	\$300.00
Motor controllers (SDC2130)	2	EE	\$175.00	\$350.00
Nuts/Bolts	1	ME	\$75.00	\$75.00
3D printing materials	1	ME/EE	\$20.00	\$20.00
Miscellaneous	2	ME/EE	\$250.00	\$500.00
Total Project General Budget				\$2,001.00

11 Project Risks

The risks for this project are divided into three groups: mechanical systems, autonomy, and general. Each group has a list of risks that fall under them along with a solution to prevent them.

1. Mechanical Systems

Collection System Failure - the actuators are unable to move the bucket ladder down to dig. **Solution** - check the functionality during testing.

Deposition System Failure - icy regolith jamming the conveyor belt and making it unable to deposit it into the bin. **Solution** - use covers to prevent icy regolith from jamming.

Wheel Motor(s) Failure - the wheels are not capable of transversing the robot through the competition pit. **Solution** - check the functionality during testing.

Chassis System Failure - the chassis breaks apart and the robot is unable to compete. **Solution** - secure the joint on the articulating chassis.

Over Mechanical Budget - spending too much on new components used for the collection and deposition systems. **Solution** - overlook all the new parts that are needed for the robot and how much each costs.

Electrical Box Failure - the location of the electrical box impedes other systems, it is not properly secured to the robot, or dust getting inside the box. **Solution** - check how all the systems work together as the robot operates, and checking how well the electrical box is mounted and the seals for the inside of the box.

2. Autonomy

Incomplete Software - the code is incomplete by the time of competition. **Solution** - have the code completed.

Sensor Failure - the sensors are reading incorrect data from calibration. **Solution** - verify the sensors are working correctly during testing.

Software Rework - changes to the code that need to be done based on new evidence from testing. **Solution** - have enough tests done to confirm the code works.

Complexity/Scope Underestimation - the amount of work needed to have complete autonomy is more than estimated. **Solution** - start working on the code as soon as possible.

Overrun Computational Resources - the computer needed to run the code is not powerful enough such as not having enough memory or a slower clock speed. **Solution** - verify during testing if the computer will work.

Loss of Source Code - files used to run the autonomy code are deleted and cannot be retrieved. **Solution** - have the code backed up on multiple storage devices.

3. General

Project is over-budget - more money is spent than what the budget currently will allow. **Solution** - Overlook all the new parts that are needed for the robot and how much each costs.

Robot is incomplete by competition date - an incomplete robot will prevent it from competing. **Solution** - have a completed working robot by the competition.

Parts difficult to source - unable to find parts of the shelf for the robot. **Solution** - manufacture the needed parts.

Mechanical Failure - the mechanical systems are not functioning as required such as the collection, deposition, and chassis systems. **Solution** - check all the systems and make sure nothing is lose to allow failure.

Autonomy Failure - the robot is unable to guide and operate by itself during the competition. **Solution** - test the autonomy as much as possible before competition.

Electrical Failure - the wiring inside the electrical box and the connections to other systems are not properly secured. **Solution** - check the electrical box and make sure everything is wired correctly.

Over-dimensioned - the robot does not fit within the required dimensions set by the NASA Robotic Mining Competition. **Solution** - design the robot within the required dimensions.

A Collection System Finite Element Analysis

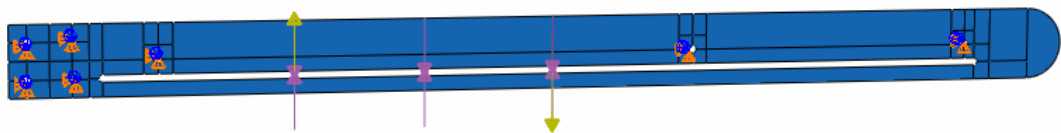


Figure 59: Loading cases used to run FEA on collection rail

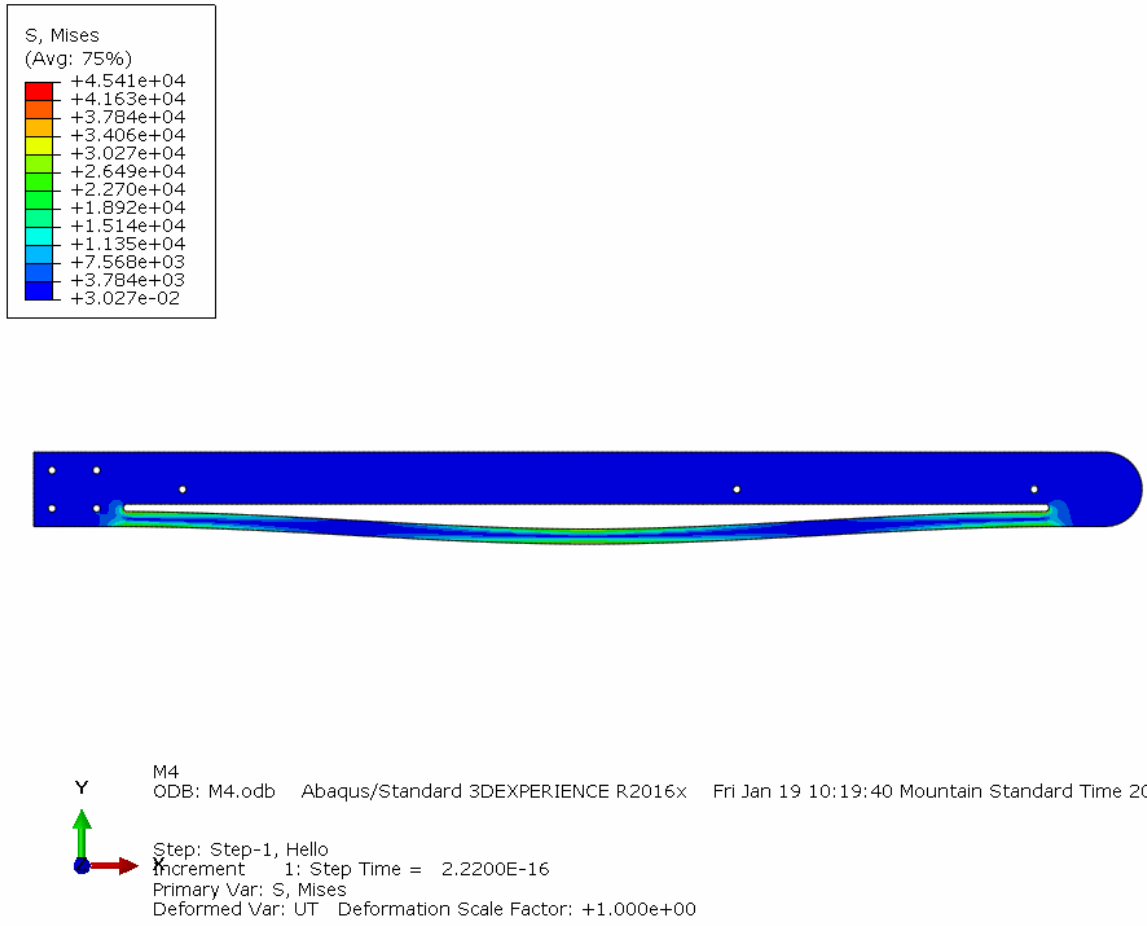


Figure 60: Finite Element Analysis post processing on collection rail

Table 17: Convergence study for FEA of collection rail.

Mesh	# Elements	# Nodes	Max Von Mises (ksi)	Percent Difference
1	2191	2493	26.66	NA
2	9233	9665	31.77	16%
3	34293	34957	38.63	18%
4	136680	135504	45.41	15%

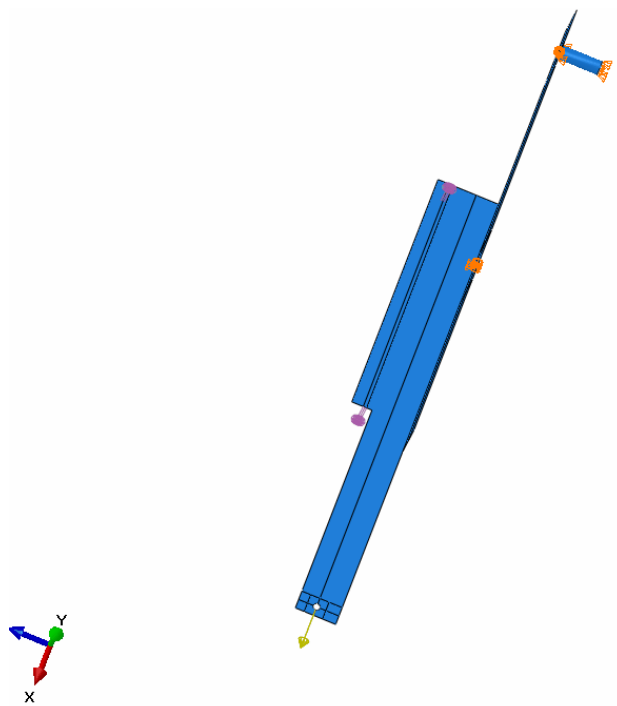


Figure 61: Loading cases used to run FEA on collection slide

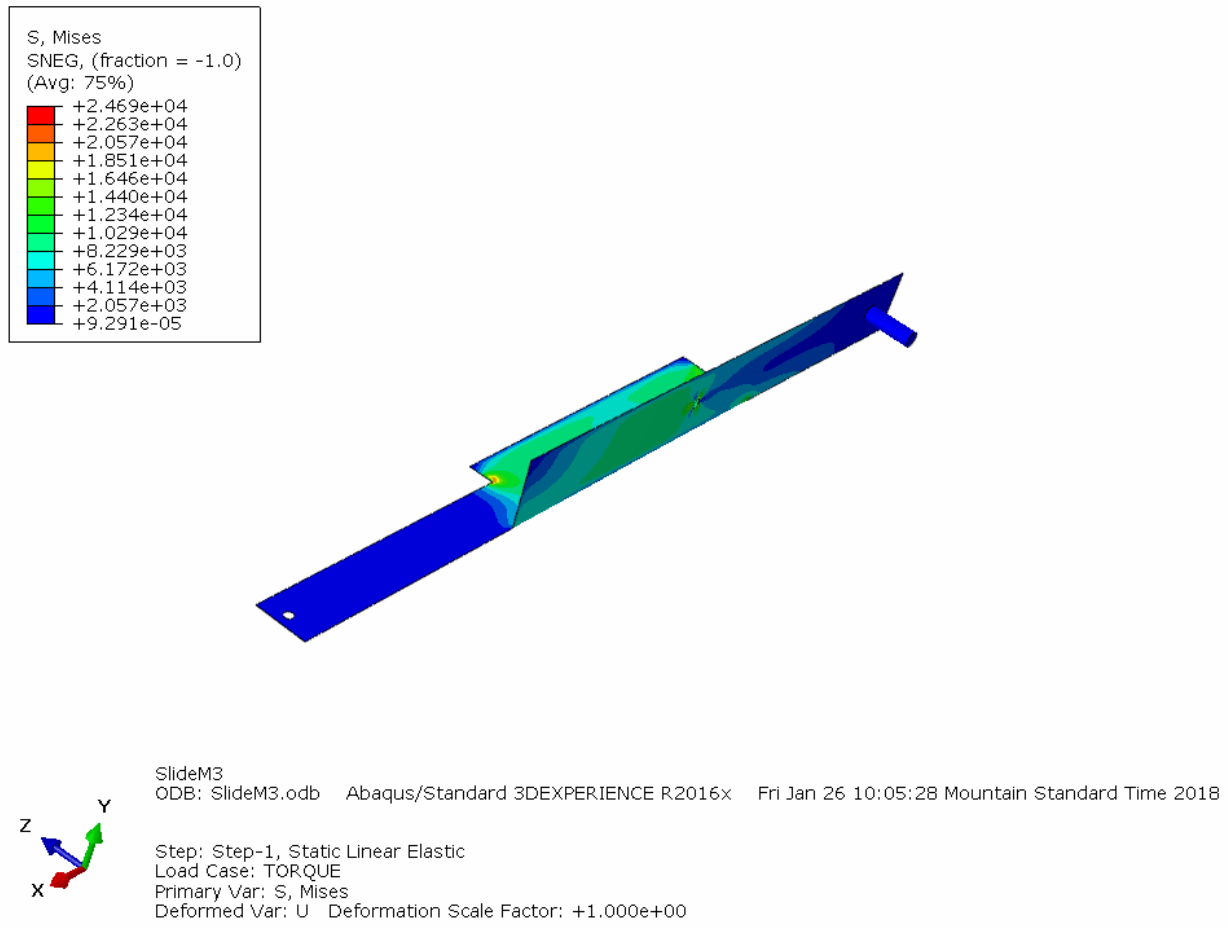


Figure 62: Finite Element Analysis post processing on collection slide

Table 18: Convergence study for FEA of collection slide.

Mesh	# Elements	# Nodes	Max Von Mises (ksi)	Percent Difference
1	1312	1489	19.05	NA
2	5070	5436	23.25	18%
3	19716	20607	24.69	6%

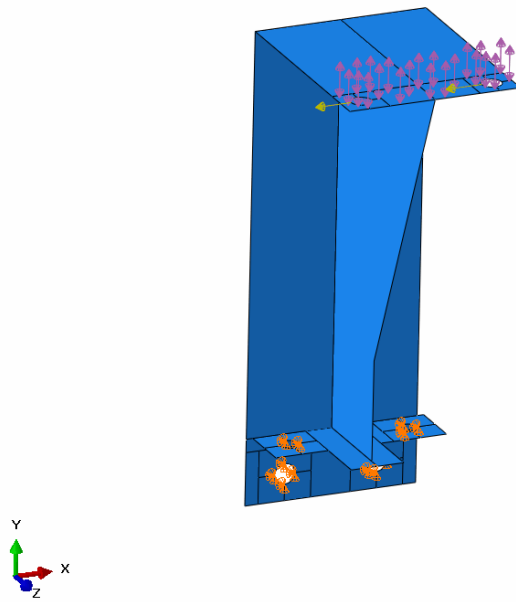


Figure 63: Loading cases used to run FEA on collection mounting structure

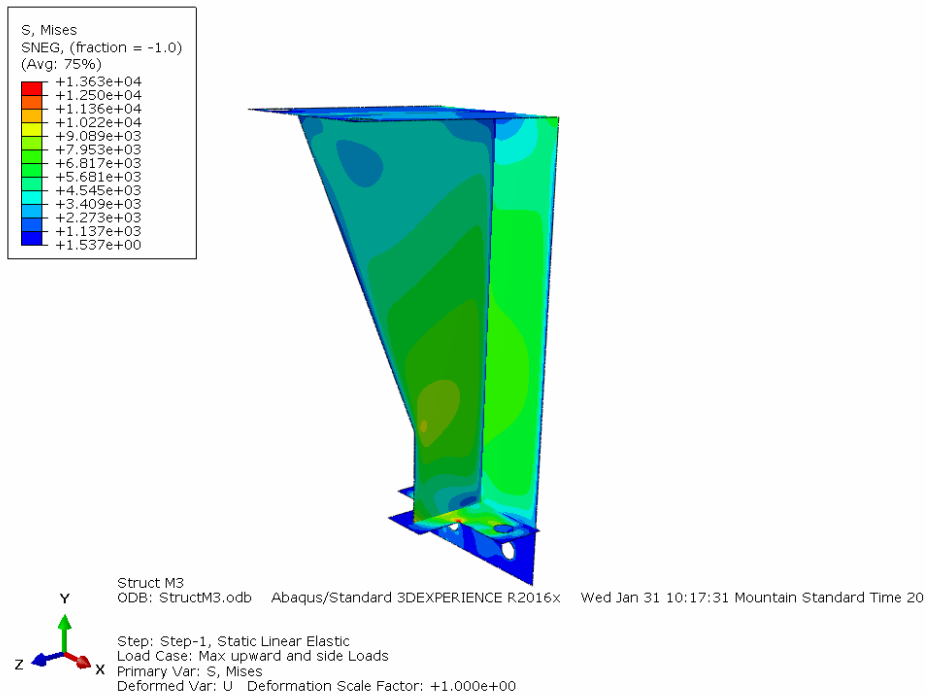


Figure 64: Finite Element Analysis post processing on collection mounting structure without hole

Table 19: Convergence study for FEA of collection mounting structure without hole.

Mesh	# Elements	# Nodes	Max Von Mises (ksi)	Percent Difference
1	5893	6075	10.23	NA
2	24905	25279	12.08	15%
3	99584	100331	13.63	11%

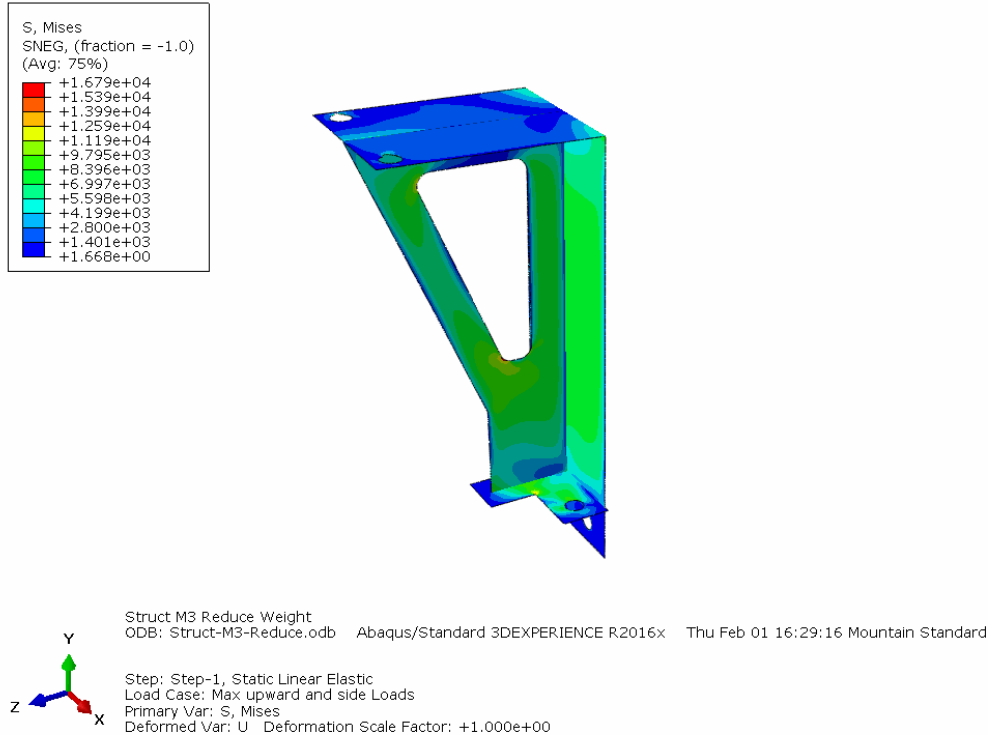


Figure 65: Finite Element Analysis post processing on collection mounting structure with hole

Table 20: Convergence study for FEA of collection mounting structure with hole.

Mesh	# Elements	# Nodes	Max Von Mises (ksi)	Percent Difference
1	6207	6448	14.338	NA
2	24014	24503	15.66	8%
3	94355	95329	16.79	7%

B Collection Subsystem Drawings

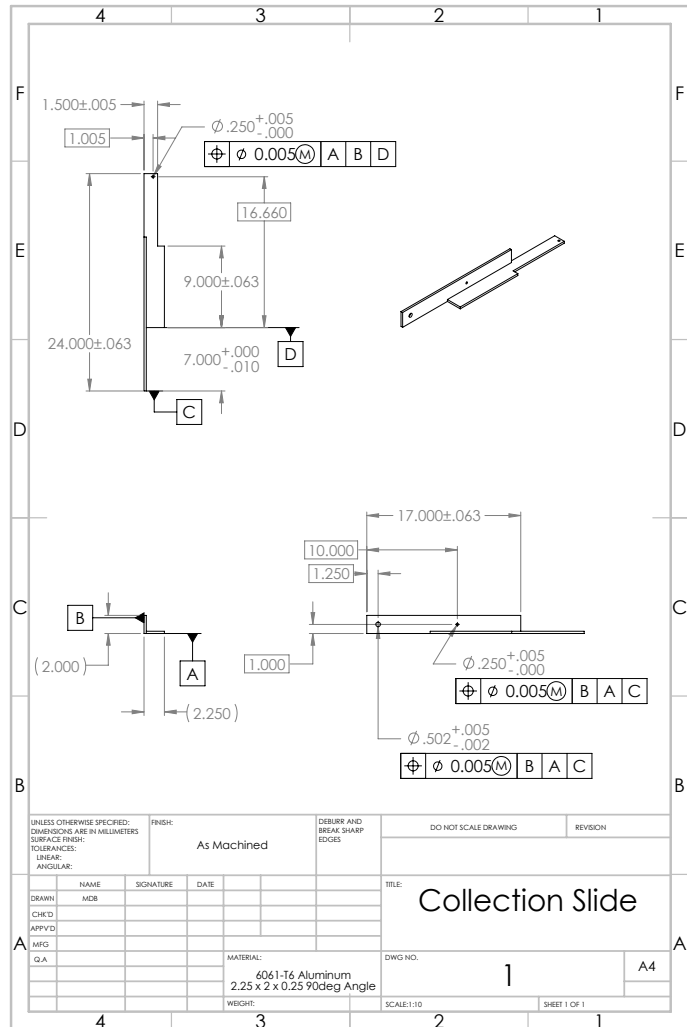


Figure 66: Collection Slide

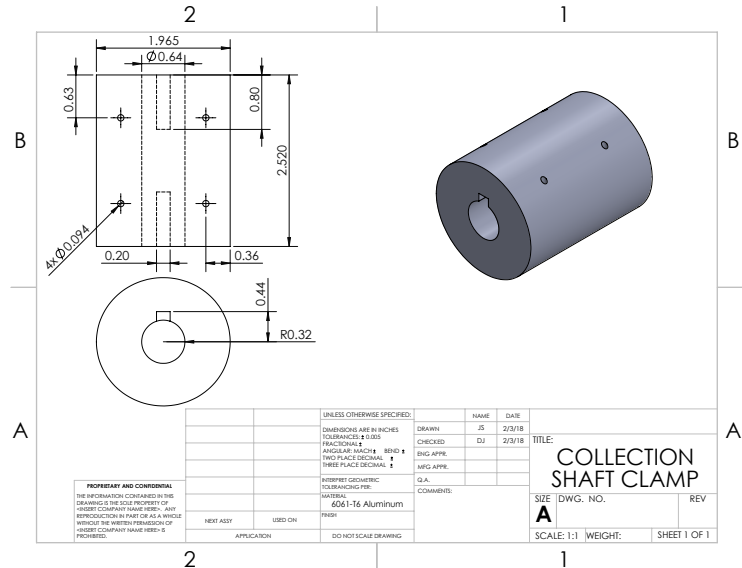


Figure 67: Collection Shaft Clamp

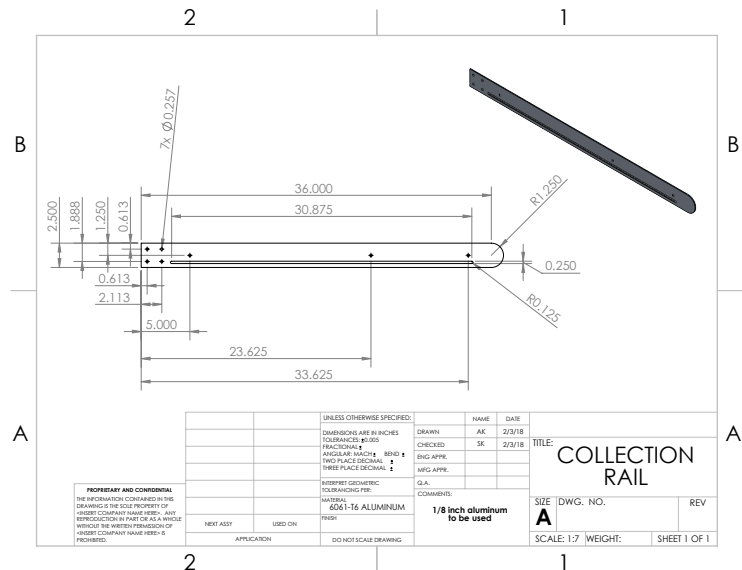


Figure 68: Collection Rail

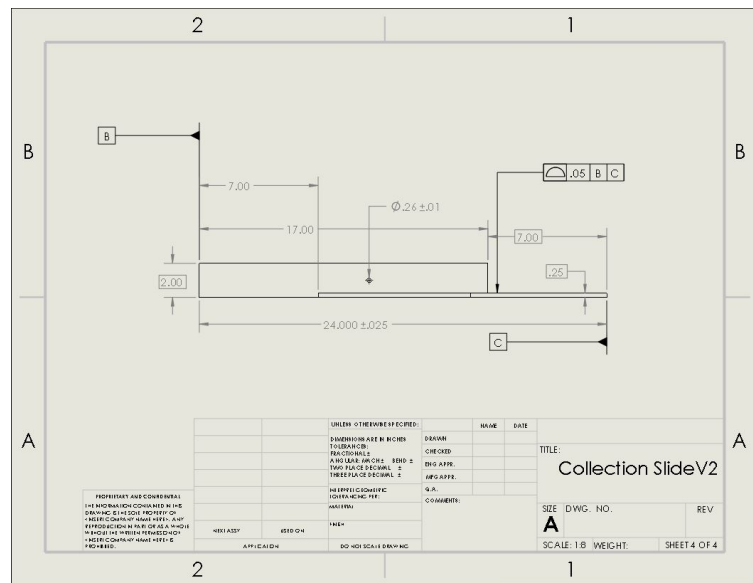


Figure 69: Collection Slide

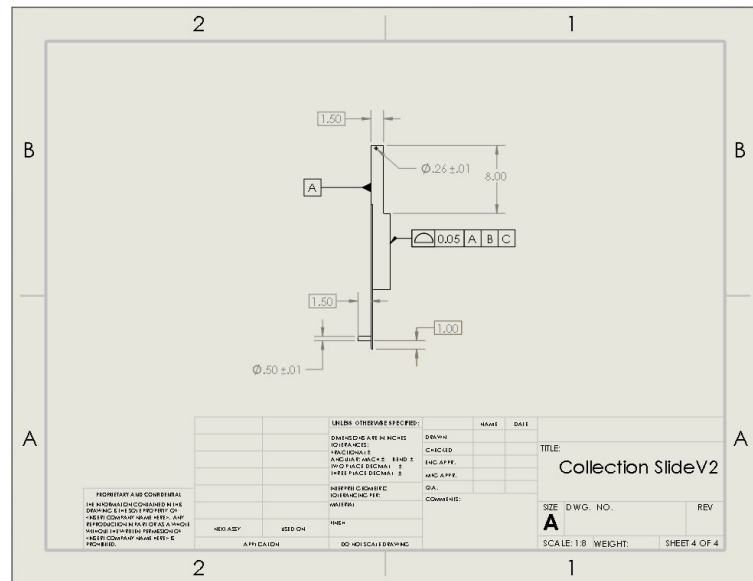


Figure 70: Collection Slide

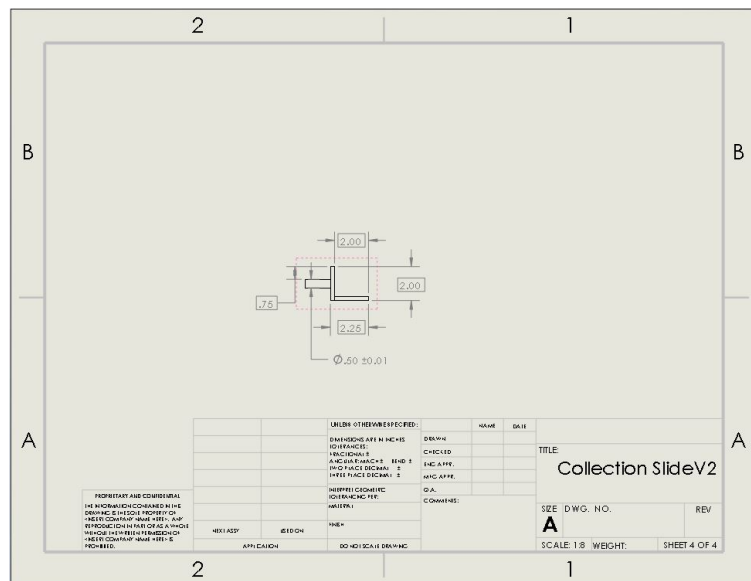


Figure 71: Collection Slide

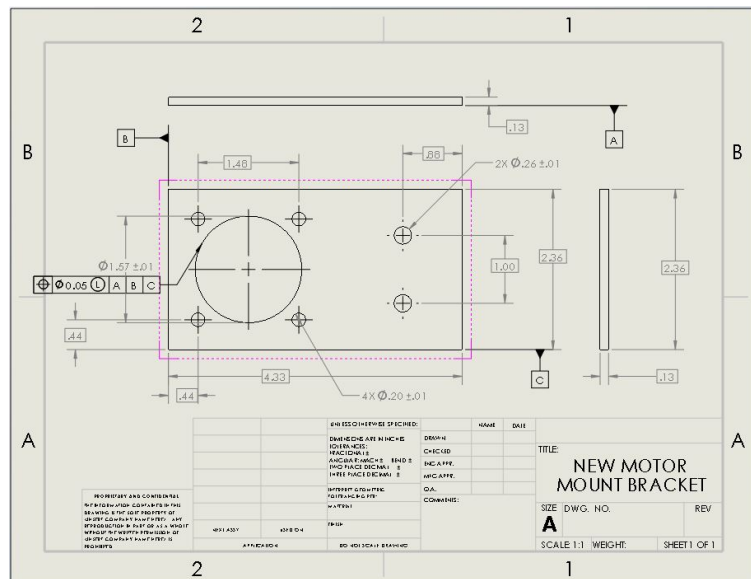


Figure 72: Collection Motor Mount

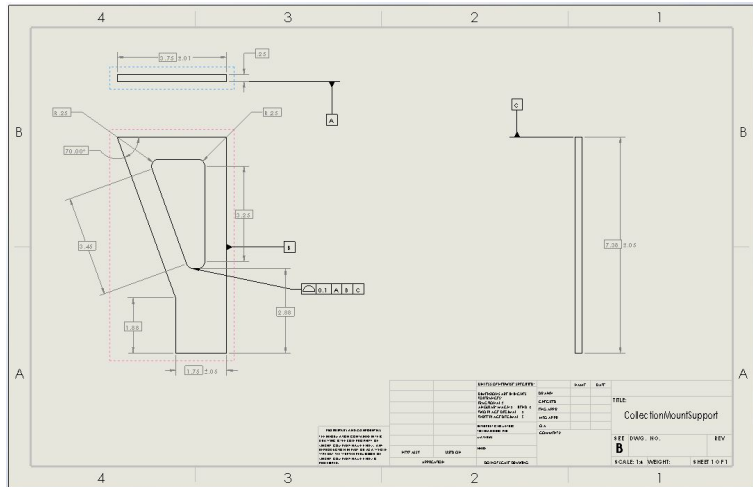


Figure 73: Collection Mount Support

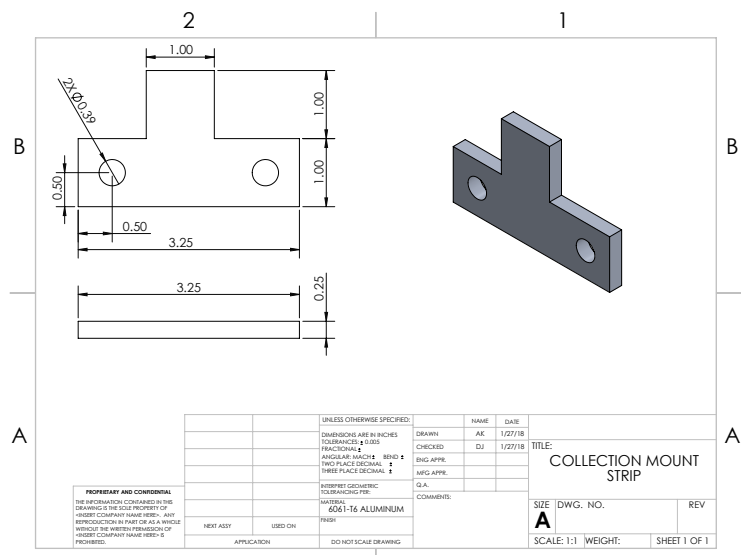


Figure 74: Collection Mount Strip

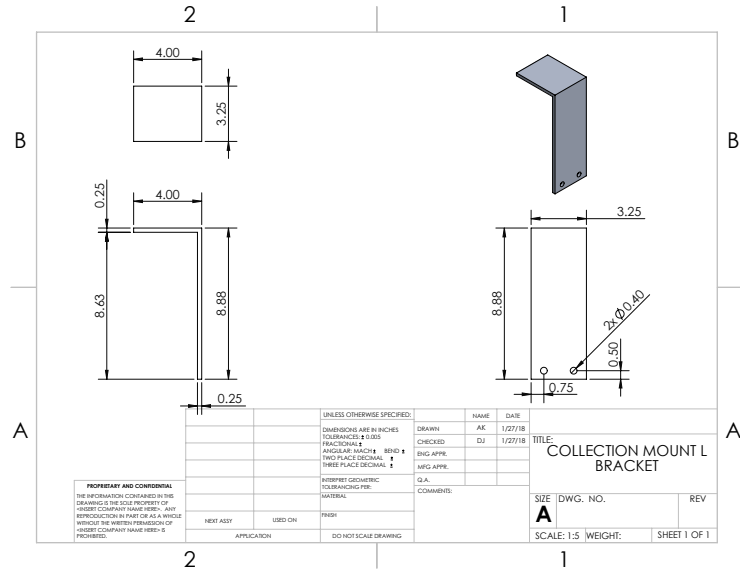


Figure 75: Collection Mount L Bracket

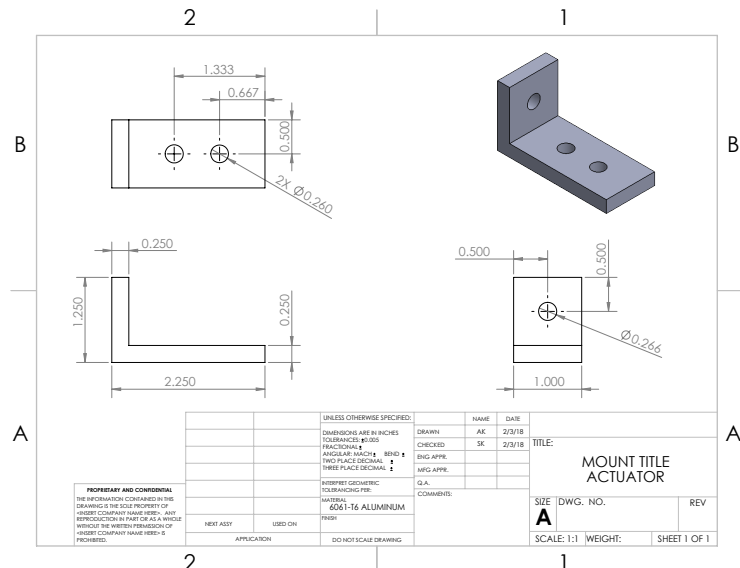


Figure 76: Mount Title Actuator

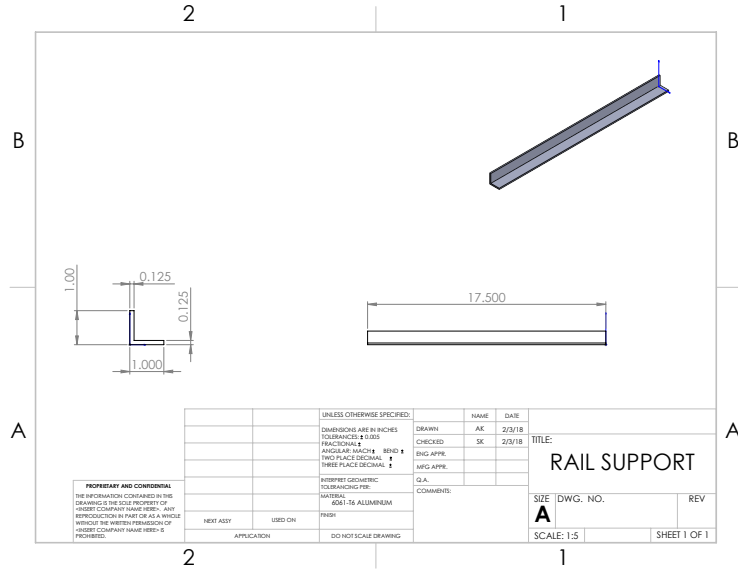


Figure 77: Rail Support

C Custom ROS Message Definitions

The ROS architecture provides a way to define and create custom messages to be used in a system. A message is a data type that has a known serialization method in the ROS ecosystem that allows it to be sent across a network connection. The custom messages defined for the Moonrocker's project are defined below.

Note: "[]" in a message definition signifies an array of the preceding data type.

Map Row (mapRow)

The map row message is an intermediary message type that defines a single row of the environment map. ROS does not support the definition of two (2) dimensional arrays of base types. This raises the need for the row message type. The map row message format is defined in Table 21. The map row ROS message definition is located in the mapRow.msg file in the autonomy_msgs project.

Table 21: Map Row Message Format

Name	Data Type	Purpose
row	float64[]	Each element contains the height of the terrain in centimeters for each point in a straight line parallel to the hopper wall. Each point is 1 centimeter from each of its neighbors.
rowLength	int16	The length of 'row'. Tells how many points are in the row.

Environment Map (envMap)

The environment map message is the message type that will carry the terrain height data within the system. The environment map message format is defined in Table 22. The environment map ROS message definition is located in the envMap.msg file in the autonomy_msgs project.

Table 22: Environment Map Message Format

Name	Data Type	Purpose
map	mapRow[] ¹	Each element contains the terrain height information in centimeters for a line of points. Each line is 1 centimeter from its neighbors.
mapHeight	int16	The length of 'map'. Tells how many rows are in the map.

¹ Data type is defined in Table 21.

Waypoint

A waypoint message is used to send a location in the robot's world. Waypoint dimensions' origin is set at the hopper.

Table 23: Waypoint Message Format

Name	Data Type	Purpose
x	float64	Distance left/right from the hopper
y	float64	Distance into the arena away from the hopper

D Custom ROS Services

The ROS architecture provides a way to define and create custom services to be used in a system. A service is an API function call that is executed by an unknown (to the client) node which requires a request message and returns a response message. The custom messages for the Moonrocker's project are defined below.

Environment Map (environment_map)

The environment map service is a service that will provide a global terrain map back to the client. This terrain map is measured in centimeters on all axes.

Table 24: Environment Map Service Format

Name	Data Type	Purpose
		Request
theMap	envMap ¹	Response This element contains the environment map.

¹ Data type is defined in Table 22.

Path

The path service will provide a set of waypoints for the robot to follow to navigate across the arena.

Table 25: Path Service Format

Name	Data Type	Purpose
target	waypoint	Request Target specifies the location the robot would like to navigate to
plan	waypoint	Response This element contains the planned path as a series of waypoints.

¹ Data type is defined in Table 22.

E State Diagrams

This section contains a preliminary version of all of the state diagrams used by the Decision Making subsystem.

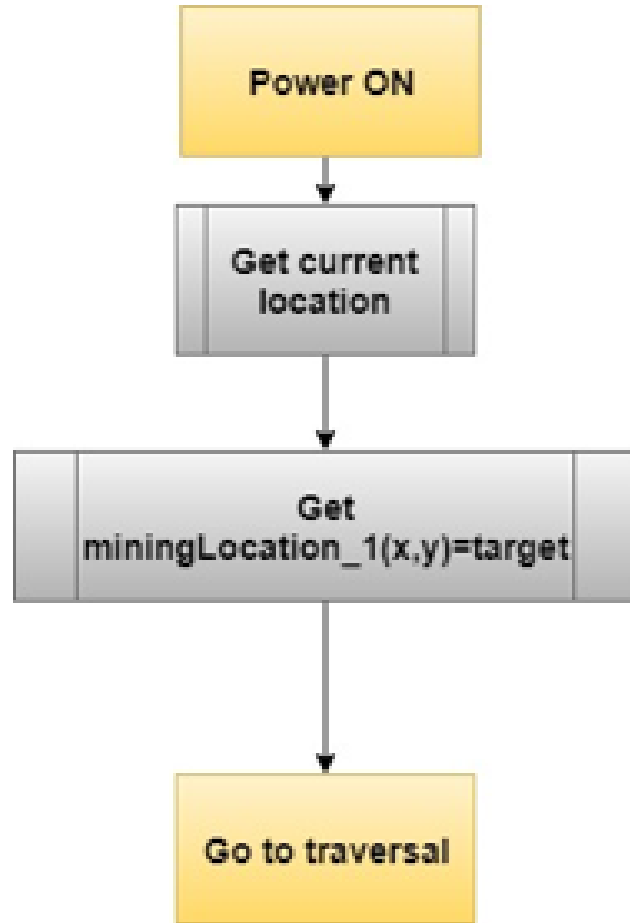


Figure 78: Startup State

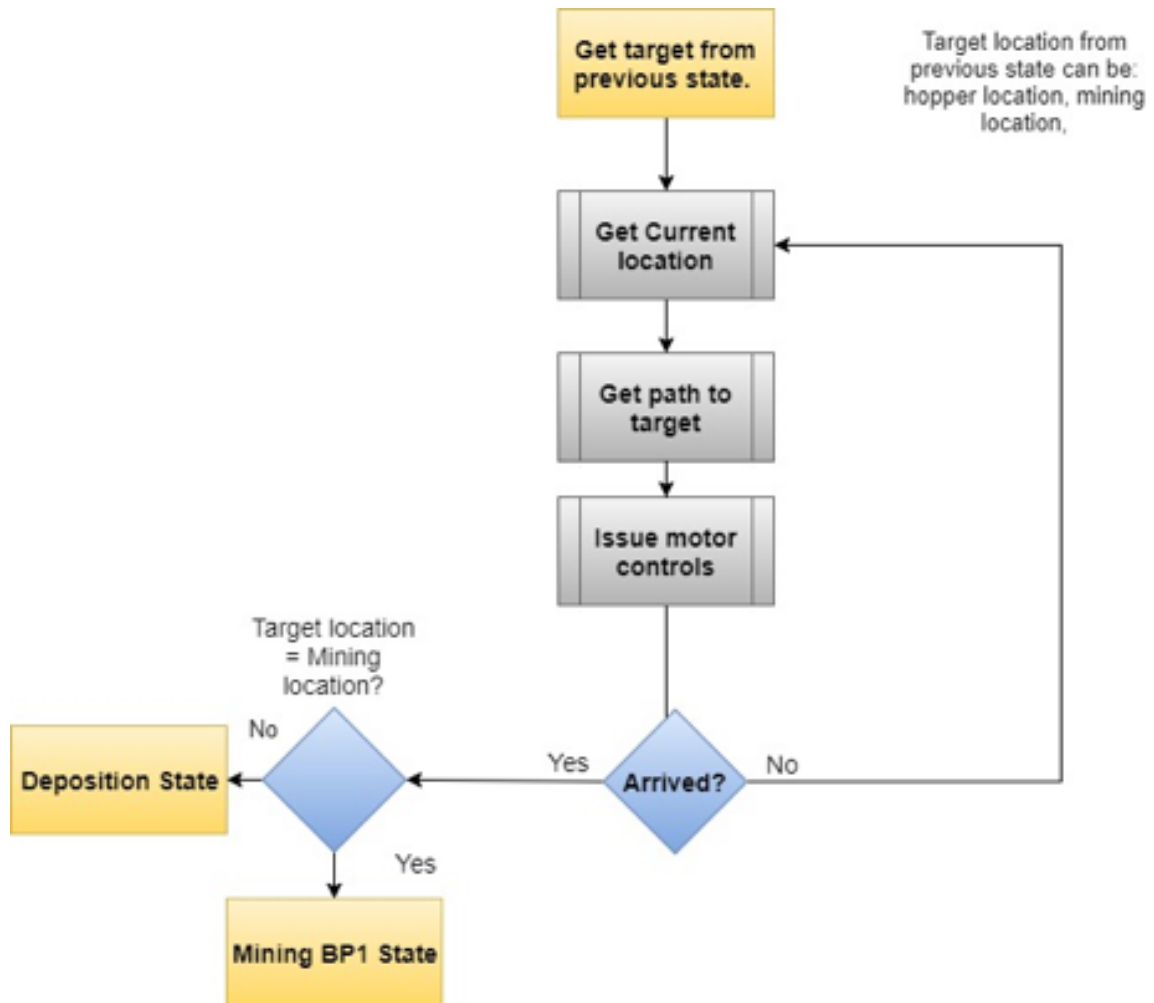


Figure 79: Traversal State

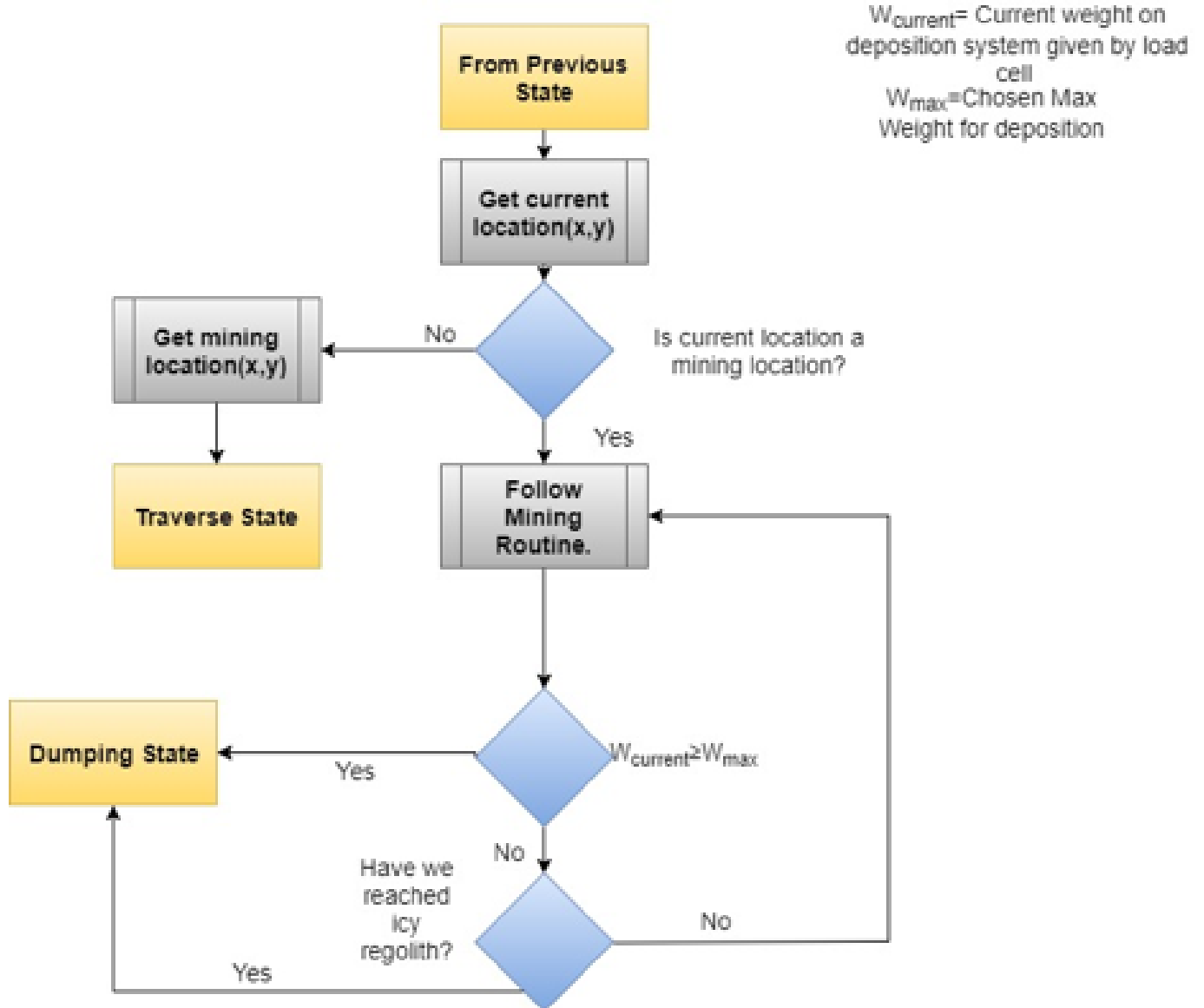


Figure 80: Regolith Mining State

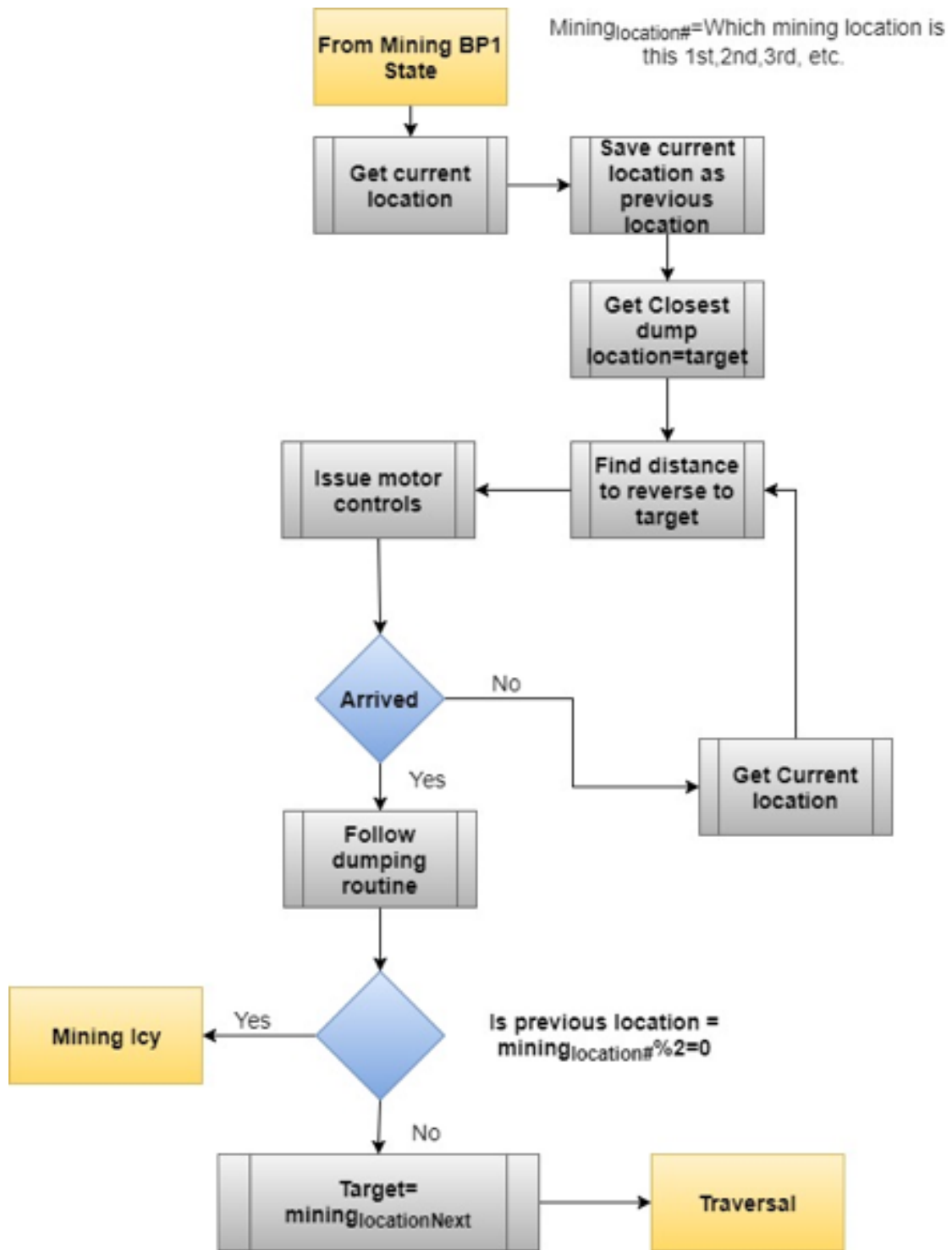


Figure 81: Dump State

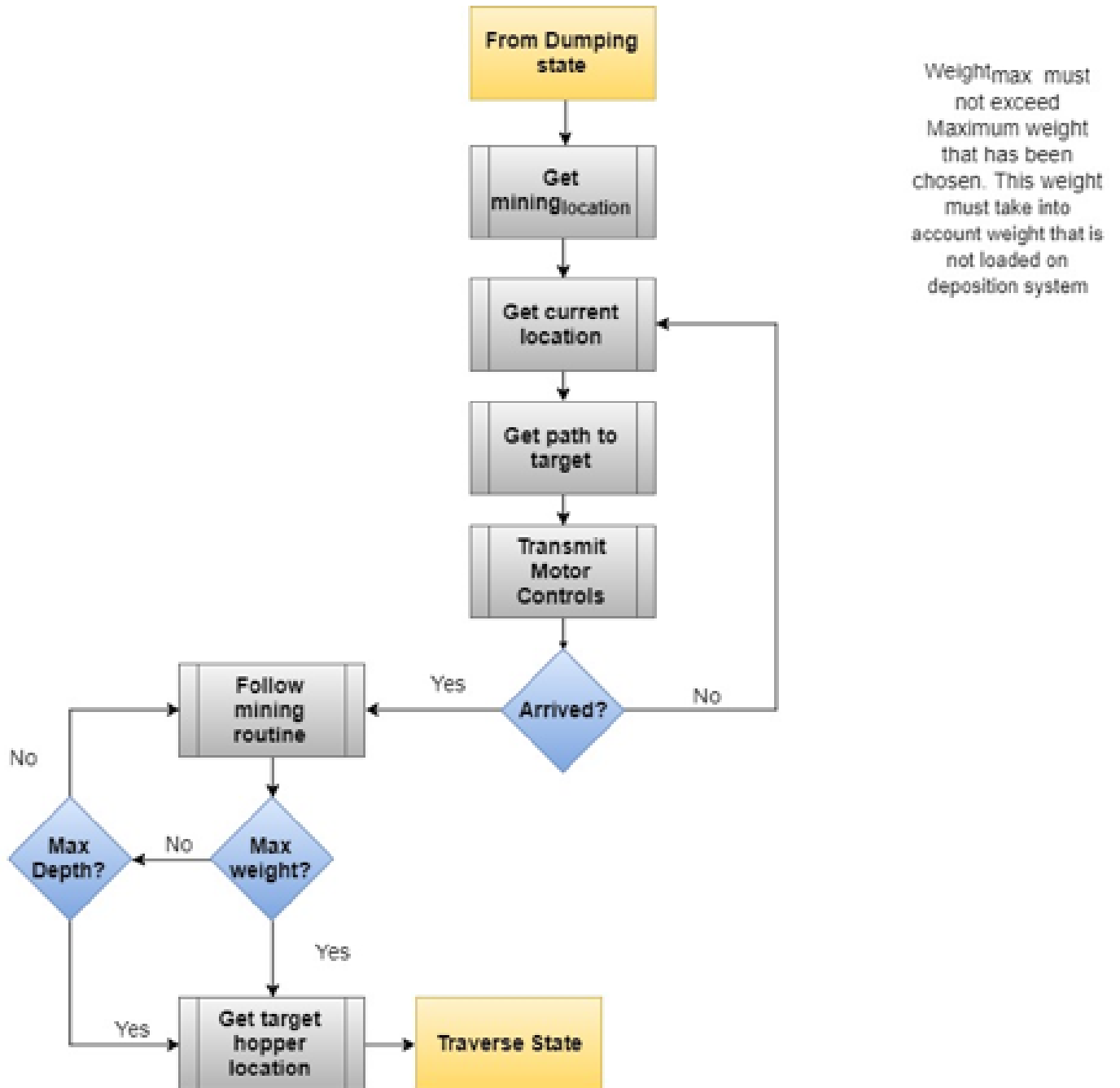


Figure 82: Icy Regolith Mining State

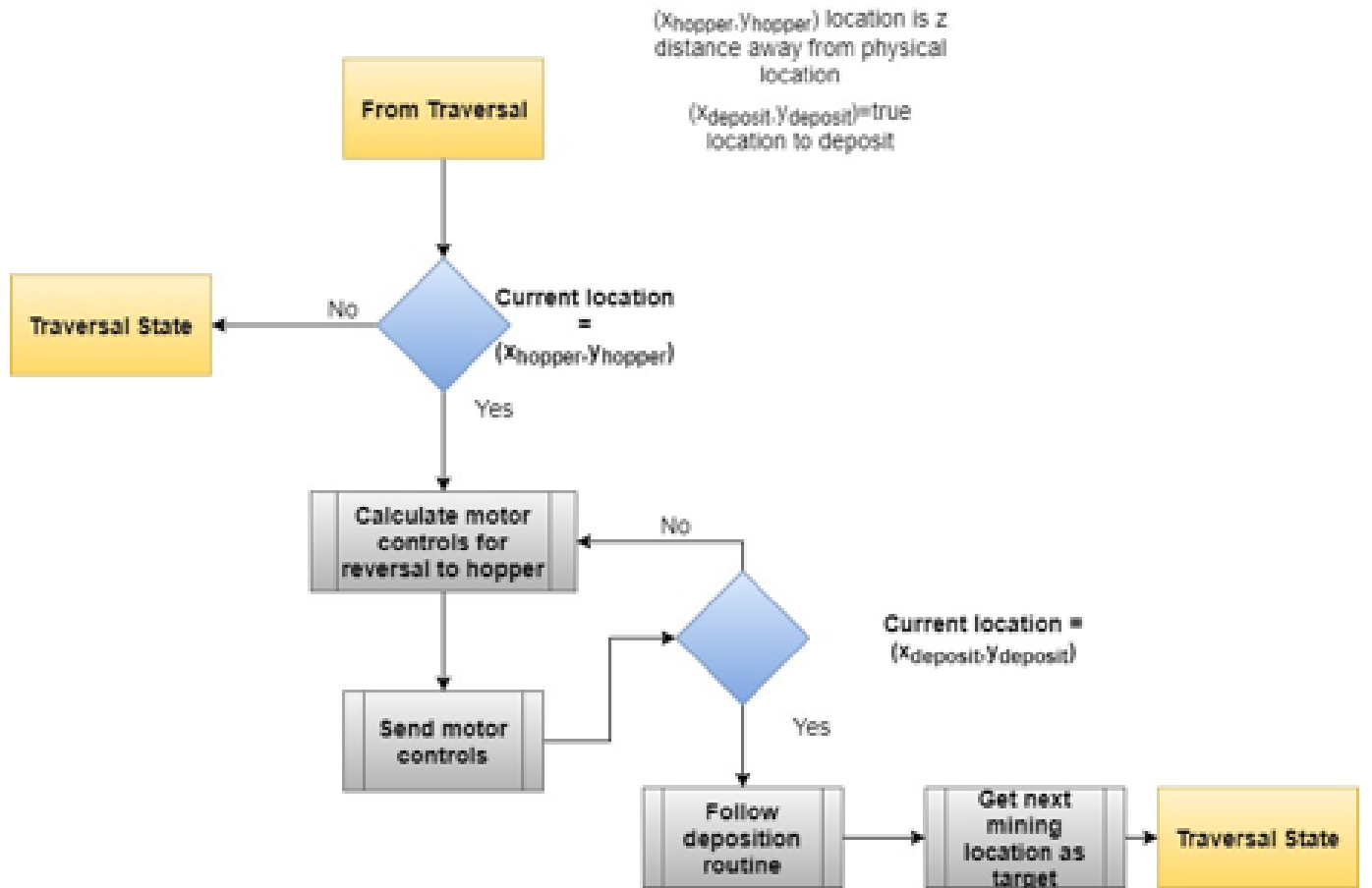


Figure 83: Deposition State

References

- [1] Jakob Engel and Dr. Daniel Cremers. Lsd-slam: Large-scale direct monocular slam. Retrieved on April 20, 2018.
- [2] Jakob Engel, Vladlen Koltun, and Dr. Daniel Cremers. Dso: Direct sparse odometry. Retrieved on April 20, 2018.
- [3] Sven Koenig and Maxim Likhachev. D* lite. Technical report, Georgia Institute of Technology and Carnegie Mellon University, <http://idmlab.org/bib/abstracts/papers/aaai02b.pdf>. Retrieved on November 15, 2017.
- [4] Timothy McJunkin. Advanced navigation for planetary vehicles applying an approximate mapping technique. Master's thesis. Retrieved on January 7, 2018.
- [5] NASA-RMC. *NASA's 9th Annual Robotic Mining Competition Rules*, 2 edition.
- [6] Eric W. Weisstein. *Point-Line Distance – 2 Dimensional*. <http://mathworld.wolfram.com/Point-LineDistance2-Dimensional.html>. Retrieved on January 7, 2018.